



<https://theses.gla.ac.uk/>

Theses Digitisation:

<https://www.gla.ac.uk/myglasgow/research/enlighten/theses/digitisation/>

This is a digitised version of the original print thesis.

Copyright and moral rights for this work are retained by the author

A copy can be downloaded for personal non-commercial research or study,
without prior permission or charge

This work cannot be reproduced or quoted extensively from without first
obtaining permission in writing from the author

The content must not be changed in any way or sold commercially in any
format or medium without the formal permission of the author

When referring to this work, full bibliographic details including the author,
title, awarding institution and date of the thesis must be given

Enlighten: Theses

<https://theses.gla.ac.uk/>
research-enlighten@glasgow.ac.uk

**THE EFFECTS OF VAPOUR SHEAR
AND INUNDATION ON ROPED TUBES**

**BY
W. JAMES FIDLER**

**SUBMITTED AS A THESIS FOR THE DEGREE OF
MASTER OF SCIENCE IN ENGINEERING**

**DEPARTMENT OF MECHANICAL ENGINEERING
UNIVERSITY OF GLASGOW**

© W.J. Fidler, September 1991

ProQuest Number: 10987060

All rights reserved

INFORMATION TO ALL USERS

The quality of this reproduction is dependent upon the quality of the copy submitted.

In the unlikely event that the author did not send a complete manuscript and there are missing pages, these will be noted. Also, if material had to be removed, a note will indicate the deletion.



ProQuest 10987060

Published by ProQuest LLC (2018). Copyright of the Dissertation is held by the Author.

All rights reserved.

This work is protected against unauthorized copying under Title 17, United States Code
Microform Edition © ProQuest LLC.

ProQuest LLC.
789 East Eisenhower Parkway
P.O. Box 1346
Ann Arbor, MI 48106 – 1346

ABSTRACT

This investigation is concerned with the effects of both vapour shear and inundation on the performance of the overall heat transfer coefficient of plain and roped tubes.

A series of experiments were conducted using a specially designed test condenser and three types of tubes to initially determine the effect of steam velocity and tube geometry on the overall heat transfer coefficient. Subsequent tests were performed to investigate the combined effects of vapour shear and inundation on bundles of condenser tubes. The main experimental variables in the tests were steam velocity, cooling water velocity and the number of equivalent tubes in a vertical array.

The results of the vapour shear tests conclusively showed that as the velocity of steam increased so did the amount of heat transferred by all of the three types of tubes. These tests also determined that the geometry of a tube bundle (i.e. staggered or in-line configurations) made little or no difference to the overall heat transfer coefficient. The multi-tube experiments confirmed that inundation reduced the heat transfer in condensers and showed that the effect of inundation was moderated through the use of a higher steam velocity. This result was convincingly shown for bundles of 2-start roped tubes but was less apparent for similar bundles of both plain and 6-start roped tubes. In all of the above experiments the roped tubes were found to consistently outperform the equivalent plain tubes with respect to the amount of heat transferred.

In addition to the experimental work, two computer programs were used to predict the effects of vapour shear and inundation on both single tubes and tube bundles. The theoretical predictions were compared with the test results and very good agreement was found for the plain tube simulations. The predictions of the roped tube simulations were judged to be less accurate than those of the plain tube, but still good considering the complex hydrodynamic and thermal processes associated with roped tubes.

Acknowledgements

The author wishes to express his appreciation to Mr. J. Cunningham for his very valuable guidance, advice and support throughout the course of this project.

Also many thanks are due to both Mr. W. Hay and Mr. J. Wilson, who supplied the technical assistance for the construction and operation of the test equipment, and to my long suffering typist Miss L. Cullen.

Finally the author would like to thank Mr. and Mrs. A. Main and particularly Dr. & Mrs. W.E. Fidler without whose encouragement and financial support this research work could not have been possible.

Table of Contents

	<u>Page No.</u>
Abstract	i
Acknowledgements	iii
Table of Contents	iv
Nomenclature	vii
List of Figures	xiii
<u>Chapter 1 - General Introduction</u>	
1.1 Introduction	1
1.2 Literature Survey	4
1.2.1 Plain Tubes	7
1.2.1.1 Vapour Shear	7
1.2.1.2 Inundation	17
1.2.1.3 Vapour Shear and Inundation	21
1.2.2 Enhancement Methods	22
1.2.2.1 Method of Roped Tube Enhancement	23
1.2.3 Roped Tubes	26
1.2.3.1 Vapour Shear	26
1.2.3.2 Inundation	27
1.2.3.3 Vapour Shear and Inundation	36
1.3 Outline of Present Research	37
<u>Chapter 2 - Computer Theory</u>	
2.1 Introduction	40
2.2 Theory of the Plain Tube Program	41
2.2.1 General Description	41
2.2.2 Correlations for the Heat Transfer Coefficients	43
2.2.2.1 Water-side h.t.c.	43
2.2.2.2 Condensing-side h.t.c.	45
2.2.3 Incremental Heat Load Calculations	45

Table of Contents (continued)

	<u>Page No.</u>
2.2.4 Estimation of the Outer Tube Wall Temperature (T_{wo})	47
2.2.5 Estimation of the Inner Tube Wall Temperature (T_{wi})	51
2.2.6 Estimation of the Cooling Water Temperature Rise (dT)	54
2.2.7 Calculation of the Heat Transfer Variables	55
2.3 Modifications to the Plain Tube Program	57
2.3.1 Introduction	57
2.3.2 Vapour Shear Correlations	57
2.3.3 Calculation of the Physical Properties of Steam	60
2.3.4 The Condensing-side h.t.c Subroutine	62
2.4 The Roped Tube Program	64
2.4.1 Introduction	64
2.4.2 Development of the Roped Tube Program	65
<u>Chapter 3 - Test Apparatus and Experimental Procedures</u>	
3.1 The Test Condenser	68
3.2 Condenser Tubes	72
3.3 The Test Condenser System	74
3.3.1 Single Tube System	74
3.3.2 The Inundation System	76
3.4 Instrumentation	78
3.4.1 Temperature Measurement	78
3.4.2 Flow Rates	79
3.4.3 Pressure Measurement	79
3.5 Experimental Program and Procedures	80
3.5.1 Experimental Program	80
3.5.2 Experimental Procedure for Single Tube Tests	82
3.5.3 Experimental Procedure for Inundation Tests	84

Table of Contents (continued)

	<u>Page No.</u>
<u>Chapter 4 - Discussion of Vapour Shear Test Results</u>	
4.1 Introduction	86
4.2 Calculations Based on Measured Results	86
4.3 Analysis of Results	89
4.3.1 Experimental Results	89
4.3.2 Theoretical and Experimental Results	93
4.3.2.1 Plain Tubes	95
4.3.2.2 Roped Tubes	99
4.4 Conclusions from the Vapour Shear Experiments	105
<u>Chapter 5 - Discussion of the Vapour Shear and Inundation Test Results</u>	
5.1 introduction	106
5.2 Analysis of Results	106
5.2.1 Experimental Results	107
5.2.2 Theoretical and Experimental Results	114
5.3 Conclusions from the Vapour Shear and Inundation Experiments	118
<u>Chapter 6 - General Conclusions</u>	
6.1 Conclusions	120
6.2 Recommendations for Further Work	121
References	122
Appendix A Derivation of the Outer Tube Wall	
Temperature Expression	127
Appendix B Derivation of the Inner Tube Wall	
Temperature Expression	134
Appendix C Polynomials for Predicting the Properties of Water	137
Appendix D The Plain Tube Program	139
Appendix E Calibration Equations for Thermocouples and Flowmeters	152

NOMENCLATURE

<u>Symbol</u>	<u>Description</u>	<u>Units</u>
A	Surface area	m ²
B	(=30) Dimensionless constant in eqn. (1.12)	-
C	Thermal entry effect in eqn. (2.3) $= 1 + \left(\frac{0.96(7/Pr)^{0.42}}{L/D_i} \right)$	-
C _p	Specific heat capacity	kJ/kg°C
D	Diameter	m
dx	Incremental tube length	m
dQ	Incremental heat flow	kW
dT	Cooling water temperature rise	°C
EF	Dimensionless enhancement factor	-
f	Friction factor	-
G	$= \left(\frac{\Delta T \lambda f}{\mu f h_{fg}} \right) \left(\frac{\rho f \mu f}{\rho g \mu g} \right)^{1/2}$ Dimensionless factor used in eqn. (1.28)	-
G ₁	Coefficient defined by eqn. (2.16)	kW/m ² °C
G ₂	Coefficient defined by eqn. (2.17)	kW/m ² °C
G _F	Vapour flow rate when test apparatus was running, eqn. (1.13)	kg/s
G ₀	Initial vapour flow rate, eqn. (1.13)	kg/s
g	Acceleration due to gravity	m/s ²
h	Enthalpy	kJ/kg
h' _{fg}	Enthalpy adjusted by eqn. (1.6)	kJ/kg
h.t.c.	Heat transfer coefficient	kW/m ² °C
K	Dimensionless coefficient defined by eqn. (2.44)	-
L	Tube length	m

<u>Symbol</u>	<u>Description</u>	<u>Units</u>
LMTD	Log mean temperature difference	°C
M	Mass flow rate	kg/s
M_C	Mass flow of condensate draining from the N^{th} tube	kg/s
M_{CN}	Mass flow of condensate generated on the N^{th} tube	kg/s
m	(=0.16) Dimensionless constant in eqn. (1.12)	-
M	Number of increments along the tube length	-
N	Number of tubes in a vertical row	-
Nu	Nusselt number ($= \alpha D / \lambda$)	-
\overline{Nu}	Mean Nusselt number	-
O.H.T.C.	Overall heat transfer coefficient	kW/m ² °C
P	Pressure	N/m ²
ΔP	Pressure change	N/m ²
p	Pitch	m
Pr	Prandtl number ($= \frac{C_p \mu}{\lambda}$)	-
Q	Heat flow	kW
q	Heat flux	kW/m ²
Re	Reynolds number ($= \frac{VD\rho}{\mu}$)	-
Re_{TP}	Two-phase Reynolds number	-
r	Tube radius	m
S	Number of starts or grooves around the roped tube circumference	-
s	(= -0.125) Non-dimensional constant used in eqn. (1.12)	-
s1	Dimensionless coefficient defined by eqn. (2.42)	-

<u>Symbol</u>	<u>Description</u>	<u>Units</u>
T_C	Average condensate film temperature	°C
T_{CW}	Mean cooling water temperature	°C
ΔT	Change in temperature	°C
T_{in}	Cooling water inlet temperature	°C
T_m	Bulk cooling water temperature	°C
T_{out}	Cooling water outlet temperature	°C
T_s	Saturated steam temperature	°C
T_{wi}	Inside tube wall temperature	°C
T_{wo}	Outside tube wall temperature	°C
t	Groove indentation depth	m
V_{CW}	Cooling water velocity	m/s
V_n	Steam velocity in the narrow space between tubes in the test condenser	m/s
V_w	Steam velocity in the widest point of the test condenser	m/s
We	Weber number $\left(= \frac{\rho V_w^2 L}{\sigma} \right)$	-
W_o	Groove width	m
X_f	Dryness fraction	-
Z^*	Dimensionless distance $= \left(\frac{4 \lambda_f L (T_s - T_{wo})}{h'_{fg} \mu_f \delta} \right)$	-

Greek Symbols

<u>Symbol</u>	<u>Description</u>	<u>Units</u>
ρ	Density	kg/m ³
λ	Thermal conductivity	kW/m°C
δ	Condensate film thickness	m
δ^*	Dimensionless film thickness	-
	$= \delta \left(\frac{\rho_f(\rho_f - \rho_g) g \sin \theta_1}{\mu_f^2} \right)^{1/3}$	
θ	Helix angle	degree
θ_1	Angle measure from top of the tube in a clockwise rotation	degree
τ	Shear stress	N/m ²
τ^*	Dimensionless shear stress	-
	$= \left(\frac{\tau}{(\rho_f - \rho_g) g \delta \sin \theta_1} \right)$	
α	Heat transfer coefficient	kW/m ² °C
α	Average heat transfer coefficient	kW/m ² °C
α_N	Average heat transfer coefficient for a vertical row of N tubes	kW/m ² °C
α_{Nu}	Nusselt's modified eqn. as defined by eqn. (1.7)	kW/m ² °C
σ	Surface tension	N/m
μ	Viscosity	$\frac{N.s}{m^2}$
ν	Kinematic viscosity	m ² /s
γ	Specific weight	N/m ³
π	Dimensionless coefficient defined by eqn. (2.41)	-

<u>Symbol</u>	<u>Description</u>	<u>Units</u>
ψ	Dimensionless correction factor for the effects of convective heat transfer and inertia forces used in eqn. (1.35) (i.e. when $Pr > 1$, $\psi = 1.0$)	-
ϵ_t	Dimensionless correction factor for physical properties of condensate, used in eqn. (1.35) $= \left(\frac{\lambda_{f,tW} \mu_f}{\lambda_f \mu_{f,tW}} \right)^{1/8}$	-
ϵ_v	Dimensionless correction factor for wavy flow of condensate $(= 0.95 Re_f^{0.04})$	-
ϵM_f	Reynold's flux dependant upon the condensation rate	-
ζ	Heat capacity effect of condensate used in eqn. (1.39) $\left(= \frac{C_p \Delta T}{h_{fg}} \right)$	-
ξ	Acceleration effect of condensate used in eqn. (1.39) $\left(= \frac{\lambda \Delta T}{\mu h_{fg}} \right)$	-

Subscripts

c	Condensate
cw	Cooling water
F	Fouling
f	Property of saturated liquid
fg	Change of phase at constant pressure
g	Property of saturated vapour
i	Inside
M	Number of increments along the tube length
N	Number of tubes in a vertical row
NG	Non-grooved
OA	Overall
OO	Heat capacity and acceleration effects are neglected
O	Outside
p	Plain
r	Roped
s	Steam
tw	Tube wall
wo	Outside wall
wi	Inside wall

List of Figures

Figure No.

- 1 Typical Shell and Tube Type Condenser
- 2 Typical Plain and Roped Condenser Tubes
- 3 Cross Sectional View of the Profile of a Roped Tube
- 4 Typical Roped Tube Configuration with the Various Characteristics
- 5 The Assumed Roped Tube Profile
- 6 A Typical Tube Increment Used in the Computer Simulation Process
- 7 Side View of the Condenser Test Cell
- 8 Flow Diagram of the Plain Tube Computer Program
- 9 Overview of the Operation of Subroutine VHT
- 10 The Assembled Test Condenser Rig
- 11 Front View of the Test Condenser
- 12 Condenser Tube Bundles
- 13 Test Section Insert
- 14 Insert Spacers
- 15 Top View of the Test Condenser
- 16 Channel Area Inside the Test Condenser
- 17 Wire Mesh Strainer
- 18 Front View of the Condenser Box Window
- 19 The Condenser Tubes Under Consideration
- 20 Schematic Diagram of the Experimental Apparatus
- 21 Front View of Test Condenser With Insulation
- 22 Side View of the Test Condenser and Inundation Tank with Insulation
- 23 Side View of the Un-assembled Test Condenser
- 24 Insulated Condensate Water Tank
- 25 Insert Position Comparison for Plain Tubes

List of Figures (continued)

Figure No.

- 26 Insert Position Comparison for 6-Start Roped Tubes
- 27 Insert Position Comparison for 2-Start Roped Tubes
- 28 OHTC Performance of Plain Tubes with Various Steam Velocities
- 29 OHTC Performance of 6-Start Tubes with Various Steam Velocities
- 30 OHTC Performance of 2-Start Tubes with Various Steam Velocities
- 31 OHTC Performance for a Steam Velocity of 0.27m/s
- 32 OHTC Performance for a Steam Velocity of 0.37m/s
- 33 OHTC Performance for a Steam Velocity of 0.51m/s
- 34 Plain Tube Results Comparison for a Steam Velocity of 0.51m/s
- 35 Plain Tube Results Comparison for a Steam Velocity of 0.51m/s
- 36 Plain Tube Results Comparison for a Steam Velocity of 0.51m/s
- 37 Plain Tube Results Comparison for a Steam Velocity of 0.37m/s
- 38 Plain Tube Results Comparison for a Steam Velocity of 0.37m/s
- 39 Plain Tube Results Comparison for a Steam Velocity of 0.37m/s
- 40 Plain Tube Results Comparison for a Steam Velocity of 0.27m/s
- 41 Plain Tube Results Comparison for a Steam Velocity of 0.27m/s
- 42 Plain Tube Results Comparison for a Steam Velocity of 0.27m/s
- 43 Vapour Shear and Inundation Experimental Results Comparison
- 44 Experimental Results Comparison for 2-Start Roped Tubes
- 45 Experimental Results Comparison for 6-Start Roped Tubes
- 46 Experimental Results Comparison for Plain Tubes
- 47 Theoretical and Experimental Results Comparison for Plain Tubes
- 48 Theoretical and Experimental Results Comparison for 2-Start Roped
Tubes
- 49 Theoretical and Experimental Results Comparison for 6-Start Roped
Tubes

Chapter 1

General Introduction

1.1 Introduction

In today's business climate a company must continue to grow and expand in order to survive. To achieve this aim, companies must be run efficiently and have progressive plans with respect to investment. In the chemical and process industries and in power generation there is a large amount of capital investment and therefore it is vitally important that a company acquires equipment that will have a long and productive life.

One of the major plant components of the previously mentioned industries is the condenser. The primary function of a condenser is to change a substance from the vapour to the liquid state. In order to perform this task the condenser must move heat from one location to another and the rate at which heat is transferred can be found using the general equation:

$$\dot{Q} = \alpha A (\Delta T)_{\text{OVERALL}} \quad (1.1)$$

In industry there are a number of types of condensers, examples of which are the vertical tube condenser, the direct contact condenser, the flat plate condenser and the horizontal shell and tube condenser. However, of the various types mentioned the horizontal shell and tube condenser, shown in Fig. 1, is the most widely used. Typically steam is the medium which condenses on the outside of the horizontal tubes, with water being the cooling fluid flowing through the inside of the tube. In order to find the amount of heat transferred by a horizontal tube in a shell and tube type condenser a variation of Eqn. (1.1) is required.

$$Q = \frac{(\Delta T)_{\text{OVERALL}}}{\frac{1}{\alpha_i A_i} + \frac{L_N(ro/ri)}{2\pi L\lambda} + \frac{1}{\alpha_o A_o} + \frac{1}{\alpha_F}} \quad (1.2)$$

It can be seen from eqn. (1.2) that there are four ways in which the heat transfer rate (Q) can be increased. This can be achieved by increasing the heat transfer coefficient (α), the surface area (A), the thermal conductivity (λ) or the change in the overall temperature (ΔT). Several of the methods mentioned though, are either not cost effective or are impractical. For example, by increasing the surface area, more material is required for the unit. This leads not only to increased cost but also the condenser will occupy much more physical space in the plant, therefore it is desirable to keep the area as small as possible. The temperature in a condenser is usually governed by the process in which it is involved and usually it cannot be altered. To improve the thermal conductivity more expensive alloys would be needed, which again leads to increased cost. The most desirable way then, to improve the heat transfer rate was to concentrate on increasing the heat transfer coefficient.

There are a number of ways in which the heat transfer coefficient can be enhanced (discussed in section (1.2.2)). These techniques do improve the heat transfer coefficient, but have the drawback of an increased frictional pressure drop on the condenser tube. This pressure drop leads, unfortunately to increased cost through the requirement of larger pump capacity. However, included in section (1.2.2) was the use of roped or spirally indented tubes, shown in Fig. 2. It has been found, with respect to horizontal shell and tube condensers, that roped tubes provide a noteworthy enhancement in heat transfer compared to the increase in frictional resistance.

Recently Pearce^[44] carried out full scale tests using a condenser bundle of 400 roped tubes at the CEGB experimental facility at Leatherhead. There it was determined that with a suitable cleaning procedure, roped tubes provided

much greater heat transfer than similar plain tubes. Roped tubes also have the additional advantage that the grooving process does not appreciably alter the outside diameter of the tube. This was a benefit as it allowed roped tubes to be fitted into existing condenser end plates when a unit is re-tubed. This was part of the rationale used by Tate and Lyle in their recent decision to use roped tubes in several condensers being upgraded.

While the CEGB study^[44] has shown that enhanced tubes can provide greater heat transfer than plain tubes, the mandate of the study was not sufficiently wide to include the effect of phenomena commonly associated with condensers.

Examples of areas not investigated were the effects of non-condensable gases, vapour shear and condensate inundation. For the purposes of this investigation the effects of vapour shear and inundation will be concentrated upon as it has been shown^[22] that non-condensables cause a very large drop in heat transfer in condensers.

A number of studies carried out using single plain tubes have shown that vapour shear not only increases heat transfer^[2,3,4,5,6,8,9,10,11,13,14,15,16] but also alters the condensate film flow from laminar to turbulent or wavy flow^[5,23]. With respect to roped tubes and vapour shear a comparatively small amount of research^[30,41] has been carried out. Consequently very little was known about how vapour shear effects a single roped tube or a tube bundle.

The inundation effect in condensers has received more attention and as a result a better understanding existed. Using plain tubes it has been shown quite conclusively^[3,18,19,26,27,28,51] that the performance of a tube bundle was lower than that of a single tube. Unfortunately inundation and roped tubes was less well understood. While a number of studies have been carried

out[31,32,38,39], various types of tubes and experimental procedures were used making comparisons very difficult.

The combined effect of vapour shear and inundation was an area that had not been widely explored using either plain[27,28] or roped tubes[41]. Consequently it was this deficiency in understanding the effect of vapour shear and inundation on single tubes and tube bundles that the present investigation focused on. The results of the combined effect were expected to be very different from Nusselt's[1] original work on condensation. This was expected because in the development of the original theory Nusselt made several assumptions which gave conservative results, assumptions such as the condensate flow was laminar, flow between tubes was continuous and that interfacial shear was negligible.

These assumptions have since been shown not to be correct in all cases and because of this the results of the present investigation should prove to be very interesting. Unfortunately a direct theoretical solution to this problem was impossible, however through careful experimentation and an understanding of the physical processes involved useful data can be obtained and correlated to provide some insight into this complex problem.

1.2 Literature Survey

The literature reviewed for this investigation has been limited to the effects of vapour shear and inundation acting separately and together on horizontal condenser tubes. The flow of the vapour was vertical from the top of the condenser in the absence of non-condensable gases. Due to the low velocity of the steam (less than 5 m/s) the effects of the separation angle[46 to 49] were not included in the scope of the investigation.

In 1916, Nusselt^[1] presented the now classic paper on condensation on a vertical plane and a horizontal tube. This particular paper has been the source of much of the research in the field of condensation. During the development of the theory a number of assumptions were made and are listed as follows:

1. The wall temperature was constant.
2. The condensate film flow was laminar.
3. The heat transfer in the condensate was by conduction perpendicular to the condensate surface only and subcooling was neglected.
4. The fluid properties within the condensate layer were constant.
5. The hydrostatic pressure, surface tension, inertia forces and vapour/liquid interfacial shear were all considered negligible compared to the viscous and gravitational forces.
6. The surrounding steam and vapour/liquid interface were both at saturation temperature.
7. The thickness of the film was small compared with the tube diameter and the effects of curvature can be ignored.

Using these assumptions Nusselt was then able to develop formulae (the derivation of which has been omitted) for the condensing-side heat transfer coefficients for an inclined plane and a horizontal tube. The developed

equations were:

$$(i) \quad \text{Inclined plane} \quad \alpha = \left[\frac{g \lambda^3_f \rho_f (\rho_f - \rho_g) h_{fg} \text{SIN } \theta}{\mu_f L (T_s - T_{wo})} \right]^{1/4} \quad (1.3)$$

$$(ii) \quad \text{Horizontal tube} \quad \alpha = \left[\frac{g \lambda^3_f \rho_f (\rho_f - \rho_g) h_{fg}}{\mu_f D_o (T_s - T_{wo})} \right]^{1/4} \quad (1.4)$$

In carrying on Nusselt's original single tube work Bromley^[20] developed a correction for the enthalpy term which allowed for a more accurate calculation of the steam side h.t.c. Bromley concentrated on Nusselt's assumption that sub-cooling of the condensate could be neglected (assumption 3) and suggested that the enthalpy term (h_{fg}) in eqn (1.4) be replaced by the following expression:

$$h_{fg} \left(1.0 + 0.4 \frac{\Delta T C_p}{h_{fg}} \right)^2 \quad (1.5)$$

The above equation allowed for the effect of heat capacity of the condensate when calculating the h.t.c. Computer simulations were also carried out and it was determined that eqn (1.5) gave satisfactory results for $\Delta T C_p / h_{fg}$ values up to 3.0. The value of 3.0 represents, Bromley concluded, the most extreme value resulting from high pressure and a large temperature difference.

Rohsenow^[21] also examined Nusselt's original assumptions closely. Rohsenow determined, using a boundary layer analysis that the temperature difference through the condensate layer was non-linear. This discovery differed from Nusselt's assumption^[4], in that the fluid properties within the condensate were constant (and therefore constant temperature). In the course of the analysis it was also determined that the enthalpy term (h_{fg}) should be replaced

in eqn (1.4) with the following corrected equation:

$$h'_{fg} = h_{fg} + \frac{3}{8} C_p (T_s - T_{wo}) \quad (1.6)$$

The corrected enthalpy term, eqn (1.6), was subsequently substituted into eqn (1.4) to produce an equation that gave a more accurate description of the condensing-side h.t.c. performance. The developed equation was as follows:

$$\alpha_{NU} = \left[\frac{g \lambda_f^3 \rho_f (\rho_f - \rho_g) h'_{fg}}{\mu_f D_o (T_s - T_{wo})} \right]^{1/4} \quad (1.7)$$

1.2.1 Plain Tubes

1.2.1.1 Vapour Shear

One of the first groups of researchers to investigate the effects of vapour shear were Rohsenow, Webber and Ling^[2]. Nusselt's original force balance was reworked to include the effect of vapour shear and a new equation for the heat transfer coefficient was developed.

$$\alpha^* = \frac{4}{3} \frac{(\zeta_z^*)^3}{z^*} + 2 \frac{\tau^* (\zeta_z^*)^2}{z^*} \quad (1.8)$$

The equation was simplified to its present form by using dimensionless groups for film thickness (ζ_z^*), distance (z^*) and interfacial shear stress (τ^*). It was determined through experiments that as the vapour velocity increased, turbulent flow of the condensate resulted and that this caused the heat transfer rate to rise. A similar rise in the heat transfer rate was noted when the Prandtl number (Pr) increased. This then was the first piece of research work that showed increased vapour velocity not only produced turbulent condensate flow but also enhanced the heat transfer coefficient.

The first experiments on the effect of vapour shear using a bundle of tubes were carried out by Fuks^[3]. The bundle consisted of eleven 19mm Do copper tubes located within a rectangular duct. Steam was allowed to flow downward through the staggered bundle at pressures ranging from 0.048 to 1.066 bar. Measurements of the cooling water inlet and outlet temperatures and the mass flow rates were then recorded for the odd-numbered tubes. With this data, Fuks was able to show that a combination of temperature difference, steam velocity and the condensate discharge affect the heat transfer coefficient (α). Fuks also developed an empirical equation for the first row of tubes in a bundle which was:

$$\frac{\alpha}{\alpha_{NU}} = 28.3 \left(\frac{V^2 w \rho_g \alpha_{NU}}{g \lambda_f \rho_f} \right)^{0.08} (Nu)^{-0.58} \quad (1.9)$$

Although the literature survey was concerned with horizontal condenser tubes, research work carried out by Chung^[4] on vertical plates in a gravitational field has been found to be very relevant to this investigation. Chung studied the liquid layer and the liquid/vapour boundary layer simultaneously by matching the interface temperature, the shear stress and the mass transfer. By doing this Chung was able to determine the major controlling factors of condensation on a flat plate. Chung found these factors to be the ratio of density and viscosity of the gas to the liquid $(\rho_g \mu_g / \rho_f \mu_f)^{1/2}$, the ratio of the temperature potential to the heat of condensation, $(C_p \Delta T / Pr h_{fg})$, and the Froude number $Fr = V_w / \sqrt{gL}$. The discovery of these controlling factors was of great importance and they were used by other researchers^[8,9,10] at a later date, to develop further theory.

In a similar manner to work by Fuks^[3], Berman and Tumanov^[5] also carried out experiments using 19mm Do, copper tubes in a vertical row. The tube bundle in the experiments consisted of 4 tubes with an active tube (cooling water flowing through it) at the bottom of the bundle and non-active half tubes located on the sides of the test rig. The pressure of the steam used

varied from 0.032 to 0.48 bar with Reynolds numbers from 46 to 864 respectively.

From the data collected, Berman and Tumanov assumed that while the condensate film flow was purely laminar the heat transfer coefficient would not significantly increase until a given Reynolds number was reached. After this particular Reynolds number, the film flow would become turbulent and as a result there would be a rapid increase in the heat transfer coefficient. Also it was assumed that as the Reynolds number continued to increase, the increase in the heat transfer coefficient would be negligible. Unfortunately the experiments did not provide enough data to establish the range over which the change in the heat transfer coefficient took place and the assumption was not verified. However the following equation was developed from the data.

$$\frac{\alpha}{\alpha_{NU}} = 1 + 9.5 \times 10^{-3} Re^{11.8/\sqrt{NU}} \quad (1.10)$$

It was found that 95% of the experimental data points were within $\pm 10\%$ of the curve generated with eqn (1.10). This showed that the equation was an important step in explaining how vapour velocity (through the Reynolds number) affected the heat transfer coefficient. Also from the experimental results Berman and Tumanov drew the following conclusions:

- 1) The effect of velocity was much greater on the heat transfer coefficient than Nusselt predicted, even at very low Reynolds numbers of steam flow.
- 2) Increased steam velocity affected the heat transfer coefficient by inducing turbulent flow and decreasing the thickness of the condensate film.

- 3) The temperature gradient and steam velocity were interrelated so that the heat transfer coefficient was greatest when the temperature gradient was high and the vapour velocity was low.

In an attempt to provide general theory on surface condensers, Silver[6] studied the various phenomena which govern the condensation process. With respect to vapour shear Silver replaced Nusselt's fifth assumption (interfacial liquid/vapour shear is negligible) with the correction factor;

$$r^2 = \frac{1}{r} + \frac{3(E_{M_f} + M_f)V_w \alpha_o}{2g \lambda_f \rho_f} \quad (1.11)$$

The outside h.t.c. term (α_o) was found with eqn (1.4) and then multiplied by eqn (1.11) to give the corrected outside h.t.c. which was then used to find the heat transfer rate in the normal manner (i.e. use of eqn (1.2)).

Up until this point the research carried out on vapour shear has concentrated on the heat transfer coefficient of a single tube. Berman[7] was the first to attempt to find the effect of vapour shear on an entire tube bundle. Using data generated previously[3,5] at the Soviet Thermal Power Institute (VTI) Berman derived several expressions. These expressions were for the velocity of the vapour between the tubes in the bundle, eqn. (1.12) and the vapour flow rate, eqn (1.13).

$$f(V_n) = B \left(\frac{V^2 N \gamma g}{g D_o \gamma_f} \right)^{m/2} \left(\frac{\gamma_f h_{fg} D_o^3}{\lambda_f \mu_f \Delta T} \right)^s \quad (1.12)$$

$$f(\Delta) = \frac{\Delta}{1 - (1 - \Delta)^{1-m}} \quad (1.13)$$

Using the heat transfer coefficient α_{NU} , eqn. (1.7), the number of vertical rows of tubes (N) in the bundle and the above expressions it was possible to determine the heat transfer coefficient for the tube bundle.

$$\alpha = \alpha_{NU} f(V_{\Gamma}) f(\Delta) \frac{0.84}{N^{0.07}} \quad (1.14)$$

In a theoretical analysis of a horizontal cylinder located in the path of flowing steam, Shekrladze and Gomelauri^[8] made several assumptions that led to the development of new equations. Shekrladze and Gomelauri assumed that the effect of the pressure gradient around the periphery of the cylinder could be neglected in comparison to the momentum transferred, and that outside of the vapour boundary layer the velocity field obeys the potential flow laws around a cylinder. Two other assumptions were that the vapour boundary layer was laminar up until the point of separation and that the inertia forces can be neglected. These general assumptions were then used to derive equations for the heat transfer coefficient and the Nusselt number when the effects of gravity are both present and absent. The following two equations (1.15 and 1.16) were applicable when gravity was absent:

$$\alpha = 0.9 \left(\frac{\lambda_f^2 \rho_f V_W}{\mu_f D_o} \right)^{1/2} \quad (1.15)$$

$$N_u = 0.9 \left(\frac{\rho_f V_W D_o}{\mu_f} \right)^{1/2} \quad (1.16)$$

When gravity was included in the calculations, equations (1.17 and 1.18) were relevant.

$$\alpha = 0.64 \left(\frac{\lambda_f^2 \rho_f V_W}{\mu_f D_o} \right)^{1/2} \times \left(1 + \left(1 + \frac{1.69 g D_o}{V_W^2 \left(\frac{C_p \Delta T}{P_r h_{fg}} \right)} \right)^{1/2} \right)^{1/2} \quad (1.17)$$

$$Nu = 0.64 \left(\frac{\rho_f V_w D_o}{\mu_f} \right)^{1/2} \times \left(1 + \left(1 + \frac{1.69}{\left(\frac{V_w^2}{g D_o} \right) \left(\frac{C_p \Delta T}{P_r h_{fg}} \right)} \right)^{1/2} \right)^{1/2} \quad (1.18)$$

The results calculated using eqn. (1.17) were compared to experimental results[5] for various pressures and most of the theoretical data was within $\pm 10\%$ of the experimentally generated curve. This theoretical investigation concluded that the greater the temperature difference between the steam and the tube wall, the greater was the effect of vapour velocity upon the h.t.c. It was also determined that the h.t.c. was greater when the vapour was moving as compared to when the vapour was virtually stagnant. These statements agree closely with conclusions reached by Fuks[3] as a result of experimentation.

Fujii et al[9] carried out a theoretical analysis of the condensation process, similar to Shekrladze and Gomelauri[8] using two-phase boundary layer equations. It was assumed in this study that outside the vapour boundary layer, the flow of steam was potential and could be expressed as $2V_w \sin \theta$. Using this assumption and theory by Chung[4] the following general expression was derived.

$$Nu = X \left(1 + \frac{0.276}{X^4 \left(\frac{V_w}{g D_o} \right) \left(\frac{C_p (T_s - T_{wo})}{P_r h_{fg}} \right)} \right)^{1/4} Re^{1/2} \quad (1.19)$$

where

$$X = 0.9 \left(1 + \frac{1}{\left(\frac{\rho_g \mu_g}{\rho_f \mu_f} \right)^{1/2} \left(\frac{C_p \Delta T}{P_r h_{fg}} \right)} \right)^{1/3} \quad (1.20)$$

For the case of very high vapour velocities (up to 70 m/s) a specific form of the general equation was developed.

$$Nu = 0.9 \left(1 + \frac{1}{\left(\frac{\rho_g \mu_g}{\rho_f \mu_f} \right)^{1/2} \left(\frac{C_p \Delta T}{Pr h_{fg}} \right)} \right)^{1/3} \left(\frac{\rho_g V_w D_o}{\mu_g} \right)^{1/2} \quad (1.21)$$

where

$$\left(\frac{\rho_g \mu_g}{\rho_f \mu_f} \right)^{1/2} \left(\frac{C_p \Delta T}{Pr h_{fg}} \right) < 10$$

The theoretical results of eqn (1.19) were found to compare favourably with experimental results by Berman and Tumanov[5]. As a result of the study it was concluded that the local heat transfer coefficients increased as the vapour velocity increased and that approximately 80% of the total condensation took place on the upper half of the tube. Also it was concluded that, unlike [5], the influence of turbulence on the liquid film with respect to increasing the h.t.c. was small.

Shekrladze[10] also used two-phase boundary equations to theoretically describe the effects of flowing vapour on the condensing-side heat transfer coefficient. The ensuing equation, eqn (1.22), was similar in form to previous theory [3,5] in that it used Nusselt's[1] original equation in the form of a ratio:

$$\frac{\alpha}{\alpha_{NU}} = 0.833 (\pi)^{1/4} (1 + s)^{1/3} \left(1 + \left(1 + \frac{1.69}{\pi(1 + s)^{4/3}} \right)^{1/2} \right)^{1/2} \quad (1.22)$$

Shekrladze also found that when the π term was less than 10, the above equation could be reduced to the following equation:

$$\frac{\alpha}{\alpha_{NU}} = 1.25 \pi^{1/4} (1 + s)^{1/3} \quad (1.23)$$

After conducting a review of past theory with respect to vapour shear, Berman[11] developed a much simpler equation for steam pressures varying from 0.03 to 1.0 bar.

$$\frac{\alpha}{\alpha_{\text{NU}}} = a + b \text{ LOG } (\pi) \quad (1.24)$$

The developed equation, eqn (1.24), was used over the range $0.01 < \pi < 20$ with the constants, ($a=1.28$ and $b=0.28$) which were extrapolated from previous work[5,45].

Kutateladze et al[12] also attempted to determine, like Berman[7], the effects of vapour shear on the performance of a tube bundle. The experiments were carried out using both in-line and staggered bundles of 16mm Do nickel tubes with freon (F-21, CHFCl_2) as the flowing vapour to be condensed. Although the present investigation was concerned primarily with steam a number of very important conclusions were drawn and for this reason was included in the literature. From the experimental results, Kutateladze et al. determined that the heat transfer coefficient depended on the number of tubes in the bundle, the vapour velocity and the temperature difference between the flowing vapour and the tube wall. Also it was determined that channel geometry (staggered or in-line) had little influence on the heat transfer coefficient. When the difference in temperature between the tube wall and the flowing vapour was high, vapour velocity was found to have less of an affect on the heat transfer coefficient than when the temperature difference was low. However, the most important discovery was that at high vapour velocities each tube in the bundle could be regarded as independent and because of this the heat transfer coefficient could be calculated using single tube formulae that included the effects of vapour velocity.

Fujii[13] developed an equation, eqn (1.25), that included the effects of vapour shear by using a dimensionless parameter, π , and a two-phase Reynolds number (Re_{TP}).

$$\frac{Nu}{\sqrt{Re_{TP}}} = \left(1.0 - \frac{0.27 (5/\pi)^{1/2} - 1.0}{(5/\pi)^{1/2} + 1.0} \right) \left(\frac{1}{\pi} \right)^{1/4} \quad (1.25)$$

The results of this theoretical equation compared favourably with previous data[49] and several conclusions were drawn. Fujii concluded that dimensionless terms, such as π , should be used in calculations as they allow for easy comparisons to be made. It was also concluded that the mainstream velocity should be used in calculations and that the direction of flow matters little in comparison to the profile of the velocity (i.e. mainstream velocity around the tube/oncoming vapour velocity).

Lee and Rose[14], analysed single horizontal tubes in a similar manner to Shekrladze and Gomelauri[8]. However, Lee and Rose included the effect of surface shear stress (τ) and assumed that the velocity at the liquid-vapour interface was smaller than the vapour velocity at the edge of the vapour boundary layer. Two equations were developed for when there was no separation of the condensate from the tube and a constant heat flux. When the effects due to gravity were neglected eqn. (1.26) should be used and when gravity was included eqn. (1.27) was appropriate.

$$\frac{\bar{Nu}}{\sqrt{Re_{TP}}} = 0.77 \quad (1.26)$$

$$\frac{\bar{Nu}}{\sqrt{Re_{TP}}} = 0.544 \left(1.0 + \left(1.0 + 1.63 \left(\frac{gh_f g (\frac{\rho_f \mu_f D_o}{v_w})^{1/2}}{q} \right)^{4/3} \right)^{1/2} \right)^{1/2} \quad (1.27)$$

The developed equations showed very good agreement with eqns (1.16) and (1.18) indicating that the original analysis carried out by Shekrladze and Gomelauri was correct.

Using an asymptotic approximation for shear stress and assuming that the pressure gradient around the tube was unimportant, Rose[15] also investigated the effects of vapour shear on a single horizontal tube. In developing eqn. (1.28) dimensionless groups were used, as previously mentioned by Fujii[13], to simplify the equations and to facilitate easy comparisons with other work.

$$\frac{\text{Nu}}{\sqrt{\text{Re}_{\text{TP}}}} = \frac{0.9 \left(1 + \frac{1}{G}\right)^{1/3} + 0.728 \left(\frac{1}{\pi}\right)^{1/2}}{\left(1.0 + 3.44 \left(\frac{1}{\pi}\right)^{1/2} + \frac{1}{\pi}\right)^{1/4}} \quad (1.28)$$

The equation was then used to generate numerical solutions which were found to compare very favourably with the experimental results of Shekrladze and Gomelauri[8].

In a recent theoretical analysis by Uehara and Dilao[16], correlations developed by Fujii[9,13] and Rose[15] were used to determine the O.H.T.C. for horizontal tube condensers. Computations were carried out using eqn's (1.19), (1.25) and (1.28) with various working fluids in order to determine which of the correlations gave the best performance.

To obtain the largest amount of data possible the velocities of the fluids (Freon -113, Freon - 114, Freon - 22, NH₃ and steam) were varied from 1.0 to 3.0 m/s. Also the fluids were to condense on a brass tube of 1mm wall thickness with a diameter and length that ranged from 10.0 to 30.0mm and 500 to 1500mm respectively. The results of the computer simulations for the correlations were compared with one another and in the case of steam the

results were contrasted with data from HEI[50]. This led Uehara and Dilao to make the following conclusions:

1. With respect to freon (at moderate velocity) all three equations gave higher O.H.T.C. values than Nusselt's predictions. Equation (1.19) gave the best results followed in order by eqn's (1.28) and (1.25).
2. Using the greatest vapour velocity (3.0 m/s) in the simulations, eqn's (1.19) and (1.28) gave much higher O.H.T.C. values than equation (1.25).
3. All of the equations had higher O.H.T.C. values, for steam, than Nusselt's prediction which was in turn higher than the values from HEI.
4. At low vapour velocities, eqn (1.28) was found to have O.H.T.C. values lower than Nusselt's predictions.

1.2.1.2 Inundation

In examining Nusselt's original theory, Jakob[17] suggested that eqn (1.4) could be successfully modified to provide the average h.t.c. for a vertical row of N condenser tubes. When the modified equation, eqn (1.29), was divided by Nusselt's original equation, eqn (1.4), an expression for the average h.t.c. of a

$$\alpha = 0.725 \left(\frac{g \lambda_f^3 \rho_f (\rho_f - \rho_g) h_{fg}}{\mu_f D_o (T_s - T_{wo}) N} \right)^{1/4} \quad (1.29)$$

vertical row of N tubes (α_N) with respect to the top tube (α_{Nu}) was determined;

$$\frac{\alpha_N}{\alpha_{Nu}} = (N)^{-1/4} \quad (1.30)$$

as shown by eqn (1.30). In order to find the h.t.c. for a given tube in the vertical row of N tubes the following equation could be used:

$$\frac{\alpha_N}{\alpha_{Nu}} = N^{3/4} - (N - 1)^{3/4} \quad (1.31)$$

It is important to note that during the derivation of eqn's (1.29), (1.30) and (1.31) it was assumed that the condensate flowed as a continuous laminar sheet from one tube to another in the vertical row. However, it has been shown that these equations underestimate the heat transfer rate^[18,51]. The probable cause of the underestimation was that the flow of condensate has been shown to splash between tubes and have a rippled or wavy flow^[5,23] while on the tube surface.

Short and Brown^[19] studied the effects of both Freon - 11 and steam as the fluids condensed through a horizontal bundle of tubes. The bundle consisted of 21 brass tubes, with 12.5mm Do, which were arranged in a vertical row. The results of the experiments were correlated and an empirical expression was developed, eqn (1.32) which related the heat transfer coefficient to the amount of condensate generated on, and falling from a given tube in the bundle.

$$\frac{\alpha_N}{\alpha_{Nu}} = \left(\frac{\sum \dot{M}_c}{M_{cN}} \right)^{-1/4} \quad (1.32)$$

Using a bundle consisting of staggered 19mm Do tubes, Fuks^[3] was the first to determine an expression for the effect that recycled condensate had on the heat transfer coefficient. This was carried out by collecting the condensate and draining it as evenly as possible over one of the top tubes in the bundle. The expression developed as a result of these experiments, eqn. (1.33), had a

very different exponent than the previously

$$\frac{\alpha_N}{\alpha_{Nu}} = \left(\frac{\sum \dot{M}c}{Mc_N} \right)^{-0.07} \quad (1.33)$$

developed eqn. (1.32). The differences in the equations was probably due to the different condensate flow pattern in the staggered bundle used by Fuks, as opposed to the in-line bundle used by Short and Brown and that condensate water was recycled over the tubes.

Labuntsov[23] carried out experiments using single horizontal tubes and developed several equations to explain how wavy flow of the condensate affected the h.t.c. The developed equations could only be used when the following condition with respect to tube diameter, eqn (1.34), was satisfied.

$$Do > 20 \left(\frac{\sigma}{g \rho_f} \right)^{1/2} \quad (1.34)$$

The first of the two equations, eqn (1.35), involved correction factors which were multiplied with eqn (1.7). These factors accounted for the effects of

$$\alpha = \alpha_{Nu} \psi \epsilon_t \epsilon_v \quad (1.35)$$

convective heat transfer and inertia forces (ψ), the physical characteristics (ϵ_t) and the effect of wavy flow (ϵ_v) in the condensate film. The second of the developed equations, eqn. (1.36), only considered how wavy flow affected the average h.t.c. (α).

$$\frac{\bar{\alpha}}{\alpha_f} \left(\frac{\delta_f^2}{g} \right)^{1/3} = 1.205 Re_f^{-1/3} \left(\left(\frac{\lambda_{fwo}}{\lambda_f} \right)^3 \frac{\mu_f}{\mu_{fwo}} \right)^{0.167} \quad (1.36)$$

Using tubes with outside diameters ranging from 20mm to 49.3mm and fluids such as benzene, ammonia, Freon - 12 and acetone it was shown that the derived expressions, eqn's (1.35) and (1.36), gave good agreement with the experimentally obtained data.

All of the developed equations mentioned thus far have come about from laboratory experiments. Kerns[24] recommended the following equations based on experience gained from operating industrial condenser units.

$$\frac{\bar{\alpha}_N}{\alpha_{Nu}} = (N)^{-1/6} \quad (1.37)$$

and

$$\frac{\bar{\alpha}_N}{\alpha_{Nu}} = N^{5/6} - (N - 1)^{5/6} \quad (1.38)$$

These equations were of a similar form to those developed by Jakob (eqns. (1.30) and (1.31)) and although little attempt has been made to compare (eqns. (1.37) and (1.38)) to experimental data, these equations were generally considered the best for inundation applications as a result of Kerns' experience.

After initial work with flat plates, Chen[25] carried out a theoretical analysis of laminar film condensation using single tubes and tube bundles. In the analysis, Chen considered the effects of heat capacity and acceleration of the condensate but assumed, as Nusselt did, that the condensate flowed in a continuous sheet between tubes. The developed theory, eqn. (1.39), was compared to existing data[18, 19]

$$\frac{\bar{\alpha}_N}{\alpha_{\infty}} N^{1/4} = \left(1 + 0.2\zeta (N - 1) \right) \left(\frac{1.0 + 0.68\zeta + 0.2\zeta^2}{1.0 + 0.95\zeta - 0.15\zeta^2} \right)^{1/4} \quad (1.39)$$

and satisfactory agreement was found.

Grant and Osment[26] carried out experiments similar to those of Fuks[3], which involved recycling condensate water through a tube bundle. The bundle consisted of 139 staggered tubes of 19.05mm Do. An empirical relationship, eqn. (1.40), was determined from the recorded data which related the mass flow of

$$\frac{\alpha_N}{\alpha_{Nu}} = \left(\frac{\sum \dot{M}_C}{M_{CN}} \right)^{-0.223} \quad (1.40)$$

condensate to the h.t.c. of the Nth tube in the bundle. As can be seen, eqn. (1.40), was similar in form to both eqns (1.32) and (1.33). However as the equation was closer in agreement to eqn. (1.32) than eqn. (1.33) it lent more support to the work of Short and Brown than Fuks.

1.2.1.3 Vapour Shear and Inundation

In an attempt to determine the effects of vapour shear and inundation, Nobbs[27] and Nobbs and Mayhew[28] carried out experiments on both a single tube and a tube bundle. Realizing that a direct theoretical approach was impossible, the test program was set up to provide data on both the combined effect of vapour shear and inundation, and on the effect of vapour shear and inundation acting independently of one another. The tests were conducted using 19.05mm Do copper tubes which were arranged in both the in-line and staggered bundle configurations with a mass flow of steam ranging from 0 to 25 kg/s. The results of the bundle experiments were more relevant to the present investigation than the single tube work as the single tube work emphasised the effects of separation which were, as previously stated, beyond the scope of this thesis. Using the collected tube bundle data the following conclusions were reached:

1. Vapour velocity was found to increase the h.t.c. on tubes in a tube bank when inundation was present and also when inundation was not present.

The increase in the h.t.c. as a result of vapour shear was also found to be larger (than the zero velocity case) as the heat flux increased.

2. Inundation generally reduced the h.t.c. of the tubes in the tube bank. The reduction in the h.t.c. due to inundation was found to decrease as the vapour velocity was increased.
3. The path of the condensate as it drained through the bundle was often found to be diagonal instead of vertically downward. This resulted in some tubes receiving a large amount of inundation.

1.2.2 Enhancement Methods

The drive for efficiency, in modern industry, has been the catalyst for research into methods of improving heat transfer. As a result, a number of methods of enhancing heat transfer in condenser tubes have been developed. The various methods have been arranged, by Bergles^[29] into three categories, which were a) passive methods, b) active methods, and c) compound methods.

a) Passive Methods

Passive Methods of improving heat transfer encompass the following:

- Treated surfaces
- Rough surfaces
- Extended surfaces
- Enhanced tubes
- Displaced enhancement devices
- Swirl flow devices
- Coiled tubes
- Surface tension devices

- Additives for liquids
- Additives for gases.

b) Active Methods

Active Methods include:

- Mechanical aides
- Surface vibration
- Fluid vibration
- Electric or electromagnetic fields

c) Compound Methods

Compound methods of heat transfer enhancement consisted of a combination of any of the previously mentioned passive or active methods.

All of the methods mentioned improve heat transfer, however the most practical methods were to be found in the first section (i.e. Passive Methods). With respect to horizontal shell and tube type condensers, roped or spirally indented tubing has been found to be particularly effective and should be investigated further.

1.2.2.1 Method of Roped Tube Enhancement

Dropwise and filmwise condensation were the two types of condensation that could occur when steam passed over the surface of a condenser tube. In industrial condensers filmwise condensation was more common and as the name suggests a thin layer or film of condensate water formed on the tube surface. This condensate layer acted as a resistance to the transfer of heat from the steam to the cooling water passing through the tube, and therefore

anything that could be done to reduce this resistance was beneficial. Using fluted tubes (Note: The ridges or profiles of a fluted tube run longitudinally along the entire length of the tube. When used to condense vapour, fluted tubes are mounted vertically inside a condenser and the condensate water runs the length of the tube, (usually from top to bottom)). Gregorig^[42] carried out a force balance between the pressure gradient, due to surface tension forces, and the viscous forces on an element of the condensate film. Gregorig showed that the heat transfer coefficient for the condensate film was much greater for the fluted tube as compared to a plain tube. A similar pattern of increased heat transfer was found to exist for horizontal roped tubes.

The increase in the heat transfer coefficient for the profiled tubes was found to be a combination of enhancement taking place on both sides of the tube wall, and as a result the various phenomena shall be explained separately.

As was previously mentioned, the surface tension of the condensate film on the outside of the fluted tube wall provided a pressure gradient. On the crest of the profile (point (1) in Fig. 3) an area of high pressure compared to the pressure of the vapour to be condensed was formed as a result of the convex shape. In the trough of the profile (point (2) in Fig. 3) a low pressure zone was created due to the concave shape. This difference in pressure induced the condensate to flow from the crest to the trough of the profile. When this occurred the film thickness on the crest of the profile was very thin and a high local heat transfer coefficient resulted. With respect to the trough, a low heat transfer coefficient was generated as the condensate flowed from crest to trough of the profile. However, the average heat transfer coefficient over the entire tube was much greater than the h.t.c. of a similar plain tube.

On the inside of the tube, the indented ridges promoted turbulence by breaking up the laminar sub-layer formed by the cooling water flow. This generated turbulence in turn led to an increase in the convective heat transfer inside the tube. Although the heat transfer was enhanced, the indentations also increased the pressure drop of the coolant as it flowed through the tube, resulting in higher pumping costs. However, in view of the larger heat transfer coefficient the pressure drop was considered a minor penalty.

It should be noted that although the methods of enhancement that take place in a roped tube are well understood a direct theoretical solution for every type of roped tube was unavailable.

Such a solution was impossible due to the variable geometric characteristics of the individual tube. To produce a given roped tube, the manufacturer began with an equivalent plain tube (of a given wall thickness) onto which a number of grooves or starts were indented. These grooves could have various indentation depths (t), helix angles (θ) or pitches (p) as shown in Fig. 4. Depending upon customer preference these characteristics could be changed to suit a particular need. The indentation depth, for example, could be made deeper or shallower to provide greater or smaller local heat transfer coefficients. The helix angle could also be altered. A small helix angle provided a short path for the condensate to flow along. This short flow path allowed the condensate to flow quickly from the tube as compared to a long flow path, generated by a large helix angle, which tended to hold the condensate on the tube for a longer period of time. If the pitch was decreased on a roped tube, more flow channels would be created over the length of the tube allowing for faster removal of the condensate and more local areas of high and low heat transfer giving the tube a better overall heat transfer rate.

With the combination of wall thickness, tube material, the number of starts, groove depth, pitch and helix angle it could be readily seen why comparing the results of experiments was very difficult.

1.2.3 Roped Tubes

1.2.3.1 Vapour Shear

Eissenberg et al^[30] were the first researchers to conduct experiments to determine how roped tubes were affected by various steam velocities. The tests were carried out as part of a larger experimental programme that investigated the effects of steam temperature, mass velocity, non-condensable gases, condensate rain, log mean temperature difference and cooling water velocity. The 3-start, 25.4mm Do enhanced tubes were mounted in a staggered bundle consisting of 163 tubes with 3 spray tubes located at the top of the bundle to simulate inundation. The steam mass velocity was varied from 500 - 12500 kg/hr -m² and it was important to note that the steam flowed horizontally across the copper-nickel alloy tubes as opposed to vertically downward over the tubes.

The resulting experimental data led to the following conclusions:

1. The top tubes in the tube bundle were generally unaffected by steam velocity.
2. The increase in the condensing side h.t.c. was greater for tubes lower down in the bundle and was found to be 25% greater than values predicted using Nusselt's theory.
3. There was an increase in the amount of condensate carry over as the steam velocity increased.

4. The water side h.t.c. was found to be 100% higher than values predicted using the Dittus-Boelter equation.

Although the experiments were carried out using steam that flowed horizontally across the tube bundle, the results show that steam velocity does have an effect on the condensing side h.t.c. of roped tubes.

1.2.3.2 Inundation

Using staggered tube bundles, Withers & Young^[31] compared the performance of 1-start roped tubes with similar plain tubes. The two types of tubes used in the experiments had outside diameters of 15.9mm and 25.4mm and were made of copper and 90-10 copper-nickel respectively. In order to obtain a variety of data two steam temperatures, 38°C and 100°C, were used. The data showed that, under isothermal conditions, the pressure drop inside the roped tubes was 5 times that of the plain tubes. No enhancement was recorded on the condensing side of the tubes but on the water or tube side the h.t.c. for the 15.9mm and 25.4mm Do tubes was found to be 2.7 times and 2.2 times greater respectively, than the corresponding plain tubes. It was concluded from the design study that roped tubes could be used to provide significant savings in cost by reducing the condenser length, tubing weight and the number of tubes in the bundle.

Catchpole and Drew^[32] studied the effect of geometry on the performance of roped tubes. The five types of tubes used in the experiments all had a 15.9mm Do and were made of 70-30 copper-nickel but each tube had a different groove depth and groove pitch. Tests were carried out on single tubes and tube bundles with a cooling water velocity of 3.05m/s and a steam pressure of 0.14 bar.

When the results of the single roped tube experiments were compared to the results of the plain tubes, it was determined that there was a 40% improvement in heat transfer. With respect to the tube bundles the roped tubes showed a 25% to 50% improvement over the plain tubes. Associated with the increase in heat transfer was an increase in the friction factor for the roped tubes. An increase of 33% to 264% was recorded for the friction factor of the roped tubes as compared to the plain tubes.

Catchpole and Drew concluded that the helix angle of the grooves greatly affected condensate drainage. A large helix angle was found to slow the drainage of the condensate by increasing the groove length from the top of the tube to the bottom. A small helix angle had the opposite effect and promoted condensate drainage. The following relation was also developed using a multiple regression analysis and the collected data.

$$\frac{\alpha_r}{\alpha_p} = 1.17 (We \cos \theta)^{0.076} \quad (1.41)$$

It can be seen from eqn (1.41) that in order to provide enhancement over the plain tubes a small helix angle (θ) and a large Weber number (We) would be required.

Cunningham & Milne^[33] also investigated the effect of helix angle on the performance of profiled tubes. The tubes used in the experiments all had 13mm Do and were made of aluminium brass. The roped tubes had the same pitch but the helix angle of the 2-start tubes was 18° and that of the 6-start tubes was 44°. The friction factor for the tubes was determined using the fanning friction equation, eqn. (1.42), and by measuring the cooling water inlet and outlet temperatures, the water side pressure drop and cooling water flow rate.

$$\Delta P = \frac{2\rho V_w^2 f L}{D_i} \quad (1.42)$$

When the results of the profiled tubes were compared with those of the plain tube it was determined that the 2-start tube had the highest resistance to the cooling water flow and that the lower the helix angle the greater the turbulence and pressure drop. With this information the following conclusions were drawn:

1. Roped tubes gave much better heat transfer performance than equivalent plain tubes but at the expense of increased pumping costs.
2. The heat transfer of roped tubes increased with a decrease in helix angle for tubes with identical ratios of indentation/diameter and pitch/diameter.

Mimura and Isozaki^[34] sought to determine how the tube side pressure drop off affected the heat transfer of roped tubes. Tests were carried out using steam at atmospheric pressure on both plain and profiled tubes made of 90-10 copper-nickel, with 15.88mm Do and 0.9mm wall thickness. The roped tubes had 1 to 3 starts or grooves, pitches ranging from 7 to 13mm and indentation depths between 0.9mm and 1.1mm. The results showed that the h.t.c. and the pressure drop for the profiled tubes were both greater than for the equivalent plain tubes and that this was caused by the pitch (p), indentation depth (t) and the number of starts or grooves. The tube side h.t.c. was found to be proportional to the expression $(p/D_i - 0.42)^{-0.15}$ with a maximum value at t_i/D_i equal to 0.05. The friction factor (f) inside the tubes was found to decrease as the number of grooves increased and was proportional to the following two expressions: $(t_i/D_i)^{1.52}$ and $(P/D_i)^{-0.94}$. Finally it was concluded that the pressure drop in the profiled tubes increased the water side h.t.c. and was proportional to the expression $(\Delta P/L)^{0.41}$.

Mehta and Rao^[35] also investigated the effect of geometry on the performance of enhanced condenser tubes. Using a single tube condenser unit, steam at atmospheric pressure was condensed on aluminium tubes with a 19.51mm Do and 1.8mm wall thickness. A plain tube was used as a comparison for the results generated from the 11 enhanced tubes, all of which had different pitch to depth ratios ($4.5 < p/t < 48.8$). In order to derive correlations for tube performance, a simplifying geometric expression was developed. This expression was known as the "severity factor", equation (1.43)

$$\phi = \frac{t_i^2}{pD_i} \quad (1.43)$$

The severity factor was then used to develop equations for the inside friction factor, the tube side h.t.c. and the condensing side heat transfer coefficient. Also it was used to explain the results of various experiments, all of which took place in the range of Reynolds numbers (Re) from 10,000 to 80,000. The experiments showed that all the enhanced tubes had an improvement, with respect to heat transfer, over the plain tube. Most of the h.t.c. values were also found to be 15% to 20% greater than h.t.c. values found using Nusselt's original theory. The water or tube side h.t.c. was found to increase continuously as the groove depth increased, showing that as the turbulence inside the tube increased so did the amount of heat transferred. Mehta and Rao concluded that for the condensing side, groove depth and groove pitch were not sufficient criteria to predict the best possible h.t.c., implicitly suggesting that some other parameters should be included.

Marto et al^[36] carried out experiments similar to those of Mehta and Rao. The five enhanced tubes (made from aluminium, copper-nickel or titanium), each with 1-start or groove and a 15.9mm Do were tested and the results compared to a similar plain tube. Each enhanced tube had a different helix angle, groove depth and pitch to generate a wide range of data. The results however, for the

condensing side h.t.c. were quite different than those of Mehta and Rao. Marto et al found that for 4 of the 5 enhanced tubes the condensing side h.t.c. was approximately 10% below that of the plain tube. The titanium tube was the only enhanced tube to have better condensing side h.t.c. results and this was a 35% improvement over the plain tube. It was also determined that most of the enhancement occurred on the tube or waterside and that an increase in pressure drop accompanied this enhancement. This later conclusion was in line with previous work^[31,32] carried out using single tube horizontal condensers.

Sethumdhavan and Rao^[37] used 5 enhanced tubes with the same helix angle ($\theta = 65^\circ$) but with different groove depths and number of starts to carry out experiments, similar to those of Mimura and Isozaki^[34], to determine the effect of turbulent cooling water flow on heat transfer.

The enhanced tubes were made of copper and had 1 to 4 starts. The results of the experiments showed that the enhanced tubes provided an improvement in the water side h.t.c. of 15% to 100% with an associated increase in the friction factor (f) in the order of 30% to 200% as compared to a plain tube. The tube that gave the greatest enhancement over the plain tube was found to have 4 starts and the highest ti/p ratio. The conclusions for single tubes that most of the enhancement takes place on the waterside and that roped tubes provide higher heat transfer coefficients were in line with the findings of previous papers^[33,34,35].

Baghernejad^[38] attempted to predict the increase in both the heat transfer rate and the friction factor of roped tubes over plain tube values under similar operating conditions. Correlations were derived for the condensing side and water side heat transfer coefficients to obtain insight into the behaviour of the entire system.

In order to develop theory for the condensing or steam side of an enhanced tube, Baghernejad made a number of simplifying assumptions which were as follows:

1. The outside surface of the roped tube consists of a succession of flat and valley regions (shown in Fig. 5).
2. The axial cross-section of the grooves approximates the arc of a circle (Fig. 5).
3. The grooves take the shape of repeated rings with the same helix angle instead of being in the shape of a helix turning around the tube.
4. The condensate was distributed on a roped tube such that the distance from the centre of the cross-section of the tube to the surface of the condensate film, at any given angle, was constant.

Using these assumptions, the Nusselt number for the non-groove sections (Nu_{NG}) of the roped tube was derived. The resulting single tube equation, eqn. (1.44), made use of the Nusselt number for an equivalent plain tube (Nu_p), shown in eqn. (1.45) and the various outside geometric characteristics such as groove width (W_o), groove depth (t_o) and pitch (p).

$$Nu_{NG} = \frac{1.0}{-0.5 + \left| 0.25 - \frac{2}{3} \left(\frac{W_o}{p} \right)^2 \frac{t_o}{D_o} \left(1 - \frac{2}{3} \frac{t_o}{D_o} \frac{W_o}{p} \right) + \frac{Nu_p + 1.0}{Nu_p^2} \right|^{1/2}} \quad (1.44)$$

In calculating the Nusselt number for the plain tube (Nu_p) eqn (1.7) was used.

$$Nu_p = \alpha Nu \frac{D_o}{\lambda f} \quad (1.45)$$

With eqn (1.44) the helix angle θ and the previously mentioned geometric characteristics, it was then possible to develop an expression for the average Nusselt number of a single roped tube (Nu_r) which was as follows:

$$Nu_r = Nu_{NG}(\cos \theta)^{1/3} \left(\frac{1.0 + Nu_{NG} \frac{t_o}{Do} \frac{Wo}{p} \left(1.0 - \frac{Wo}{p}\right)}{1.0 + Nu_{NG} \frac{2}{3} \frac{t_o}{Do} \frac{Wo}{p}} \right) \quad (1.46)$$

An enhancement factor, eqn. (1.47), was arrived at by dividing eqn. (1.46) by eqn. (1.44), making it possible to express the amount of enhancement that resulted from the roped tube as compared to a plain tube for the same operating conditions.

$$EF = \frac{Nu_r}{Nu_p} \quad (1.47)$$

Using the same method Baghernejad developed equations for a bank of roped tubes. The term Nu_p , in eqns. (1.44) and (1.45), was changed to Nu_{pN} to represent the N^{th} equivalent tube in a plain tube bundle. To evaluate the new term (Nu_{pN}) it was first necessary to evaluate the heat transfer coefficient (α_N) in eqn (1.45) using one of the tube bundle equations found in section (1.2.1.2). Once the h.t.c. (α_N) was found it was then possible to determine the Nu_{pN} term, as shown in eqn. (1.48)

$$Nu_{pN} = \alpha_N \frac{Do}{\lambda f} \quad (1.48)$$

The equivalent plain tube bundle equation, eqn. (1.48), was then used to find a new expression for the Nusselt number of the non-grooved section of the

roped tube (Nu_{NGN}), which was as follows:

$$Nu_{NGN} = \frac{1.0}{-0.5 + \left(0.25 - \frac{2}{3} \left(\frac{Wo}{p}\right)^2 \frac{to}{Do} \left(1 - \frac{2}{3} \frac{to}{Do} \frac{Wo}{p}\right) + \frac{Nu_{NGN} + 1.0}{Nu_{NGN}^2}\right)^{1/2}} \quad (1.49)$$

The average Nusselt number for the N^{th} equivalent roped tube, eqn (1.50), was then derived using equations (1.48) and (1.49).

$$Nu_{rN} = Nu_{NGN} (\cos \theta)^{1/3} \frac{1.0 + Nu_{NGN} \frac{to}{Do} \frac{Wo}{p} \left(1.0 - \frac{Wo}{p}\right)}{1.0 + Nu_{NGN} \frac{2}{3} \frac{to}{Do} \frac{Wo}{p}} \quad (1.50)$$

With respect to the water or tube side h.t.c. Baghernejad again considered the geometric characteristics of roped tubes and tried to develop correlations that could be used, not only to predict the tube-side h.t.c. but the friction factor as well. Baghernejad found that the water side h.t.c and the friction factor were both dependent upon the severity factor^[35]. With the severity factor, eqn (1.43), and previously published data^[33,52] the following relations for the friction factor and the constant C in the Dittus-Boelter equation were determined using a semi-empirical method.

$$f_r - f_p = 1.5 \left(\frac{1}{S}\right)^{1.25} \left(\frac{ti}{p}\right)^{1.5} \quad (1.51)$$

$$c_r - c_p = 5 \left(\frac{ti}{S.p.Di}\right)^{0.7} \quad (1.52)$$

After their development, the various equations were compared to experimental data from other sources. With respect to the condensing side equations, the single tube, eqn. (1.46), was found to compare favourably (maximum error of 18%) with previous data^[33,35,52,53]. The multi-tube

expressions were then compared to data generated in experiments by Baghernejad. Unfortunately the comparison proved inconclusive as a result of vapour shear and dropwise condensation, present in the 5 tube, in-line bundle, that was not accounted for in the theory.

When eqn (1.52) was used in the Dittus-Boelter equation, it was found to have fairly good agreement with previous water side h.t.c. data^[33] with a maximum error of 27%. Equations (1.51) and (1.52) were also compared to design data for condenser tubes^[52] and a maximum error of 16% was found for both equations.

In recently completed work by Ben Boudinar^[39,40] the effects of inundation on roped tube bundles was examined. Experiments were carried out using steam at atmospheric pressure with 3 different types of 13mm Do, aluminium-brass tubes. The test bundles consisted of 3 in-line tubes, the top tube in the bundle being used to re-circulate hot condensate water in order to simulate up to 9 equivalent tubes deep in a condenser. Plain tubes were used as the control bundle and the results of the 2-start and 6-start, with helix angles of 18° and 44° respectively, bundles were compared with it. In addition to the experimental work carried out, two computer programs that simulated the performance of a condenser were developed. The first of these programs simulated the effect inundation has on plain tubes. The theoretical results for a single plain tube were found to have a maximum deviation from the experimental results of only 8%. Similarly the plain tube program successfully predicted heat transfer coefficients for the tubes in the bundle affected by inundation. The results showed that the developed program was sound. The second program was modified using Baghernejad's^[38] correlations in order to predict the performance of roped tubes affected by inundation. The theoretical results for a single 6-start tube compared very well with the experimental results, giving a maximum deviation of just 9%. The 2-start tube theoretical

results tended to underestimate the values for the heat transfer coefficients when compared to the experimental results. The error for the 2-start tubes was found to be about 17%.

As a result of the comparison between the computational work and the experimental results, the following conclusions were reached:

1. Spirally indented or roped tubes provided significant improvements in the overall heat transfer coefficient.
2. Inundation was found to adversely affect the performance of roped tubes. The 2-start roped tubes were affected to a greater extent by inundation than the 6-start tubes.
3. In the computer programs, Kerns'[24] equation was used successfully to predict the effect of inundation on the tube bundles.
4. When Baghernejad's[38] correlations were used in conjunction with Kerns'[24] equation the results of the roped tube program were found to give good agreement with the experimental results, particularly after the tube was flooded.

1.2.3.3 Vapour Shear and Inundation

Cunningham and Baghernejad[41] carried out experiments using 21-tube bundles to determine the combined effects of vapour shear and inundation on roped tubes. The tubes used in the experiments were made of aluminium-brass with an outside diameter and wall thickness of 13mm and 1mm respectively. The roped tubes had 2-starts and 6-starts with helix angles of 18° and 44° respectively but with the same groove depth and groove pitch. The tube

bundles consisted of 3 columns of 5 tubes and 2 columns of 3 tubes that were set in-line with each other.

The variables in the experiments were cooling water velocity, log mean temperature difference and steam velocity, which ranged from 22 m/s to 27 m/s. It was determined from the experiments that the O.H.T.C. increased as the cooling water velocity increased, and that for any given cooling water velocity the 2-start tubes gave the highest O.H.T.C. followed by the 6-start and plain tubes. Also it was observed that a reduction in the O.H.T.C. occurred in tubes lower down in the bundle as a result of inundation and that as the heat flux increased the vapour velocity in the tube bundle decreased. From these observations the following conclusions were drawn:

1. Inundation could be a problem even in condenser bundles as shallow as 5 tubes.
2. The performance of individual tubes in a bundle could be greatly affected by the vapour flow pattern.
3. The effect of inundation on a roped tube was no worse than that of a plain tube if the surface indentation was not severe (i.e. 6-start).
4. Inundation was a problem in bundles only a few rows deep when tubes designed to give high heat transfer (i.e. 2-start) were used.

1.3 Outline of Present Research

The main aim of the present investigation was to study the effects of vapour shear and inundation upon the OHTC performance of both plain and roped tubes.

This study was carried out by first designing a test condenser system that was capable of operating both above and below atmospheric pressure. The

various components of the system were subsequently constructed in the Glasgow University workshops and then installed in the Two-phase flow laboratory of the Mechanical Engineering Department.

Within the test condenser it was possible to simulate the effects of vapour shear and tube bundle geometry through the use of two inserts that had half tubes mounted on them, as shown in figure 13. The position of these inserts could be moved both horizontally and vertically with respect to the tube bundle so that the channel area and hence the steam velocity (as discussed in section (4.2)) could be altered and both the staggered and in-line tube bundle configurations could be simulated. The effect of inundation was imitated by using a bundle of three condenser tubes and an external hot water supply. The top tube in the bundle had uniformly drilled holes running along its length so that by altering the flow rate of water from the external supply, the active tube (located under both the inundation and dummy tubes) became more representative of a tube located lower down in the tube bundle.

Experiments were initially carried out to determine whether the tube geometry affected the OHTC performance of the plain and the two types of roped tubes (described in section (3.2)), and to determine the operational reliability of the test system. Tests were then performed on the non-inundated tubes using three different steam velocities. The results of the experiments involving roped tubes were then compared to those of the plain tubes in an attempt to provide an insight into the relative performance of roped tubes.

The latter part of the test programme focused on the combined effects of vapour shear and inundation on the condenser tubes. The experimental data was contrasted with results from previous inundation tests to determine the effects of steam velocity on inundated condenser tubes.

In addition to the experiments carried out using the condenser system, an attempt was made to simulate the effects of vapour shear and inundation theoretically. To this end two computer programs, developed by Ben Boudinar^[39] were modified using existing vapour shear theory. The operation of the programs, the theory involved and the required modifications were discussed in detail in Chapter 2.

Chapter 2

Computer Theory

2.1 Introduction

The theoretical simulation of an industrial process can often be a challenging and difficult problem. This was certainly true with respect to condensation. It was determined that the solution of numerous complex iterative equations would be required to imitate the operation of a condenser and as a result it was decided that the ideal method of solution was with the use of a computer.

As with the development of most theory, the simulation process of a condenser has been developed and improved upon by several researchers. Hilarionos^[54] developed a successful finite element model for use with single plain tubes. This model was used by Ben Boudinar^[39], together with developed theory by Baghernejad^[38] to produce two computer programs. These programs simulated the operation of a condenser, for either plain or roped tubes, when the effect of condensate inundation was present in a tube bundle.

These two programs, written in Fortran 77 on an IBM 3090 computer, were subsequently improved with the use of vapour shear theory (section 2.3.2). Both the plain and roped tube programs were enhanced so that it was possible to predict the performance of a condenser when both the effects of vapour shear and inundation were present. This was an important step forward as very few papers^[27,28,41] have been published in this area.

The theory developed by Baghernejad^[38] required a knowledge of the equivalent plain tube program results and as such the logic of the roped tube

program was very similar to that of the plain tube program. As a result of this similarity, a detailed description of the plain tube program, with inundation, has been provided (section 2.2) with separate sections to describe how the program was changed to include vapour shear (section 2.3) and how the program was converted for use with roped tubes (section 2.4).

2.2 Theory of the Plain Tube Program

2.2.1 General Description

The basic method used to evaluate the performance of the test condenser was called the Pointwise Heat Exchanger method. This method involved subdividing every tube in the condenser into sections and analysing each section as if it were an individual tube.

This process was carried out by setting up the tube bundle in the form of a 2-dimensional (i, j) matrix. The tubes in the bundle were firstly numbered from $i=1$ to N down the vertical row from the steam inlet, which was located at the top of the test condenser. The individual tubes were then divided into sections, as mentioned previously, perpendicular to the flow of cooling water and numbered from $j=1$ to M , beginning at the cooling water inlet. Once the matrix was established, calculations for each section or increment were carried out beginning at the cooling water inlet of the top tube. The flow characteristics of successive increments were determined using the temperature rise over the preceding increment. The tubes located below the top tube in the bundle also included the effects of condensate inundation in the calculations.

It can be determined from the above description that a large number of iterations were required to evaluate the condenser's performance. To begin the iterative process, initial starting points or guesses were necessary for the cooling water temperature rise through the increment (dT), the outer tube wall

temperature (T_{wo}) and the inner tube wall temperature (T_{wi}). The Newton-Raphson iterative method (shown in section 2.2.3) used these initial starting points and improved upon them continually until a pre-set convergence criterion was satisfied.

When the final values of T_{wo} , T_{wi} and dT were found, it was then possible to continue the calculations to determine the condensation rate and the overall heat transfer coefficient (O.H.T.C.) for each increment of the tube. The condensation rate for the increment was found with a heat balance using subroutines to provide the required properties of steam and water. The overall heat transfer coefficient (O.H.T.C.) was calculated by adding the heat transfer coefficients of the tube wall (obtained using the tube dimensions and thermal conductivity), the water-side (section (2.2.6.1)) and the condensing-side (section (2.2.6.2)).

In order to complete the above calculations with a high degree of accuracy but also keep the number of calculations to a reasonable level the following assumptions were made:

- 1) Steam flowed perpendicular to the tubes
- 2) Steam pressure drop across the tubes was neglected
- 3) Absence of non-condensable gases
- 4) The steam was completely saturated.

These assumptions simplified the complex process of condensation somewhat but did not affect the performance of the programs greatly.

2.2.2 Correlations for the Heat Transfer Coefficients

In the computer programs, Ben Boudinar^[39] included a number of correlations to calculate both the water-side and the condensing-side heat transfer coefficients. This was carried out so that combinations of these correlations could be used in comparison with the measured results, to determine which equations gave the closest agreement with the experimental data.

2.2.2.1 Water-side h.t.c.

The equations used to find the water or tube-side heat transfer coefficient were comprised of a mixture of both theoretical and empirical approaches. Cooling water properties such as velocity and specific heat were correlated using the Reynolds (Re) and Prandtl (Pr) number and the numerical constants were determined from experimental data.

The water-side correlations used in the program described performance with the Nusselt number (Nu) in the form:

$$\text{Nu} = \frac{\alpha_j D_j}{\lambda_{\text{CW}}}$$

and were as follows:

1) The Dittus-Boelter Equation

$$\text{Nu} = 0.023 \text{ Re}^{0.8} \text{ Pr}^{1/3} \quad (2.1)$$

The properties of the cooling water were evaluated using the bulk cooling water temperature (T_M), as described in section (2.2.4).

2) The Seider-Tate Equation

$$Nu = 0.027 Re^{0.8} Pr^{1/3} \left(\frac{\mu}{\mu_{wi}} \right)^{0.14} \quad (2.2)$$

The Seider-Tate equation was devised for use when the viscosity of the cooling fluid was susceptible to temperature. The sensitivity of the cooling fluid was accounted for by using two viscosity terms which were evaluated at different temperatures. The " μ " term was calculated using the mean cooling water temperature (T_{CW}), shown in section (2.2.4), and the " μ_{wi} " term was found using the inner tube wall temperature (T_{wi}). All other fluid properties were evaluated with the bulk cooling water temperature (T_M).

3) The Allan and Eckert Equation

$$Nu = 0.00127 C Re Pr^{0.42} \left(1 + 25Re^{-0.27} \right) \left(\frac{\mu}{\mu_{wi}} \right)^n \quad (2.3)$$

The viscosity terms in the Allan and Eckert equation were identical to those in eqn. (2.2) and could be evaluated using the previously mentioned temperatures. The exponent, (n), used with the viscosity terms was dependent upon the Reynolds number (Re). When the Reynolds number was less than 62500 ($Re < 62500$) the following expression was used:

$$n = \left(\frac{Re}{87000} \right)^{0.84}$$

when the Reynolds number was greater than or equal to 62500 ($Re \geq 62500$) then $n=0.11$.

2.2.2.2 Condensing-side h.t.c.

To evaluate the condensing-side h.t.c. for single tubes and the top tube in a horizontal tube bundle it has been determined (section (1.2.1.2)) that eqn. (1.7), Nusselt's original equation, eqn. (1.4), modified by eqn. (1.30), provided good agreement with much of the available experimental data.

With respect to a vertical row of horizontal tubes where the effects of inundation were present, Ben Boundinar^[39] included several correlations, eqns (1.31), (1.33), (1.38) and (1.40), for use in the program. The various expressions were included as a result of the diversity among the equations themselves and to determine which equation gave the closest agreement with the measured results.

In order for the specific workings of the general theory, explained thus far, to be more fully understood, Figure 6 has been included. Figure 6 shows a single element for a horizontal tube and the location of the component parts described in detail in sections (2.2.3) to (2.2.7).

2.2.3 Incremental Heat Load Calculations

i) Overall heat transfer:-

$$dQ = \alpha_{OA} \cdot A_O \cdot LMTD \cdot dX \quad (2.4)$$

where

$$LMTD = \frac{T_{out} - T_{in}}{\ln\left(\frac{T_s - T_{in}}{T_s - T_{out}}\right)} \quad (2.5)$$

ii) Heat transfer through the cooling water:-

$$dQ = M_{CW} \cdot C_{pCW} \cdot dT \quad (2.6)$$

where

$$M_{CW} = \rho_{CW} \cdot A_i \cdot V_{CW} \quad (2.7)$$

and also,

$$dQ = \alpha_i A_i (T_{wi} - T_{CW}) \quad (2.8)$$

where

$$T_{CW} = T_{in} + \frac{dT}{2} \quad (2.9)$$

The α_i term in eqn. (2.8) was found using eqn (2.1), (2.2) or (2.3).

iii) Heat transfer through the tube wall:-

$$dQ = \frac{2\pi \lambda_{tw} dX}{\ln\left(\frac{r_o}{r_i}\right)} \cdot (T_{wo} - T_{wi}) \quad (2.10)$$

iv) Heat transfer through the condensate film:-

$$dQ = \alpha_o A_o (T_s - T_{wo}) \quad (2.11)$$

where the α_o term was found using eqn. (1.7), the modified Nusselt equation and,

$$dQ = h_{fg}' dM_C \quad (2.12)$$

where h_{fg}' was found using eqn. (1.30) and assuming that the steam was dry saturated.

2.2.4 Estimation of the Outer Tube Wall Temperature (T_{wo})

In order for the outside tube wall temperature (T_{wo}) to be continually re-evaluated as the iteration process took place, it was necessary for T_{wo} to be expressed in terms that were similarly being re-calculated, namely T_{wi} and dT . An overview of the derivation of T_{wo} has been provided in this section. A more complete derivation can be found in Appendix A. The derivation was begun using eqn. (2.8) which was re-arranged to the following form:

$$dX = \frac{dQ}{\pi D_i \alpha_j (T_{wi} - T_{cw})} \quad (2.13)$$

Equation (2.13) was then substituted into eqn. (2.10) in order to eliminate the dQ term.

$$dQ = \left(\frac{2\pi \lambda_{tw}}{\ln\left(\frac{r_o}{r_i}\right)} \right) (T_{wo} - T_{wi}) \left(\frac{dQ}{\pi D_i \alpha_j (T_{wi} - T_{cw})} \right)$$

which resulted in:

$$T_{wi} \left(D_i \alpha_j + \left(\frac{2 \lambda_{tw}}{\ln\left(\frac{r_o}{r_i}\right)} \right) \right) = D_i \alpha_j T_{cw} + \left(\frac{2 \lambda_{tw}}{\ln\left(\frac{r_o}{r_i}\right)} \right) T_{wo} \quad (2.14)$$

Equation (2.13) was also substituted into eqn. (2.11)

$$dQ = \pi D_o \alpha_o (T_s - T_{wo}) \frac{dQ}{\pi D_i \alpha_j (T_{wi} - T_{cw})}$$

which produced:

$$T_{wi} = T_{cw} + \frac{D_o \alpha_o}{D_i \alpha_j} (T_s - T_{wo}) \quad (2.15)$$

The two newly generated equations were then used to develop an expression for T_{WO} by substituting eqn. (2.15) into eqn. (2.14). The expression for T_{WO} was found to be unwielding and was simplified by the use of the following constants:

$$G1 = \frac{2 \lambda_{tw}}{D_o \ln\left(\frac{r_o}{r_i}\right)} \quad (2.16)$$

and

$$G2 = 1 + \frac{2 \lambda_{tw}}{D_i \alpha_i \ln\left(\frac{r_o}{r_i}\right)} \quad (2.17)$$

Thus, the expression for ' T_{WO} ' resulting from the substitution of eqn. (2.15) into eqn. (2.14) was found to be:

$$T_{WO} = \frac{T_{CW} G1 + \alpha_o T_S G2}{\alpha_o G2 + G1} \quad (2.18)$$

Unfortunately the α_o term in eqn. (2.15) was a direct function of T_{WO} and as such had to be expressed in another form. This was achieved by substituting eqn. (1.30) into eqn. (1.4), yielding:

$$\alpha_o = 0.725 \left(\frac{p h_{fg}}{\Delta T} + RA \right)^{1/4} \quad (2.19)$$

where

$$P = \frac{\rho_f^2 g \lambda_{tw}}{\mu_f D_o} \quad (2.20)$$

and

$$RA = 0.68 C_{pf} \quad (2.21)$$

also

$$\Delta T = T_s - T_{wo}$$

To obtain an expression for T_{wo} , eqn. (2.19) was substituted into eqn. (2.18). However this resulted in a non-linear equation. To solve this expression the Newton-Raphson method was chosen, from several numerical methods, because of its simplicity and high degree of accuracy.

The Newton-Raphson method of solving non-linear equations required the function to be in $f(X) = 0$ form and also needed the function's first derivative, $f'(X) = 0$. An initial guess, X_1 , was made and the following format observed:

$$X_2 = X_1 - \frac{f(X_1)}{f'(X_1)}$$

$$X_3 = X_2 - \frac{f(X_2)}{f'(X_2)}$$

until the difference between the X_n and X_{n-1} terms was approximately zero.

Finally, after substituting eqn. (2.19) into eqn. (2.18) the following function, eqn. (2.22) and its first derivative, eqn. (2.23), for T_{wo} were combined

$$f(T_{wo}) = \alpha_o G2 (T_{wo} - T_s) + T_{wo} G1 - T_{cw} G1 \quad (2.22)$$

$$f'(T_{wo}) = \left(\frac{d \alpha_o}{d T_{wo}} \right) G2 (T_{wo} - T_s) + \alpha_o G2 + G1 \quad (2.23)$$

with the Newton-Raphson method to derive an expression, eqn. (2.24), to estimate the outside tube wall temperature (T_{wo}),

$$T_{wo_{n+1}} = T_{wo_n} - \frac{f(T_{wo_n})}{f'(T_{wo_n})} \quad (2.24)$$

where T_{wo_n} was a first estimate followed by a number of iterations until the difference between $T_{wo_{n+1}}$ and T_{wo_n} was negligible.

It should be noted that the average condensate film temperature, T_c , used in the evaluation of eqns (2.19) and (2.20) was determined using the following expression:

$$T_c = \frac{(T_s + T_{wo})}{2}$$

In order to calculate the average condensate temperature it should also be noted that the T_{wo_n} term must be adjusted to the $T_{wo_{n+1}}$ term generated in the previous iteration.

When the calculations for G_2 , eqn. (2.14), were carried out it was necessary to estimate a value for the water side h.t.c. (α_j). This involved the use of the Reynolds number (Re) and the Prandtl number, both of which needed to be evaluated using the bulk cooling water temperature (T_m) where:

$$T_m = \frac{(T_{cw} + T_{wi})}{2}$$

As the T_m term contained T_{wi} and T_{cw} contained dT it was necessary to make initial estimates for both T_{wi} and dT (both of which were unknowns) in order to calculate α_j and G_2 .

2.2.5 Estimation of the Inner Tube Wall Temperature (T_{wi})

In section (2.2.4) in order to find a value for the outside tube wall temperature (T_{wo}) it was necessary to estimate a value for the inside tube wall temperature (T_{wi}). This initial value of T_{wi} permitted the calculation of the water-side h.t.c. (α_i), using one of the equations in section (2.2.2.1), which in turn led to finding a value for T_{wo} . However, in order to generate predicted results with confidence an accurate value for T_{wi} was required, not only to find a value for T_{wo} but also to determine the temperature rise of the cooling water (dT) through the increment of the tube, dX .

To derive an expression that produced an accurate value of T_{wi} , eqns (2.14) and (2.15) from section (2.2.4) were used. It should be noted at this point that simply substituting the previously determined value of T_{wo} into either eqn. (2.14) or (2.15) would not yield an accurate value of T_{wi} as T_{wo} was arrived at using an initial estimate of T_{wi} . The value of T_{wi} was found by re-arranging eqn. (2.15) into an expression for T_{wo} and then substituting into eqn. (2.14) which resulted in an expression of T_{wi} in terms other than T_{wo} .

Thus, eqn. (2.15) was reorganised into an expression for T_{wo} yielding:

$$T_{wo} = T_s + \left(\frac{D_i \alpha_i}{D_o \alpha_o} \right) T_{cw} - \left(\frac{D_i \alpha_i}{D_o \alpha_o} \right) T_{wi} \quad (2.25)$$

Rearrangement of eqn. (2.14) was also carried out to give the following expression:

$$T_{wi} \left(1 + \frac{2 \lambda_{tw}}{D_i \alpha_i \ln\left(\frac{r_o}{r_i}\right)} \right) = T_{cw} + \left(\frac{2 \lambda_{tw}}{D_i \alpha_i \ln\left(\frac{r_o}{r_i}\right)} \right) T_{wo}$$

The above expression was then simplified with the use of eqn. (2.17) which resulted in:

$$T_{wi} G2 = T_{cw} + \left(\frac{2 \lambda_{tw}}{D_i \alpha_i \ln\left(\frac{r_o}{r_i}\right)} \right) T_{wi} \quad (2.26)$$

Equation (2.25) was then substituted into eqn. (2.26), shown below,

$$T_{wi} G2 = T_{cw} + \left(\frac{2 \lambda_{tw}}{D_i \alpha_i \ln\left(\frac{r_o}{r_i}\right)} \right) \left(T_s + \left(\frac{D_i \alpha_i}{D_o \alpha_o} \right) T_{cw} - \left(\frac{D_i \alpha_i}{D_o \alpha_o} \right) T_{wi} \right)$$

which finally produced:

$$T_{wi} \left(G2 + \frac{G1}{\alpha_o} \right) - T_{cw} \left(1 + \frac{G1}{\alpha_o} \right) - T_s (G2 - 1) = 0 \quad (2.27)$$

The constants G1 and G2 were defined by eqns (2.16) and (2.17) respectively and the α_o term came from substituting eqn. (1.30) into eqn. (1.4), as shown in Appendix A. A complete derivation of eqn. (2.27) has been provided in Appendix B.

In order to use eqn. (2.27) to determine a value of T_{wi} it was necessary to employ the Newton-Raphson method used in section (2.2.4). This method of solution was required since the α_i term in eqn. (2.17) was dependent upon T_{wi} (shown in Appendix B). Therefore eqn. (2.27) was re-written in the following form:

$$f(T_{wi}) = T_{wi} \left(G2 + \frac{G1}{\alpha_o} \right) - T_{cw} \left(1 + \frac{G1}{\alpha_o} \right) - T_s (G2 - 1) \quad (2.28)$$

Thus with eqn. (2.28) and its derivative, eqn. (2.29)

$$f'(T_{wi}) = G2 + \frac{G1}{\alpha_0} \quad (2.29)$$

it was possible to find an expression for the calculation of T_{wi} , which was as follows:

$$T_{wi_{n+1}} = T_{wi_n} - \frac{f(T_{wi_n})}{f'(T_{wi_n})} \quad (2.30)$$

To begin the iterative process to find the accurate final value of T_{wi} , it was necessary to use the initial estimated T_{wi} value from section (2.2.4). The iterations were then carried out until $T_{wi_{n+1}}$ was approximately equal to T_{wi_n} or satisfied a pre-set convergence criterion. Prior to each new iteration it was necessary to re-calculate the α_i term using the latest value of T_{wi} .

It is important to note that after the final value of T_{wi} was determined, it was necessary to compare the $T_{wi_{n+1}}$ value with the T_{wi} value used as an initial estimate used to find T_{wo} in the previous section. If the two values were similar, i.e. $T_{wi_{n+1}} \cong T_{wi_{initial}}$ then the program continued on, if the two values were dissimilar then the entire process described in sections (2.2.4) and (2.2.5) must be repeated. The T_{wo} value was then re-calculated using new values of T_{wi} until

$$(T_{wi_{n+1}})_{l+1} = (T_{wi_{n+1}})_l$$

where: $n =$ the number of iterations to find T_{wi}

$l =$ the number of iterations involved in calculating both T_{wo} and T_{wi} to achieve a suitable degree of accuracy for the T_{wi} value.

2.2.6 Estimation of the Cooling Water Temperature Rise (dT)

In order to use an iterative process to determine a final value for 'dT', it was necessary to carry out a heat balance for the increment under examination. The heat balance, dQ, was found using eqn. (2.11) and the most recent estimated values of T_{wO} and α_o resulting from the iterative processes described in sections (2.2.4) and (2.2.5). It should be noted that the T_{wO} and α_o values used in calculating the heat balance at this point were obtained using an initial estimate of 'dT' that was made at the beginning of section (2.2.4). The combination of eqn. (2.11) and the estimated values of T_{wO} and α_o produced the following equation:

$$dQ_{est} = \alpha_{o_{est}} A_o (T_s - T_{wo_{est}}) \quad (2.31)$$

The initial estimate of 'dT' was then used to find the mean cooling water temperature through the increment with eqn. (2.9). The mean cooling water

$$T_{cw} = T_{in} + \frac{dT_{est}}{2} \quad (2.9)$$

temperature (T_{cw}) was used to calculate the density (ρ), for the mass flow of cooling water (\dot{M}_{cw}), and the specific heat capacity (C_p) of the cooling water.

With the estimated heat load (dQ_{est}) and the calculated physical properties of the cooling water it was then possible to set up an iterative process using eqn. (2.6).

$$dQ = \dot{M}_{cw} C_{p_{cw}} dT \quad (2.6)$$

The equation was then re-arranged to the following form:

$$dT_{n+1} = \frac{dQ_{n_{est}}}{\dot{M}_{cw_n} C_{p_{cw_n}}} \quad (2.32)$$

so that a new value of dT could be found. The new estimate of ' dT ' was then used to re-calculate dQ_{est} , \dot{M}_{CW} and Cp_{CW} until dT_{n+1} approximately equalled dT_n ($dT_{n+1} \doteq dT_n$) in which case the next part of the program could begin. If dT_{n+1} did not equal dT_n ($dT_{n+1} \neq dT_n$) then the entire iterative procedure from section (2.2.4). was repeated using dT_{n+1} as the initial estimate for dT .

The above description of the iterative process to find dT was for a single tube. In order to find the dT value for a vertical row of horizontal tubes where inundation was present it was necessary to use one of the correlations mentioned in section (2.2.2.2) to find the appropriate value of α_0 . Once the multi-tube value for α_0 had been determined the iterative process described could then be used.

2.2.7 Calculation of the Heat Transfer Variables

As the program worked through each of the increments in every tube in the bundle to find values for T_{wo} , T_{wi} and dT it also calculated various heat transfer variables. These variables were then stored using the matrix system discussed in section (2.2.1). Therefore in order to determine heat transfer values for a single tube or a bank of tubes, all that was required was a summation of the relevant increments. The relevant heat transfer values were as follows:

- i) Total heat transferred through the tube bundle, Q_{TOT}

$$Q_{TOT} = \sum_{i=1}^N \sum_{j=1}^M dQ_{i,j} \quad (2.33)$$

ii) Average cooling water outlet temperature, $T_{out,avg}$

$$T_{out,avg} = T_{in} + \frac{\sum_{i=1}^N \sum_{j=1}^M dT_{i,j}}{N} \quad (2.34)$$

iii) Total mass flow of condensate produced, \dot{M}_C

$$\dot{M}_C = \sum_{i=1}^N \sum_{j=1}^M d\dot{M}_{C,i,j} \quad (2.35)$$

iv) Average overall heat transfer coefficient, α_{OA}

$$\alpha_{OA} = \frac{\sum_{i=1}^N \left(\frac{\sum_{j=1}^M \alpha_{O,i,j}}{M} \right)}{N} \quad (2.36)$$

v) Average water-side heat transfer coefficient, $\alpha_{i,avg}$

$$\alpha_{i,avg} = \frac{\sum_{i=1}^N \left(\frac{\sum_{j=1}^M \alpha_{i,i,j}}{M} \right)}{N} \quad (2.37)$$

vi) Average condensing-side heat transfer coefficient, $\alpha_{O,avg}$

$$\alpha_{O,avg} = \frac{\sum_{i=1}^N \left(\frac{\sum_{j=1}^M \alpha_{O,i,j}}{M} \right)}{N} \quad (2.38)$$

2.3 Modifications to the Plain Tube Program

2.3.1 Introduction

In previous work carried out by Ben Boudinar^[39] it has been shown that the predicted results from the plain tube program agreed very well with experimental data. This confirmed that the basic logic of the program was sound and that any modifications undertaken should not disrupt the calculation method used. This, therefore was the first constraint that arose when changes to this program were considered. The second constraint was that the program was written to simulate the effect of stagnant or low velocity stream on the condensation process.

With the above design constraints, the problem of simulating vapour shear, in a condenser, was overcome with equations that determined the condensing-side h.t.c. by including the effect of low velocity steam and the use of subroutines. The following sections describe the correlations, the calculation of physical properties and the subroutines that were used to simulate the effect of vapour shear in a horizontal shell and tube type condenser.

2.3.2 Vapour Shear Correlations

In order to simulate the effects of vapour shear on horizontal condenser tubes, great care was taken in the selection of appropriate theory. A number of the available expressions were based on the modified Nusselt equation, eqn. (1.7). As this expression has been shown, in section (1.2), to provide theoretical results that agreed very well with experimental data it was decided to select theory that incorporated this particular equation. Also it was decided that a number of expressions should be selected so that a performance comparison could be carried out to determine which equation should be used in the final simulation.

Thus, four equations that included the effects of low vapour velocity and the above mentioned theory were selected in order to modify the plain tube program. It should be noted that the equations do not include the effects of the separation angle, pressure drop across the tube or the effect of non-condensable gases as these characteristics were not included in the scope of research.

The correlations used to simulate vapour shear were as follows:

1) Fuks Equation

$$\frac{\alpha}{\alpha_{\text{Nu}}} = 28.3 \left(\frac{V_w^2 \rho_g \alpha_{\text{Nu}}}{g \lambda_f \rho_f} \right) (\text{Nu})^{-0.58} \quad (2.39)$$

The Fuks equation was used for calculating the condensing-side h.t.c. when the Reynolds number (Re) for steam was between 500 and 6000. The steam velocity (V_w) used in this expression was the approach velocity which was found in the entry channel of the condenser above the tube bundle shown in Fig. 7. The properties of the condensate water were evaluated at the average temperature of the steam and the outside wall, i.e.:

$$T_c = \frac{T_s + T_{wo}}{2}$$

using polynomial expressions from a subroutine. The polynomial expressions can be located in Appendix C.

2) Shekrladze Equation

$$\frac{\alpha}{\alpha_{\text{Nu}}} = 0.833(\pi)^{1/4} (1+S)^{1/3} \left(1 + \left(1 + \frac{1.69}{\pi(1+S)^{4/3}} \right)^{1/2} \right)^{1/2} \quad (2.40)$$

where

$$\pi = \frac{\lambda_f (T_s - T_{wo}) V_w^2}{g D_o \mu_f h_{fg}} \quad (2.41)$$

and

$$S = Pr_f K \left(\frac{\rho_g \mu_g}{\rho_f \mu_f} \right)^{1/2} \quad (2.42)$$

The Prandtl number (Pr_f) for the condensate and the constant K were evaluated with the following equations:

$$Pr_f = \frac{\mu_f C_{p_f}}{\lambda_f} \quad (2.43)$$

and

$$K = \frac{h_{fg}}{C_{p_f}(T_s - T_{wo})} \quad (2.44)$$

The properties of the condensate water were evaluated using the average condensate temperature (T_c) with the polynomials from Appendix C, the steam properties were interpolated using the method described in section (2.3.3).

It should be noted that when eqn. (2.41) produced a value greater than 10, ($\pi > 10$), then Shekrladze's eqn., (2.40), may be reduced to the following form:

$$\frac{\alpha}{\alpha_{Nu}} = 1.25 \pi^{1/4} (1+S)^{1/3} \quad (2.45)$$

3) Berman Equation

$$\frac{\alpha}{\alpha_{Nu}} = a + b \log(\pi) \quad (2.46)$$

The constants a and b had values of 1.28 and 0.28 respectively over the range $1 \leq \pi \leq 20$, and were extrapolated from experimental results by Berman and Tumanov^[5]. The π term in eqn. (2.46) was evaluated using eqn. (2.41).

4) Berman and Tumanov Equation

$$\frac{\alpha}{\alpha_{Nu}} = 1.0 + 9.5 \times 10^{-3} Re_{\pi}^{11.8/\sqrt{Nu}} \quad (2.47)$$

This equation was used over the range $500 < Re_{\pi} < 6000$ with the Reynolds number (Re_{π}) being calculated with the following equation:

$$Re_{\pi} = \frac{V_w D_o \rho_g}{\mu_g} \quad (2.48)$$

The physical properties of steam and water were evaluated in the same manner as the previous equations.

It was important to note that all of the numerical constants and exponents of eqns (2.39), (2.40), (2.46) and (2.47) were empirically determined from experimental data that involved the use of plain tubes.

2.3.3 Calculation of the Physical Properties of Steam

In order to provide the necessary physical properties of steam used to calculate the condensing-side h.t.c., using the equations from section (2.3.2), two subroutines were written and added to the plain tube program. The CALL statements (Note: the CALL statement, as used in Fortran 77, not only activated the subroutine, but also sent information to and received information from the subroutine) were located at the very top of the main program so that the

various physical properties of steam were available for use throughout the rest of the program.

The first subroutine made use of the steam pressure (P_S), an input variable in the data file, to interpolate values for the steam temperature (T_S), the specific volume (the inverse of steam density, ρ_f), and the specific enthalpy (h_{fg}) between the pressure range of 0.2 to 2.0 bar. The second subroutine interpolated a value for the viscosity of steam (μ_f), using the steam temperature obtained in the first subroutine, over the temperature range of 60 to 120°C.

The method used to interpolate the required data was quite straight forward. Once the subroutine had been activated by the CALL statement, information was then sent from the main program to the subroutine (i.e. either pressure (P_S) or temperature (T_S)). The subroutine then checked if the information that had been received was within the range of data available for interpolation.

The subroutine then worked through the one dimensional array that contained either the pressure or temperature data, taken from steam tables^[55], using an IF statement, shown below for pressure, to determine the

```
IF (PST - C(I)) 30, 40, 50
```

data necessary for the interpolation. This was achieved, first in the bracketted section of the IF statement which determined whether the inputted value (i.e. PST) was less than, equal to or greater than C(I). The data selection for the interpolation was then carried out at one of the above numbered statement locations and calculations performed. The calculated data was then sent up to the main program, with the use of a return statement. A complete listing of the modified plain tube program, located in Appendix D, shows the exact computer coding used to carry out the interpolation.

2.3.4 The Condensing-side h.t.c. Subroutine

As was mentioned in section (2.3.1), the most efficient and least disruptive method of modifying the plain tube program was with the use of subroutines. With a CALL statement (described in section (2.3.3)) information could be sent down to a subroutine where calculations were performed and then new information sent back up to the main program. This then was a very powerful tool as new information could be obtained with the addition of a single statement that did not interrupt the logical flow of operation.

In order to make use of the advantage offered by a subroutine, great care was taken in the positioning of the CALL statement to obtain the best theoretical results. The question of where to position the CALL statement was partially solved by the selected vapour shear theory (section (2.3.2)). All of the selected equations, eqns. (2.39), (2.40), (2.46) and (2.47) required the use of the condensing-side h.t.c. (α_{NU}) as found with eqn. (1.7) in order to simulate the effects of vapour shear.

Upon closer examination of the theory in the original plain tube program it was also determined that the condensing-side h.t.c. played an important role in the iterative processes used to calculate values for T_{wO} and T_{wi} , as shown by eqns. (2.22), (2.23), (2.28) and (2.29) in sections (2.2.4) and (2.2.5). Thus with this information it was decided that modifications should take place in the section of the plain tube program that evaluated both the inner and outer tube wall temperatures, T_{wi} and T_{wO} respectively.

In analysing the operational layout of the plain tube program, shown in Fig. 8, it was determined that T_{wO} and T_{wi} were evaluated in a subroutine of the main program called TAR. This subroutine calculated the temperature rise of the

cooling water (dT) through the increment dX in the top tube of the tube bundle. In order to calculate the final value for dT , subroutine TAR called another subroutine, BOU, to evaluate the final values of both T_{wO} and T_{wi} . It was within subroutine BOU that the condensing-side h.t.c. (α_{Nu}) was calculated using eqn. (1.7) in order to begin the Newton-Raphson iterative process. Thus, the CALL statement for the vapour shear subroutine was located directly underneath eqn. (1.7) in subroutine BOU.

In order to evaluate the effects of vapour shear the new subroutine, VHT, made use of the condensing-side h.t.c., provided by eqn. (1.7), the physical properties of steam and water and the coefficient COVV that decided which correlation (section (2.3.2)) should be used. The properties of steam were sent down from the main program by modifying the CALL statements of both subroutines TAR and BOU to allow the extra required information to pass through the two subroutines to subroutine VHT. The properties of water were obtained by calling subroutine ETA1 which contained the polynomial equations, shown in Appendix C, for density, viscosity, specific heat and thermal conductivity.

Once the new value for the condensing-side h.t.c. (α_o) had been determined, as shown in Fig. 9, it was sent back up to subroutine BOU with a return statement. The new condensing-side h.t.c. was then used in the iterative process to calculate both T_{wO} and T_{wi} . It should be noted that subroutine VHT was called upon to produce an updated version of α_o for every iteration until the pre-set convergence criterion was satisfied in both subroutine BOU and subroutine TAR.

The above description of subroutine VHT detailed how the effects of vapour shear were applied to the top tube in the bundle. To calculate the

effects of vapour shear and inundation on the tubes lower down in the bundle the same condensing-side h.t.c. (α_O) value was used. In section (2.2.2.2) it was shown that the inundation eqns (1.31), (1.33), (1.38) and (1.40) made use of the information from the top tube to simulate tubes deeper down in the vertical row of horizontal tubes. Thus the value of α_O , found in subroutine VHT, was used instead of the previous value α_{Nu} , found using eqn. (1.7). The use of the modified condensing-side h.t.c. and the inundation eqn (1.38) produced results that agreed very well with experimental data, as shown in Chapter 5.

It should be noted that in order to run the plain tube program it was necessary to use the AUTODBL(DBL4) function. This function instructed the computer to carry out calculations using double precision (i.e. to carry 16 decimal places).

2.4 The Roped Tube Program

2.4.1 Introduction

The result of the computer work carried out with plain tubes was the development of a program that simulated the operation of a condenser. Using previous correlations and iterative methods, described in sections (2.2) and (2.3), the program was able to predict the overall heat transfer coefficient (O.H.T.C.), the condensing-side and water-side (α_O and α_i respectively) heat transfer coefficients, the heat flow (Q) and both the inside and outside tube wall temperatures (T_{wi} and T_{wo} respectively).

Ben Boundinar^[39] determined that the developed plain tube program could be modified using Baghernejad's^[38] theory to predict the behaviour of roped tubes under similar conditions. The roped tube program was then used to predict results which were compared to carefully obtained experimental

data^[39,40] so that it was possible to evaluate Baghernejad's theory with confidence.

As was mentioned in section (2.1), the method of evaluation used in the roped tube program was almost identical to the method used in the plain tube program. Therefore, as a result of this similarity, it was decided that the following section should concentrate on the modifications required to firstly change the plain tube program to a program for roped tubes and secondly to account for the effects of vapour shear in the simulation process.

2.4.2 Development of the Roped Tube Program

In order to change the plain tube program into a program to predict results for a roped tube only a few modifications were necessary. It was shown in section (1.2.3.2) that to use Baghernejad's theory a knowledge of the plain tube performance was required. The subroutine TAR was used to determine final values for T_{wO} , T_{wi} , dT , α_i and α_o in the normal manner (section (2.2)). This information was then used in the correlations derived by Baghernejad to convert the plain tube into a roped tube for the purpose of further simulation. The equations that performed this task were inserted directly underneath the CALL statement for subroutine TAR in the main program.

Once the program had converted the plain tube to a roped tube a second subroutine, ROP1, was called. This subroutine was very similar to the plain tube subroutine TAR in that it calculated values for T_{wO_r} , T_{wi_r} , dT_r , α_{i_r} and α_{o_r} . However, to begin the iterative process in subroutine ROP1, only initial estimations for T_{wi_r} and dT_r were required. The initial value of α_{o_r} could be found from eqn. (1.44), which when used with the initial estimates for T_{wi_r} and dT_r and eqn. (2.18) resulted in an equation, (2.49), to find T_{wO_r} without an initial estimate being required

$$T_{wo_r} = \frac{T_{cw_r} G1 + \alpha_{o_r} T_s G2_r}{\alpha_{o_r} G2_r + G1} \quad (2.49)$$

The α_{o_r} term used in eqn. (2.49) was determined with eqn. (1.46) and G1 was a constant used to simplify the expression, as defined by eqn. (2.16). The cooling water temperature (T_{cw_r}) and the G2_r constant were defined as follows:

$$T_{cw_r} = T_{in} + \left(\frac{dT_r}{2}\right) \quad (2.50)$$

and

$$G2_r = 1 + \frac{2 \lambda_{tw}}{D_i \alpha_{i_r} \ln\left(\frac{r_o}{r_i}\right)} \quad (2.51)$$

The α_{i_r} term in eqn. (2.51) was evaluated by substituting eqn. (1.52) for the numerical constant in the Dittus-Boelter equation, eqn. (2.1), which produced the following expression:

$$\alpha_{i_r} = \frac{\lambda_{cw}}{D_i} \left(Cp + 5 \left(\frac{t_j}{Sp D_i} \right)^{0.7} \right) Re^{0.8} Pr^{1/3} \quad (2.52)$$

The iterative process used to evaluate both T_{wi_r} and dT_r was exactly the same as described in sections (2.2.5) and (2.2.6) for T_{wi} and dT respectively. The two values, T_{wi_r} and dT_r , were then used to find T_{wo_r} . Once all of the temperature values (T_{wo_r} , T_{wi_r} and dT_r) were determined the simulation process was then continued using the same method as was previously outlined in section (2.2).

In order to simulate the effects of both vapour shear and inundation the same subroutines used in the plain tube program were used in the roped tube program. It was decided that the CALL statements for the subroutines should

be located in the same positions, as Baghernejad's theory required a knowledge of the plain tube performance. Thus the effect of vapour shear was determined in subroutine TAR and then the information was used to predict the performance of both single roped tubes and roped tube bundles through the use of Baghernejad's theory and subroutine ROP1.

Chapter 3

Test Apparatus and Experimental Procedures

In order to determine the effect that both vapour shear and inundation had on plain and roped tubes a test condenser system was devised. The following sections detail the design criteria and procedures that were used in the construction and operation of the condenser system as well as the instrumentation used to record the experimental data.

3.1 The Test Condenser

To construct the test condenser it was necessary to satisfy a number of design criteria, which were as follows:

- (1) The condenser unit should be capable of operating at both sub-atmospheric and atmospheric conditions and the steam loss during operation should be kept to a minimum.
- (2) The physical dimensions of the test section should allow the condenser tubes to be long enough so that there was an adequate cooling water temperature rise (to allow the accurate estimation of the heat transferred).
- (3) The velocity of the steam flowing inside the condenser should be variable.
- (4) The test condenser should be capable of simulating both the staggered and in-line tube bundle configurations.
- (5) The steam entering the test section should be of good quality and have a uniform distribution along the tubes under examination.

- (6) The condenser should allow different types of tubes to be used in the test section and be capable of simulating the condensation process of a deep tube bundle.
- (7) Permit visual observation of the experiments in progress.

In order to satisfy condition (1) and allow the evacuator system located in the Two-phase flow laboratory to reduce the steam pressure to sub-atmospheric conditions, the test section needed an air tight seal. To achieve this air tight seal the mild steel plates that formed the three components of the assembled test rig (which had dimensions of 485 x 180 x 830mm as shown in Figure 10) were carefully welded together. The welded seams on the inside of the condenser were then covered with silicon sealant, as a further precaution, to fill in any pin holes that might have resulted from the welding process. Thick rubber gaskets were also mounted between the welded flanges of the three components which were held together using 5/16in Whitworth bolts that were spaced at approximately 60mm intervals around the flanges, as shown in Figure 11. This arrangement provided a very good seal between the components of the test condenser as no steam was observed to leak from between the flanges during any of the experiments.

To remove the condensate from the test section and still maintain sub-atmospheric conditions, a sloping baffle was tack welded into the bottom portion of the condenser. This sloping baffle forced the condensate that dripped from the tube bundle to flow toward a discharge pipe mounted in the base of the condenser. The condensate then flowed down the drainage pipe, through a gate valve into a Corning QVF glass cylinder located under the test rig. The gate valve through which the condensate flowed could then be shut (to preserve sub-atmospheric conditions in the test rig) and the collecting cylinder emptied as discussed in the operating procedures.

To comply with conditions (2) and (6), a series of three tubes were mounted between two end plates, as shown in Figure 12. In the three tube bundle only the bottom tube was active with cooling water flowing through it. The middle tube was a dummy tube, used to simulate the conditions of the condensate flow pattern over the active tube. The top tube in the bundle was used to simulate condensate inundation at rates equivalent to a number of overhead condenser tubes. The length of the tubes inside the test section was 485mm which allowed an adequate cooling water temperature rise that was measured with thermocouples. The bundles were inserted into the test section and the endplates were screwed to both sides of the condenser so that the bundles were fixed in place for the duration of the test run. Also, steam-tight gaskets were placed between the endplates and the condenser wall to provide a tight seal and prevent steam from escaping. This particular arrangement allowed the tube bundles to be removed and replaced so that a number of tests could be performed.

It was possible to satisfy conditions (3) and (4) by designing and building inserts for the condenser test section, as shown in Figure 13. These inserts were held in position inside the condenser with 4 bolts and were used to reduce the channel area through which the steam flowed. By reducing the area the steam flowed through the velocity of the steam was increased, as the mass flow of a fluid is constant. This can be seen from eqn. (3.1)

$$\text{Mass Flow Rate } (\dot{M}) = \text{Density} \times \text{Area} \times \text{Velocity} \quad (3.1)$$

The width of the channel was determined by using aluminium spacers, Figure 14, that sat on top of the bolts used to hold the inserts in position. Three sets of spacers were used with lengths of 45mm, 35mm and 22mm which approximated distances of 4, 3 and 2 tube diameters respectively. Also shown

in Figure 14 are two of the sheet metal plates that were used to cover the gap (at the top of the insert) between the edge of the insert and the inside of the condenser wall, to force the steam flow through the channel created by the inserts. The channel created by the 22mm spacers and the inserts can be seen in Figures 15 and 16.

With respect to simulating staggered and in-line bundle configurations, it can be seen from Figure 13 that half tubes were mounted on the insert and that the slots cut into the top and bottom of the insert were of different depths. The slot depths were altered so that when the inserts were bolted into the first position the half tubes sat in line with the 3 tubes in the tube bundles, shown in Figure 12. When the inserts were rotated 180° they sat approximately 6mm lower in the condenser and as a result were staggered with respect to the tube bundle. With this method it was possible to imitate, through the use of the half tubes and different slot depths, staggered and in-line condenser bundles.

To achieve an even condensation rate over the entire length of the tubes under consideration it was necessary for the steam flow to be as uniform as possible (condition (5)). The uniform flow of the steam through the test section was possible through the use of a deflecting baffle mounted in the top of the condenser box and a strainer. The deflecting baffle was mounted adjacent to the steam inlet pipe and forced the steam to flow upwards at approximately a 90° angle towards the very top of the condenser.

After being deflected and prior to flowing through the channel created by the inserts the steam passed through a strainer that was mounted in the top of the central component of the condenser. The strainer was made from a honeycomb of wire mesh, shown in Figure 17, that was 60mm thick and had a cross-sectional area that was the same as the inside of the condenser (i.e.

485mm x 180mm). The purpose of the strainer was twofold, firstly it removed water droplets that might have been present in the steam upon entry to the condenser. The second function of the strainer was to straighten the steam flow so that when the steam passed over the tube bundle it was uniformly distributed along the entire length of the tubes.

During the experiments it was important that visual observation of the tubes took place to determine that the type of condensation was filmwise and not dropwise. Design criteria (7) was facilitated by mounting windows in both the outside wall of the condenser and one of the inserts. The two windows on the condenser wall were made of heat treated shatter proof glass and were 8cm x 10cm in size. The windows were set into a machined slot, with a rubber gasket between the glass and the mild steel condenser wall and then a cover plate was screwed into place to hold the glass securely. The edges of the cover plate were then coated with silicon sealant to prevent any steam loss. The windows mounted in the insert were 10cm x 13cm in size and were held in place with aluminium supports, that were fixed to the insert with screws. Rubber gaskets, similar to those used on the outside windows, were placed between the glass and the aluminium to prevent the glass breaking due to distortion of the inserts caused by the high temperature. As shown in Figure 18 it was possible to obtain a good view of the tubes under examination despite the half tubes mounted on the insert.

3.2 Condenser Tubes

During the course of the experiments, three types of condenser tubes were used. The experimental results of the plain tubes were compared with those of two types of roped tubes, in order to determine how both vapour shear and inundation affected the performance of enhanced tubing. The tubes,

as shown in Figure 19, were all supplied by Yorkshire Imperial Metals^[52] and made from aluminium brass.

The enhanced or roped tubes were manufactured using apparatus that indented grooves on equivalent plain tubes. With this process it was possible to vary the number of grooves or starts, the groove width, the depth and pitch of the groove as well as the helix angle so that a great number of different enhanced tubes could be produced.

During the roping process great care was taken by Y.I.M. so that the outside diameter of the crest of the groove was identical to that of the original plain tube. As a result of this and the fact that the indentation depth of the roped tube grooves was only 0.2mm, it was assumed, for the purposes of the computer programs, that the roped tube dimensions with respect to inner and outer diameters and wall thickness were the same as those of the plain tube. Therefore the dimensions of all three tubes were as follows:

Active Length = 485mm

Inside Diameter = 11mm

Wall Thickness = 1mm

With respect to the two types of roped tubes the indentation depth and pitch of the profiles were 0.2mm and 6.4mm respectively. The roped tubes differed only in the number of starts or grooves and the helix angle. The first type of tube had 2 starts ($S=2$) and the second type had 6 starts ($S=6$) which resulted in helix angles of 18° and 44° respectively.

3.3 The Test Condenser System

3.3.1 Single Tube System

The schematic line diagram represented in Figure 20, which included the inundation system discussed in section (3.3.2), shows the equipment used to simulate the effects of vapour velocity on condenser tubes. The steam for the experiments was supplied by the departmental boilers and fed to the Two-phase flow laboratory at a pressure of 10.2 atmospheres. To conduct the experiments the steam from the main line was reduced in pressure, to just over one atmosphere, and then fed through a water trap and a separator to remove any excess moisture content before being introduced into the condenser. Once inside the test section the steam flow was straightened and filtered once again using the strainer (Figure 17) prior to condensing on the tubes under examination.

As the steam was flowing through the test section, cooling water from a supply tank was pumped through a calibrated flowmeter (section (3.4.2)) to the active tube in the bundle. Prior to the cooling water entering the test condenser it was necessary to ensure that the flow of water was fully developed. This was achieved by reducing the diameter of the cooling water pipe from 0.032m to 0.013m for a distance of 0.4m outside the test section. The length of 0.4m corresponded approximately to 31 tube diameters. Any steam that was not condensed by the cooling water flowing through the active tube was removed by the evacuator system to a series of dump condensers and a sprayer (as discussed in section (3.1)).

The condensate water that dripped from the tube bundle was channelled towards the collecting cylinder (mounted under the test rig) by a sloping baffle located in the base of the condenser. Once the cylinder was full the condensate was removed in the manner discussed in section (3.5.2).

Not shown in the schematic line diagram (Figure 20) was the insulation used to keep the heat loss from the test condenser to a minimum. Sheets of 20mm thick Jablite polystyrene were cut and shaped to form two layers around the condenser (as shown in Figures 21 and 22) as it was much easier and safer to use than glass fibre insulation.

During the course of the experimental program the positions of the inserts and the tube bundles were frequently changed. This was achieved by first removing the layers of insulation, the steam and cooling water lines and the various thermocouples (section (3.4.1)). The three components of the test condenser were then unbolted and, after removing the top section, the middle section was rotated 90° (Figure 23) using an overhead crane. This rotation allowed easy access to the interior of the test condenser so that changes could be made to either the inserts or the tube bundles.

The position of the inserts were changed by simply loosening the four bolts that held each insert in place, changing the aluminium spacers (that sat on top of the bolt shafts) and re-bolting the inserts into their new positions from the inside of the condenser wall. To change the tube bundle a similar process was used. First the inserts were un-bolted, next the aluminium spacers were removed and then the inserts were slid back as close to the inside wall of the condenser as was possible. The endplates of the tube bundle were then unscrewed and the bundle drawn out of condenser.

To avoid the presence of dropwise condensation the bundles under consideration were cleaned with a clean cloth and tap water prior to being inserted into the test section. This method of removing any dirt or oil from the tube surface was found to be sufficient as no dropwise condensation was observed during any of the experiments.

After the changes to either the position of the inserts or the tube bundles were complete the test condenser system was re-assembled in preparation for the next experiment in the series.

3.3.2 The Inundation System

In order to simulate the effects of condensate inundation (at atmospheric conditions) during the experiments, the equipment shown in the previously mentioned schematic line diagram (Figure 20) and in Figure 24 was used. It can be seen from the schematic diagram that water was heated in the 0.08m³ brass tank using two 1.5kW heating elements and an ISL temperature controller (model CRL 453). The temperature controller was equipped with a platinum resistance thermometer in order to monitor the temperature rise of the water inside the inundation tank so that the heating elements would be automatically switched off once the desired temperature had been reached.

It has been shown by previous researchers^[27,28,39] that the temperature of heated water, introduced into test condensers to simulate condensate inundation, quickly rose due to the condensation of steam. In past experiments the temperature of the inundation water was 2-3°C below the saturation temperature so that as the hot water passed over dummy tubes (in a shallow bundle) it reached saturation temperature before coming into contact with the active tubes. In the present investigation the water temperature could only be heated to within 5°C of the saturation temperature. This was due to cavitation in the low N.P.S.H. pump caused when the water temperature was higher than 95°C. Although the water temperature used was marginally lower than in previous experiments, it was not expected to significantly affect the outcome of the experiments.

To ensure thorough heating of the inundation water, two Gallenkamp variable speed stirrers were used to circulate the water inside the holding tank. Then, once the water in the tank was at the correct temperature it was pumped, using a Grundfos low N.P.S.H. pump, through plastic tubing (to minimise vibration) to two flowmeters. The two tri-flat Fisher and Porter flowmeters (section (3.4.2)) were then used to regulate the water flow rate to the inundation tube in order to simulate the effects of condensate falling from overhead tubes in a condenser bundle.

With respect to the inundation tube, Ben Boudinar^[39] conducted several small experiments to determine the most effective way of uniformly distributing inundation water across the active tube and avoid the more complicated design methods of Van der Hegge Zijnen^[56]. Ben Boudinar experimented with various pitches and diameters of holes and arrived at the following conclusions

- 1) The condensate water should flow upwards through holes located on the top of the inundation tube.
- 2) The hot condensate water should be pumped into both ends of the inundation tube.
- 3) For inundation rates of less than 1.7 l/min, it was found that 1mm diameter holes spaced at a distance of 4mm apart on the inundation tube provided satisfactory distribution of the condensate.
- 4) When the inundation rate ranged from 0.9 l/min to 3.2 l/min, an inundation tube with 1.25mm diameter holes drilled at a pitch of 8mm provided a uniform distribution.

Based on the above information the inundation tubes used in the present investigation were mounted in the tube bundle so that the condensate water flowed upwards through 1mm diameter holes that were spaced 4mm apart over the length of the tube. Also the inundation water was pumped into both ends of the inundation tube to minimise pressure variation along the length of the tube.

It should be noted that since the inundation experiments were carried out at atmospheric conditions the gate valves mounted above and below the condensate collecting cylinders were left open. This allowed the condensate to flow continuously through the collecting cylinder to the drain without the use of the Grundfos pump.

3.4 Instrumentation

3.4.1 Temperature Measurement

During the experimental program the various temperatures were recorded in degrees Celsius using type K (Ni-Cr/Ni-Al) thermocouples.

To ensure that accurate values were recorded the thermocouples were calibrated over two particular ranges of operation (i.e. 15°C to 50°C for the cooling water thermocouples and 75°C to 97°C for the steam and condensate water thermocouples). The thermocouple calibrations were carried out by first recording the temperature of a water bath with the thermocouples and a Schlumberger 3530 Orion data logger and then comparing the results with those obtained using a platinum resistance thermometer. With the recorded data, a calibration equation for each thermocouple (shown in Appendix E) was then determined using linear regression. The resulting equations were then incorporated into the short program discussed in section (4.2) and used to calculate the OHTC.

A total of eight thermocouples were used to record the following temperatures:

- Steam temperature inside the test condenser
- Steam inlet temperature
- Steam outlet temperature
- Cooling water inlet temperature
- Cooling water outlet temperature
- Temperature of the condensate water in the collecting cylinder
- Inundation water inlet temperature

3.4.2 Flow Rates

The flowmeters used to measure the cooling water and inundation water flow rates were made by Fisher and Porter, and calibrated with a graduated cylinder and a stop watch. Using the measured data, calibration equations were determined for each flowmeter (shown in Appendix E) with the same linear regression method used to find calibration equations for the thermocouples.

With respect to the flow rate of steam, a mercury manometer was used pressure drop (ΔP) and a calibration equation (Appendix E) for the orifice it was possible to determine the mass flow of steam in kg/hour.

3.4.3 Pressure Measurement

An attempt was made to measure the pressure difference between the top and bottom of the test section with tappings through the side walls of the condenser and water manometers. The attempt was unsuccessful due to large and irregular fluctuations caused by the evacuator system. For the purposes of calculation, the pressure was determined by measuring the steam temperature (section (3.4.1)) and then using steam tables^[55].

3.5 Experimental Program and Procedures

3.5.1 Experimental Program

Using the apparatus described in section (3.3) and the tubes supplied by Y.I.M., two sets of experiments were carried out. The first set of tests were used to determine the effect of vapour shear on condenser tubes while the second set focused on the combined effects of both vapour shear and inundation.

The first half of the test program (i.e. vapour shear effects) was carried out by altering the vapour velocity and the bundle configuration, inside the condenser, using the inserts discussed in section (3.1). Each of the three tubes under investigation (i.e. plain, 2-start and 6-start) were subjected to three different steam velocities and two different bundle configurations (using the highest vapour velocity). During each test the cooling water velocity was altered from approximately 1.1m/s to 4.16 m/s. In this manner a large amount of experimental data was recorded and used to make comparisons between the tubes themselves and also with the computer generated results.

It should be noted that the experiments involving vapour shear and single tubes were run at sub-atmospheric conditions. This was carried out so that the recorded data would provide a closer approximation of the actual performance of an industrial condenser affected by vapour shear. The operation of power condensers at conditions less than atmospheric is a common industrial practice to lower the temperature difference between the steam and the cooling medium, which in turn improves the **CYCLE EFFICIENCY.**

With respect to the simulation of condenser tubes deeper down in the bundle, experiments were carried out using a single vapour velocity and a set cooling water flow rate in a similar manner to tests conducted by Ben Boudinar[39]. This test method was used so that the experimentally obtained vapour shear and inundation data could be contrasted with both previous inundation data[39] and the predicted results obtained using the computer programs, previously discussed in Chapter 2.

Prior to beginning the experiments, it was decided that the most effective method of evaluating the performance of the condenser was through the use of the overall heat transfer coefficient (OHTC). The OHTC was the chosen method of evaluation because it could be independently determined using both theoretical and experimental data.

In both the plain and roped tube computer programs the OHTC was calculated using a number of iterative processes to find the various components of eqn. (3.2), shown below:

$$\text{OHTC} = \frac{1}{\frac{1}{\alpha_i} + \frac{WT}{\lambda} + \frac{1}{\alpha_o}} \quad (3.2)$$

where: WT = Wall thickness of the tube.

Using the measured data from the test condenser the OHTC was determined directly using eqn. (3.3). The method of calculation involving eqn. (3.3), shown below, was discussed in greater detail in section (4.2).

$$\text{OHTC} = \frac{Q \times \text{LOG} \left(\frac{T_s - T_{IN}}{T_s - T_{OUT}} \right)}{\pi D_o L (T_{OUT} - T_{IN})} \quad (3.3)$$

In order to carry out the experimental program discussed in this section, a set of specific operating procedures was devised for both the vapour shear tests (section (3.5.2)) and the inundation simulations (section (3.5.3)).

3.5.2 Experimental Procedure for Single Tube Tests

The following procedure was used to start up and run the test rig for the single tube vapour shear experiments:

- 1) The overhead extractor fan system was switched on.
- 2) The cooling water supply for both the test condenser and the dump condensers was turned on and adjusted to the desired flow rates.
- 3) The steam supply to the test rig was then turned on and set to the desired mass flow rate. The condensate collecting cylinder was left open to the atmosphere at this point for a few minutes in order to blow away any air that had accumulated inside the test section.
- 4) The test section was then closed off from the atmosphere using gate valves located under the test rig and the evacuator system was turned on to simulate sub-atmospheric conditions.
- 5) A careful check of the test condenser was then made to ensure that there were no steam leaks and then the polystyrene insulation was placed around the outside of the test section.
- 6) During the period of time required for the test system to reach stable conditions it was necessary to empty the condensate from the collecting

cylinder. This was achieved by first closing the gate valve, located above the collecting cylinder, through which the condensate flowed. When this gate valve was closed the sub-atmospheric conditions inside the condenser were maintained so that the test run could be continued. Once the gate valve above the collecting cylinder was closed another valve underneath the cylinder was opened and the Grundfos low N.P.S.H. pump was switched on. When the condensate water had been removed from the cylinder the pump was switched off, the gate valve under the cylinder closed and then the valve under the test rig opened to allow the removal of more condensate water from the test section.

- 7) After stable conditions were reached (determined by approximately constant inlet and outlet cooling water temperatures for a given flow rate) temperature measurements were then taken with the Orion data logger.

The recorded temperatures were as follows:

- Steam temperature inside the test section
- Inlet and outlet steam temperatures
- Inlet and outlet cooling water temperatures
- Temperature of the condensate in the collecting cylinder.

After taking temperature measurements a new cooling water flow rate was selected, and the test system was again allowed time to reach stable conditions. Once stable conditions were achieved the above procedure was repeated from step (7). Using this method, temperature measurements were recorded for cooling water velocities ranging from 1.1 m/s to 4.16 m/s for each of the three types of tubes.

After the test was completed, the apparatus described in steps (1) - (4) was turned off and the test condenser stripped down in the manner described in section (3.3.1) in order to prepare for the next experiment.

3.5.3 Experimental Procedure for Inundation Tests

The general procedure for simulating the effects of inundation was to maintain a given cooling water flow rate through the active tube and then re-cycle the equivalent amount of condensate produced. By re-introducing the condensate into the test section through the inundation tube, the active tube imitated the next tube down in the condenser bundle. During the experiments the inserts were positioned very close to the tube bundle (by using the 45mm spacers) so that the highest vapour velocity, of the series of three used in the vapour shear test program, would result and the effects of vapour shear would be more pronounced.

The steps involved in simulating vapour shear and inundation were as follows:

- 1) The overhead extractor fan system was switched on.
- 2) The inundation water tank was filled with tap water and the immersion heaters and stirrers were switched on and time allowed (usually overnight) for the inundation water to reach a temperature in excess of 95°C.
- 3) The following morning the cooling water supply for both the test rig and dump condensers was switched on and adjusted to the desired flow rates.
- 4) The steam supply to the test rig was then turned on and set to the desired mass flow rate.

- 5) Once stable conditions had been achieved in the test section (determined by approximately constant cooling water inlet and outlet temperatures) a set of temperature measurements (as discussed in section (3.4.1)) were recorded with the Orion data logger.
- 6) The mass flow rate of the condensate (\dot{M}_C) was then calculated using the short computer program discussed in section (4.2).
- 7) The Grundfos N.P.S.H. pump located under the inundation tank was then switched on and the required flow rate (i.e. the previously calculated mass flow in step (6)) was set using the two tri-flat flowmeters (section (3.4.2)).
- 8) Time was allowed for the test system to reach stable conditions to ensure that the temperature levels and flow rates were constant and then the process was repeated from step (5).

This entire process was repeated for each of the three types of tubes under consideration in the present investigation.

Chapter 4

Discussion of the Vapour Shear Test Results

4.1 Introduction

Prior to investigating the combined effects of vapour shear and inundation on a condenser tube bundle, it was decided to examine the effect that vapour shear had on a single tube. The single tube experiments were carried out to determine whether tube geometry affected the condensation process and to record the effects of various vapour velocities on the three types of tubes under examination. The recorded experimental data also served as a valuable check on the operational reliability of the test condenser.

4.2 Calculation based on the Experimental Results

In order to facilitate the comparison of experimental and theoretical data, discussed in section (3.5.1), a short computer program was written. This program calculated the overall heat transfer coefficient (O.H.T.C.) using the measured experimental data, that was refined in the program with the calibration equations found in Appendix E, and the following equation:

$$\text{OHTC} = \frac{Q \times \text{LOG}\left(\frac{T_s - T_{\text{IN}}}{T_s - T_{\text{OUT}}}\right)}{\pi D_o L (T_{\text{OUT}} - T_{\text{IN}})} \quad (3.3)$$

The steam temperature (T_s) and the cooling water inlet and outlet temperatures (T_{IN} and T_{OUT} respectively) used in the equation were measured directly with thermocouples and the Orion data logger (section (3.4.1)). However, there were two possible methods of assessing the heat flow (Q) used in eqn. (3.3)

The heat flow (Q) could be determined by either evaluating the heat lost by the steam in the test condenser or the heat gained by the cooling water flowing through the condenser tube. In order to calculate the heat flow using the first method (i.e. heat lost by steam) it was necessary to collect the condensate flowing from the test rig over a time interval so that the mass flow rate could be evaluated. The mass flow rate was then multiplied by the enthalpy of the steam (which was assumed to be dry saturated) to find the heat flow, as shown in eqn. (4.1)

$$Q = M_c h_{fg} \quad (4.1)$$

The second method of evaluating the heat flow (Q) involved measuring the mass flow rate of the cooling water and the cooling water inlet and outlet temperatures. The specific heat capacity (C_p) of the cooling water was then evaluated using an average cooling water temperature (i.e. $(T_{IN} + T_{OUT})/2$) and the polynomial expression for heat capacity found in Appendix C. All of the above mentioned information was then substituted into eqn. (4.2) to calculate the heat flow.

$$Q = C_{p_{CW}} M_{CW} (\Delta T_{CW}) \quad (4.2)$$

To determine which of the two methods produced the most accurate results, the heat flow was calculated using various cooling water flow rates and eqns (4.1) and (4.2), for plain tubes. The results were then compared with previously measured data^[39] and it was determined that eqn. (4.2) produced heat flow values that were very similar to those found by Ben Boudinar.

The heat flow values found using eqn (4.1) were found to be approximately 125% greater than both the results found using eqn (4.2) and

those determined by Ben Boudinar. This very large discrepancy between the results could perhaps be attributed to the steam condensing on many other locations inside the test section such as the inserts, the dummy tubes or the sub-cooled condensate layer on the active tube. The fact that the steam condensed on many locations others than the active tube or that the steam was wet would have caused much more condensate to be produced, resulting in a greater condensate mass flow (M_C) which in turn would increase the heat flow (Q).

As a result of the very good agreement found between the results of eqn (4.2) and the previous data, as well as the ease with which the necessary data could be recorded, it was decided that eqn (4.2) should be used to calculate the heat flow (Q) component of eqn (3.3).

The short measured data program was also used to calculate the velocity of the steam inside the test condenser. This was carried out by first determining the pressure difference (ΔP) across the calibrated orifice in the steam line using a mercury manometer. With the pressure difference and the calibration equation shown in Appendix E it was possible to calculate the mass flow of steam (M_S). The density of the steam was then found by taking the inverse of the specific volume, interpolated using data from the steam tables^[55] and the steam temperature inside the test rig.

The calculated values for the mass flow and steam density, together with the channel area were then substituted into the rearranged form of eqn (3.1) to find the velocity of the steam

$$\text{Steam Velocity } (V_W) = \frac{\text{Mass Flow Rate } (M_S)}{\text{Density } (\rho) \times \text{Channel Area}} \quad (3.1)$$

4.3 Analysis of Results

4.3.1 Experimental Results

Using the inserts in both the staggered and in-line positions inside the test condenser (as discussed in section (3.1)) and a steam velocity of 0.51m/s (obtained when the 45mm spacers were used) it was determined that the O.H.T.C. was not seriously affected by the tube bundle geometry.

It can be seen from Figures 25 to 27 that there was little difference in the tubes' performance when the inserts were in the staggered or in-line positions. With respect to the plain tubes, it was found that when the inserts were in-line with the tube bundle the averaged O.H.T.C. was 7.5% higher than when the inserts were in the staggered position. However for both of the two types of roped tubes it was determined that there was slightly better heat transfer when the inserts were in the staggered position. The O.H.T.C. values for the 2-start and 6-start tubes were found to average +2% and +5% greater respectively than the results found when the inserts were in-line with the condenser tubes.

These results were found to be consistent with work carried out by Kutateladze et al^[12]. Kutateladze et al showed, using inserts with half tubes mounted on them, that the amount of heat transferred in a condenser was determined by the number of tubes in the bundle, the vapour velocity, the temperature head and hardly at all depended on the channel geometry.

The differences in the O.H.T.C. values for the staggered and in-line tube bundles may be attributed to variations in the steam and inlet cooling water temperatures. This variation in temperature could have been caused by the time required to change the inserts from the staggered to the in-line position (discussed in section (3.3.1)) which forced the experiments to be carried out on separate days.

These initial test results not only showed that tube geometry had little effect on the O.H.T.C. but also that the test condenser was capable of producing results that were both consistent and reproducible.

With the inserts in the in-line position and the three different steam velocities (0.27m/s, 0.37m/s and 0.51m/s) it was determined for the three types of tubes under examination that as the vapour velocity increased so did the O.H.T.C. The plain tube results, (Figure 28), showed that as the vapour velocity was increased from 0.27m/s to 0.37m/s an average enhancement of 5% was recorded. When the steam velocity was further increased to 0.51m/s a 33% improvement was noted in comparison to the data obtained with a vapour velocity of 0.27m/s. For the same changes in vapour velocity, improvements in the performance of O.H.T.C. were also noted for both the 6-start and the 2-start tubes (Figures 29 and 30). These improvements have been tabulated and may be located on Table 1.

TABLE 1: Percentage improvement of the OHTC as the vapour velocity was increased

Tube	Vapour Velocity (m/s)	% Improvement
2-start	0.37	+16
2-start	0.51	+27
6-start	0.37	+14
6-start	0.51	+24

During the course of the experiments it was observed, through the windows in the test condenser and insert, that as the vapour velocity increased the condensate flowed faster from the condenser tubes. This quick removal of condensate from the tubes could partially explain the increase in the O.H.T.C. in that as the hold up of the condensate was reduced the condensate film on the top of the tube would become thinner. A thin film or layer of condensate would offer much less resistance to heat transfer and a very high temperature gradient between the steam and the tube wall would be created. The resulting large temperature ~~GRADIENT~~ would in turn create a higher local heat transfer coefficient which would lead to increased values of the O.H.T.C.

Generally the improvements in the O.H.T.C. values, when the vapour velocity was increased, were of a similar magnitude for all three of the tubes under investigation. The only exception was for the plain tube when the steam velocity was increased from 0.27m/s to 0.37m/s. There were several reasons that could account for this smaller increase in performance. Non-condensable gases, such as air, could have entered the test section through either pin hole sized cracks in the welds or up through the collecting cylinder during the process used to remove condensate from the test rig. The presence of air in the test section would have acted as another resistance around the active tube and reduced the heat transfer. Other possible reasons for the small increase in performance of the plain tube could have been a heavy condensate loading due to wet steam or fluctuations in the evacuator system causing slight changes in pressure inside the test section.

When the O.H.T.C. results of the three tubes for each vapour velocity (Figures 31 to 33) were compared, it was determined that the performance of both roped tubes was much greater than that of the equivalent plain tube. The performance improvement of the roped tubes as compared to the equivalent

TABLE 2: Percentage improvement of the O.H.T.C. of roped tubes as compared to plain tubes

Tube	Vapour Velocity (m/s)	% Improvement
2-start	0.27	+40
2-start	0.37	+56
2-start	0.51	+34
6-start	0.27	+20
6-start	0.37	+36
6-start	0.51	+21

plain tube located on Table 2, not only shows the improvement of the roped tubes over the plain tube but also that the 2-start tube provided higher O.H.T.C. values than those of the 6-start tube.

These results were found to be very similar to the outcome of experiments carried out by Ben Boudinar^[39] and Cunningham and Milne^[33] using the same types of tubes. With respect to the enhanced performance of the 2-start tube as compared to the 6-start tube, Cunningham et al determined that the heat transfer increased as the helix angle or number of starts was decreased for roped tubes having the same indentation/diameter and pitch/diameter ratios.

It was believed, based on the above information, that the smaller helix angle of the 2-start tube (discussed in section (3.2)) was responsible for the

enhanced performance of the O.H.T.C. in the following manner. As the cooling water flowed through the 2-start tube a great amount of turbulence was created, resulting in a high water-side h.t.c. This improved performance on the water-side (as compared to the other tubes under examination) made it possible to transfer more heat which in turn produced more condensate on the outside surface of the tube.

Since the 2-start tube had a much thicker condensate layer it was expected that the O.H.T.C. of this tube would be more greatly affected (than the 6-start or plain tubes) as the vapour velocity was increased. This was expected as comparatively more condensate would have been removed, resulting in a lower condensate loading and increased heat transfer. Table 2 shows that this expectation was correct as the improvement in the O.H.T.C. as compared to the plain tube was greater for the 2-start tube than the 6-start tube for all three vapour velocities.

After the measured single tube data had been analysed to determine the relative performance of the various tubes under examination, the data was then compared to the theoretically calculated results. This comparison determined how well the theory discussed in section (2.3.2) simulated the effects of vapour shear on both plain and roped tubes and was discussed in section (4.3.2).

4.3.2 Theoretical and Experimental Results

In the discussion of the computer theory (Chapter 2) it was shown that there were a number of equations that could be used to evaluate both the water-side and the condensing-side heat transfer coefficients. By substituting these heat transfer coefficients into eqn (3.2) it was determined that there were 12 different ways in which the O.H.T.C. could be calculated, as shown in Table 3.

TABLE 3: The combinations of water-side and condensing-side h.t.c. equations used to theoretically evaluate the O.H.T.C.

Combination	Water-side h.t.c. eqn	Condensing-side h.t.c. eqn.
A	Dittus-Boelter	Fuks
B	Dittus-Boelter	Shekriladze
C	Dittus-Boelter	Berman
D	Dittus-Boelter	Berman & Tumanov
E	Seider-Tate	Fuks
F	Seider-Tate	Shekriladze
G	Seider-Tate	Berman
H	Seider-Tate	Berman & Tumanov
I	Allan-Eckert	Fuks
J	Allan-Eckert	Shekriladze
K	Allan-Eckert	Berman
L	Allan-Eckert	Berman & Tumanov

To determine which of the above combinations provided the best approximation of the operation of a steam condenser, the theoretical results were compared to the previously discussed experimental data (section 4.3.1). In order for the comparison to be more readily understood the results have been arranged over a series of three figures for each vapour velocity and type of tube under consideration. Each figure, in the series of three, contains the four condensing-side equations that were used with one of the water-side equations to calculate the O.H.T.C. and the corresponding experimental data.

4.3.2.1 Plain Tubes

With respect to plain tubes, it can be seen from Figures 34 to 42 that the majority of the theoretically evaluated results overestimated the experimental data.

The largest overpredictions of the experimental data were found when the condensing-side eqn. by Berman and Tumanov (eqn. 2.47)) was used to theoretically evaluate the O.H.T.C. Combinations D, H and L (shown on Table 3) produced O.H.T.C. values for the three vapour velocities that ranged from +95% (combination D, Figure 40) to +106% (Figure 36, combination L) greater than the equivalent experimental data.

The O.H.T.C. results evaluated using Fuks and Shekriladze's condensing-side h.t.c. equations (respectively eqns (2.39) and (2.40)) were found to be very similar, but like the data calculated using Berman and Tumanov's eqn the results overpredicted the experimental data to large degree. The overestimation of the experimental results was found to range from +19% and +20% (for combinations A and B with a cooling water velocity of 1.11m/s as shown in Figure 34) to +91% and +82% when the cooling water was flowing at 4.16m/s in combinations E and F in Figure 38.

These large differences between the theoretical and experimentally obtained OHTC results may have been caused by a number of reasons such as the constants in equations (2.39), (2.40) and (2.47), a non-uniform outer tube wall temperature and the temperature distribution through the condensate layer.

The constants used in equations (2.40) and (2.47) were extrapolated from experimental data collected by Berman and Tumanov using steam pressure

that was varied from 0.032 to 0.48 bar. This range of stream pressure was different than the pressure used in the present investigation (i.e. just under 1 bar) and as a result the extrapolated constants may have affected the evaluation of the condensing-side h.t.c., which in turn would affect the O.H.T.C. Based on the theoretical data, it was believed that the extrapolated constants should only be used over the previously specified pressure range and that if the equations are to be used at steam pressures greater than 0.48 bar that new constants should be developed.

Rohsenow^[21], in a study of Nusselt's assumptions, determined that the temperature distribution in the condensate layer around a tube was non-linear and developed a correction factor (eqn. (1.6)) for the enthalpy (h_{fg}) term in Nusselt's original equation, eqn (1.4). In the plain tube program the temperature of the condensate was evaluated using an average of the outside tube wall temperature (T_{wo}) and the steam temperature (T_s), which was a linear distribution. This difference in the temperature distributions may have caused different physical properties of the condensate (such as density, viscosity and thermal conductivity) to be evaluated. These initial differences in the physical properties of the condensate would then have been compounded by numerous iterations so that the theoretically evaluated condensing-side h.t.c. would have been quite different than the actual value.

With respect to the theoretical evaluation of the condensing-side h.t.c., Nobbs^[27] stated that the assumption of a constant outside tube wall temperature led to an overestimation of the experimentally determined condensing-side h.t.c. Nobb's conclusion appears to be sound as the computer program used in the present investigation evaluated the outside tube wall temperature by assuming a constant temperature over the entire surface area of an increment and overpredictions of the experimental data resulted. Also it

seems logical to assume that with condensate being removed, as a result of increased vapour velocity, from both the top and the sides of the tube that the wall temperature in these locations would be much different than in locations such as the bottom of the tube. Thus, the assumption of a constant wall temperature may have contributed greatly to the overprediction of the experimentally obtained O.H.T.C. results.

The closest agreement between the theoretical and the experimentally obtained data, for all three vapour velocities, was determined with the use of combination C in the plain tube program. The theoretical data evaluated with the combination of Berman's condensing-side h.t.c. eqn. and the Dittus-Boelter water-side h.t.c. eqn. agreed very well with the experimental data yielding deviations that ranged from as little as -2% to a maximum of -18%, as shown in Table 4.

TABLE 4: Deviation of the theoretical plain tube results from the equivalent experimental data.

Vapour Velocity (m/s)	Combination	Min Deviation (%)	Max Deviation (%)	Average Deviation (%)
0.27	C	+3	-18	-10
0.37	C	+3	+9	+6
0.51	C	-2	+8	-1.5

When the steam in the test section was flowing at a velocity of 0.37m/s a slight overprediction of the experimental data resulted, as shown in both Table 4 and Figure 37. These results were found to be very similar to the findings of the single plain tube experiments carried out by Ben Boudinar^[39]. Ben Boudinar stated that a maximum deviation of +8% was found between the theoretical

O.H.T.C. data evaluated with the plain tube program and the O.H.T.C. of the recorded experimental data.

With respect to the theoretical results for the O.H.T.C., when the vapour velocity was 0.51m/s and 0.27m/s (Figures 34 and 40 respectively) a general underprediction of the experimental results was noted. Several reasons that may explain this trend of underprediction are as follows.

It is well known that one of the ways to compress a large scatter of experimental data is through the use of logarithms. In equation (2.46) Berman used a logarithmic expression and it was believed that the use of this term caused the values of the condensing-side h.t.c. to be depressed. When these low values of the condensing-side h.t.c were substituted into eqn. (3.2) in section (3.5.1) much larger values of $1/\alpha_0$ would have resulted, which in turn would have contributed towards smaller values of the O.H.T.C.

The presence of dropwise condensation inside the test section may also have contributed to the theoretical results underpredicting the experimental data. During the experimental program, visual observations were carried out, however there were sections of the condenser tube bundle towards the endplates that could not be observed. Dropwise condensation could have been promoted in these areas as a result of contaminants such as oil, grease or dirt. The presence of dropwise condensation on the active tube in the bundle would have caused higher experimental O.H.T.C. values to be calculated due to a larger amount of the tube surface being exposed to the steam flow as compared to when filmwise condensation was present.

The outcome of the analysis of the theoretical and experimental data was that the plain tube computer model was valid. Using available theory it was possible to simulate the operation of a condenser affected by various vapour

velocities with a deviation range of +9 to -18%. It should also be noted that the closest agreement between the theoretical and experimental data was found when the steam was flowing at the highest (0.51m/s) of the three velocities tested.

As a result of the success of the computer model with plain tubes, the similarly modified roped tube program was used to carry out an analysis of the performance of roped tubes, as discussed in section (4.3.2.2).

4.3.2.2 Roped Tubes

Using the previously discussed method of analysis, the theoretical results of the roped tube program were compared with the data from both the 2-start and 6-start tube experiments.

During the course of the data comparison, it was determined that the theoretical combinations employing Berman and Tumanov's condensing-side h.t.c. equation greatly overpredicted the experimental results. This overprediction was found to be of approximately the same magnitude as that of the plain tube analysis with respect to both the 2-start and the 6-start roped tube experimental data. As a result of the large overestimations of both the plain and roped tube experimental data, it was believed that eqn. (2.47) should not be used when the experimental conditions differ from those used by Berman and Tumanov^[5].

The theoretical combinations that involved the use of Berman's equation were also found to provide results that did not closely approximate the experimental data. Combinations C, G and K provided theoretical data that consistently underpredicted the experimental results. As these sets of equations furnished data that more closely approximately the plain tube experimental

data, particularly combination C, they should be restricted to use with the plain tube program.

The closest agreement between the theoretical and experimental data was found when combinations B, E and F were used in the roped tube program, as shown in Tables 5 and 6.

TABLE 5: Deviation of the theoretical 2-start tube results from the equivalent experimental data.

Vapour Velocity (m/s)	Combination	Min Deviation (%)	Max Deviation (%)	Average Deviation (%)
0.27	B	-5	-19	-14
0.37	E	+5	+19	+12
0.51	E	+1.5	+11	+5

TABLE 6: Deviation of the theoretical 6-start tube results from the equivalent experimental data.

Vapour Velocity (m/s)	Combination	Min Deviation (%)	Max Deviation (%)	Average Deviation (%)
0.27	B	+0	+26	+4
0.37	B	+0	-8	+0
0.51	F	+0	-10	-1

The good theoretical approximation of the (6-start tube and the low velocity 2-start tube) experimental results found using Shekrladze's condensing-side h.t.c. equation (combinations B and F) may have been caused by the inclusion of a larger number of the physical properties of both steam and water in the equation. The π term (eqn. (2.41)) that was used in Berman's equation (eqn. (2.46)), which provided very good agreement with the plain tube experimental data, only considered the thermal conductivity (λ) and viscosity (μ) of the condensate water, the steam temperature (T_s) and enthalpy (h_{fg}). Shekrladze's equation included all of the above mentioned physical properties but also included the density (ρ) and viscosity of steam as well as the density and specific heat capacity of the condensate water. With the inclusion of these extra physical properties it was believed that Shekrladze's equation provided a better approximation of the interaction between the steam and the condensate water which in turn allowed a more complete evaluation of the heat transferred.

With respect to the 2-start tube results for the higher steam velocities (i.e. 0.37m/s and 0.51m/s), the close agreement between the theoretical and experimental results may have been caused by several factors inherent to the roped tube program. During a similar analysis, Ben Boudinar^[39] found that the roped tube program, prior to modification for the present investigation, underpredicted the experimental results for both the condensing-side and the water-side heat transfer coefficients. It was believed that the underprediction from the original program was moderated by the overprediction of the experimental data found using Fuks equation (discussed in section (4.3.2.1)) in order to produce theoretical results that closely approximated the experimental data.

Although the theoretical data found using the roped tube program (Tables 5 and 6) agreed very well with the experimental results, both underpredictions and overpredictions did occur. These differences from the experimental results

may be explained in terms of the roped tube theory developed by Baghernejad^[38].

Baghernejad's assumption (3), section (1.2.3.2), stated that the grooves on a roped tube took the shape of repeated rings with the same helix angle instead of being in the shape of a helix turning around the tube. This assumption may have caused the program to overestimate the experimental results as it does not allow for the possibility of condensate hold up on the tube as the grooves were considered to be independent of each other. When a great deal of condensate is located on the surface of a roped tube (due, for example, to condensate hold-ups caused by long drainage channels) the resistance to heat transfer would be increased. This increased heat transfer resistance would in turn reduce the O.H.T.C. and cause deviations between the experimental and theoretical results.

With respect to the 6-start tube data, as shown in Table 6, Ben Boudinar^[39] also found very good agreement between the theoretical and experimental results. An estimated maximum deviation of +9% was determined between the results. This very close approximation of the 6-start tube experimental results found by Ben Boudinar and the results of the present investigation indicated that Baghernejad used data (in order to promote the theory discussed in section (1.2.3.2)) from experiments carried out on roped tubes with characteristics similar to those of the 6-start tubes. If this assumption was correct then Baghernejad's theory should be limited to use with 6-start roped tubes and further correlations should be developed to predict the performance of the wide range of profiled tubes available.

The underpredictions of the experimental data may be explained by examining assumptions (1) and (4) used by Baghernejad to promote the roped tube theory discussed in section (1.2.3.2). Baghernejad's assumptions were as

follows:

- (1) The outside surface of the roped tube consists of a succession of flat and valley regions.

- (4) The condensate was distributed on a roped tube such that the distance from the centre of the cross-section of the tube to the surface of the condensate film, at any given angle, was constant.

These assumptions may have led to the roped tube program underestimating the experimental data as the beneficial effects of surface tension have been neglected. Surface tension, as discussed in section (1.2.2), was shown by Gregorig^[42] to be the basis of the enhanced heat transfer performance of roped tubes as compared to the equivalent plain tubes. These assumptions seem to consider that the only advantage of the roped tubes, with respect to the plain tubes, was that a larger amount of condensate could be accommodated in the groove profiles, resulting in better drainage from the tube.

Assumption (4) may have contributed significantly to the underprediction of the experimental results as it has been shown [17] that the condensate layer around the circumference of a tube was not constant. The condensate layer was found, in the absence of appreciable vapour velocity, to be thinner at the top of the tube and much thicker towards the bottom.

There were also a number of factors which, by improving the performance of the experimentally obtained O.H.T.C. values, would have led to a further theoretical underprediction of the experimental data. It has been shown for plain tubes, that as the velocity of steam was increased the condensate layer on the top of the tube was thinned [5] and that turbulent or wavy flow of the condensate [5,23] was induced. It has also been determined,

again for plain tubes, that increased vapour velocity can shear condensate from the surface of one tube and carry it over to other tubes in the bundle[30]. These factors, which cannot yet be simulated by a computer, all reduce the resistance to heat transfer caused by the condensate layer and as a result the experimental O.H.T.C. values would be improved. It would be logical to assume that a similar pattern of improvement was present with respect to roped tubes causing the roped tube program to produce results that were less than the experimentally obtained data.

The roped tubes themselves may have also contributed to the underestimation of the experimental results in a way not discussed in section (1.2.2). Y.I.M.[52] stressed that the outside diameter of the roped tubes remained the same as that of the equivalent plain tube. However, the process of imprinting the grooves on plain tubes may have resulted in slight differences in the wall thickness around the tube. It would be logical to assume that the wall thickness at the base of the profile (shown in Figure 3), where the actual deformation took place, would be less than in other areas of the tube such as the side walls of the profile. A thinner tube wall would offer less resistance to heat transfer and as such contribute towards higher experimental O.H.T.C. values.

Although a number of points of contention have been raised with respect to Baghernejad's assumptions it should be noted that the task of mathematically interpreting the performance of roped tubes is very difficult indeed. These assumptions simplified the mathematical interpretation of roped tubes and allowed Baghernejad to conduct a Nusselt type analysis, culminating in the equations discussed in section (1.2.3.2). The developed equations provide a very useful starting point for both the analysis of this very complex problem and for the development of further theory.

4.4 Conclusions from the Vapour Shear Experiments

The following conclusions were drawn as a result of the experimental and theoretical investigations carried out on single horizontal condenser tubes with various steam velocities:

- 1) The O.H.T.C. of the three types of tubes under investigation (plain, 2-start and 6-start) was found to increase as the steam velocity was increased.
- 2) The performance of the roped tubes with respect to the O.H.T.C. was superior to the equivalent plain tube.
- 3) The order of performance of the tubes with respect to the O.H.T.C. was found to be, from highest to lowest, 2-start, 6-start and plain tubes respectively.
- 4) The geometry of the test bundle (i.e. staggered and in-line tubes) was found to have little affect on the performance of the tubes under investigation.
- 5) Using available theory it was possible to simulate the performance of condenser tubes within the following error ranges:
 - i) plain tubes +9% to -18%
 - ii) 2-start tubes +19% to -19%
 - iii) 6-start tubes +26% to -10%

The above margins of error for the simulations are considered to be very good as the results of an uncertainty analysis carried out on similar experiments^[39] showed that the experimental results had an error band of $\pm 15\%$.

Chapter 5

Discussion of the Vapour Shear and Inundation Test Results

5.1 Introduction

In the previous chapter it was shown that the velocity of the steam inside the test condenser affected the OHTC performance of single tubes. To determine whether the above conclusion applied to tube bundles further experiments were carried out and the results compared with previous inundation data that was recorded when the vapour was virtually stagnant.

5.2 Analysis of Results

In order to simulate the effects of both vapour shear and inundation on condenser tubes, the previously discussed test apparatus and the experimental procedures outlined in section (3.5.2) were used. The measured data program that was discussed in section (4.2) was also used, in conjunction with the test apparatus, to determine the amount of "condensate" water that should be pumped from the external hot water supply to the inundation tube.

During the vapour shear and inundation experiments of the present investigation a single cooling water velocity of 2.66m/s was used. This condition was chosen so that the recorded data could be compared with previous inundation results^[39]. The highest of the three vapour velocities (i.e. 0.51m/s) was used during all of the experiments in an attempt to make the vapour shear effects more pronounced in comparison to the preceding data^[39] which was recorded using a near stagnant steam velocity of 0.15m/s.

It should be noted that during the course of the experimental programme it was only possible to simulate the 2-start tube bundle to a depth of seven tubes, as compared to nine tubes for both the plain and 6-start tubes. This was due to insufficient pumping capacity and to the large amount of condensate generated by the 2-start tubes.

5.2.1 Experimental Results

It can clearly be seen from the experimental results, shown in Figure 43, that condensate inundation decreases the OHTC performance of tubes lower down in a condenser bundle. This result was identical to previous work carried out for both plain and roped tubes, as discussed in sections (1.2.1.2) and

TABLE 7: Percentage decrease in the OHTC performance as compared to the top tube in the condenser tube bundle

Tube No.	Plain Tubes	2-Start Tubes	6-Start Tubes
2	-5	-2	-11
3	-9	-9	-13.5
4	-11	-10	-19
5	-13	-14	-21
6	-14	-16	-22
7	-16	-18	-26
8	-18	-	-27
9	-20	-	-29

(1.2.3.2) and showed that the inundation system and test procedures were valid. Table 7 illustrates that the decrease in performance due to inundation ranged from as little as -2% for tube number 2 in the 2-start tube bundle to as much as -29% for the ninth tube in the 6-start roped tube bundle.

Figure 43 also shows that the pattern of OHTC performance of the investigated tubes was the same as both the vapour shear results, Figures 31-33, and previous inundation work^[39]. The 2-start roped tube bundle was found to have OHTC values that were much greater than every tube in the equivalent plain tube bundle. An averaged improvement of +61% was found for

TABLE 8: Percentage improvement of the OHTC for the roped tube bundles as compared to the equivalent plain tube bundle.

Tube No.	2-Start Tubes	6-Start Tubes
1	+62	+39
2	+67	+30
3	+63	+33
4	+64	+28
5	+59	+26
6	+57	+26
7	+58	+23
8	-	+23
9	-	+23
Average	+61	+28

the 2-start tube bundle in comparison to the plain tube bundle. The 6-start tube bundle also had higher OHTC values than the plain tube bundle, with an averaged improvement of +28% as shown in Table 8.

When the vapour shear and inundation results for the 2-start roped tubes were compared to those of Ben Boudinar, as shown in Figure 44, it was determined that increased vapour velocity enhanced the OHTC performance of inundated tubes. It can be seen from Table 9 that there was an improvement in the OHTC for every tube in the bundle and that the amount of improvement increased as the depth of the bundle increased. Also it can be seen in Table 9 that the spread of experimental data for the present investigation was less than that of the previous data. For the inundation data^[39] there was a 32% decrease in performance between the 1st and 7th tubes as compared with an 18% performance decrease for the vapour shear and inundation data.

TABLE 9: Percentage improvement in the OHTC for the 2-start roped tube bundle as compared to previous inundation data^[39].

Tube No.	OHTC(kW/m ² °C)		% Improvement
	Inundation Data ^[39]	Vapour Shear and Inundation Data	
1	5.85	5.97	+2
2	5.47	5.84	+7
3	4.70	5.44	+16
4	4.58	5.37	+17
5	4.37	5.13	+17
6	4.19	5.02	+20
7	3.99	4.88	+22

The increased OHTC performance of the experimental results of the present investigation as compared to Ben Boudinar's results was believed to have been caused by the increased steam velocity thinning the condensate layer on the tubes. It was shown in Chapter 4 that the performance of tubes with a heavy condensate loading (i.e. 2-start tubes) was enhanced with an increase in the steam velocity. The higher steam velocity (0.51m/s) not only thinned the condensate layer on the top of tubes but induced wavy or turbulent flow in the condensate layer and caused the condensate to splash between tubes resulting in increased heat transfer.

The findings of the 2-start roped tube comparison were very similar to the results of vapour shear and inundation tests carried out on plain tubes by Nobbs^[27]. Nobbs stated that the effect of inundation was generally to reduce the heat transfer and that the rate of reduction with increase in inundation rate was smaller as the vapour velocity was increased.

When the experimental data for the present investigation was compared with the previous inundation data^[39] for both the 6-start roped tubes (Figure 45) and the plain tubes (Figure 46) the results were found to be less conclusive than those of the 2-start roped tubes.

The 6-start roped tube results, shown in Figure 45, were virtually identical. The maximum deviation between the curves was just +6%, for the 6th tube in the bundle, and a minimum deviation of +0% was found for the 5th tube. With respect to the plain tube experimental results comparison, shown in Figure 46, the inundation data^[39] was greater than the data from the present investigation by an averaged value of +11%.

As a result of a close examination of the description of the test apparatus and experimental methods used in the inundation tests^[39] and the present

apparatus and methods (Chapter 3), several reasons were discovered that may explain the lower than expected OHTC performance of the vapour shear and inundation experiments.

During the course of the vapour shear and inundation experiments, the steam pressure inside the test cell was maintained at slightly above atmospheric pressure. This was carried out in order to allow the removal of the large amounts of condensate water, generated by the experiments, through the use of the condensate collecting cylinder (which was open to the atmosphere by way of a gate valve) and the low N.P.S.H. pump. However, the evacuator system in the Two-phase flow laboratory that was used to maintain the steam pressure and remove excess steam from the test cell may have introduced non-condensable gases (such as air) into the condenser unit through this open gate valve. Once inside the test cell, air would have formed a layer around the condenser tubes under examination creating another resistance to heat transfer. This further resistance would have greatly reduced the performance of the OHTC as it has been previously shown^[22] that air is a very potent obstruction to heat transfer in condensers and could partially explain why the results of the previous data^[39] were higher than those of the present investigation

The lower than expected OHTC results of the vapour shear and inundation tests may also have been caused by the method used by Ben Boudinar to determine the condensate mass flow rate. During the inundation experiments^[39] the condensate flow rate was evaluated as the difference between the amount of the total condensate water collected, over a period of time, in the measuring can located underneath the test condenser and the metered flow of "condensate" water pumped into the inundation tube. It was believed that this method was prone to errors that may have artificially enlarged the mass flow of the condensate such as wet steam condensing on locations inside the test cell other than the active tube (such as the condenser

walls, the dummy tube and the wire mesh strainer). Fluctuations in the inundation or "condensate" water flow rate due to head loss in the external hot water tank and measurement errors when using the inundation water flowmeters could also have contributed to discrepancies in the condensate mass flow rate.

If the condensate flow rate was increased as a result of the previously mentioned errors, the heat flow rate (\dot{Q}), eqn. (4.1), would also have been increased. As the heat flow was used in the evaluation of the OHTC, using eqn. (3.3), any increases in the heat flow rate would have caused enlarged OHTC values to be calculated. These enlarged OHTC results would have subsequently caused the OHTC data from the vapour shear and inundation experiments to have appeared low and inaccurate in comparison.

Another possible reason that may have contributed toward the slightly lower OHTC values of the present investigation was the difference in the inundation water temperature used in the two sets of experiments. As discussed in section (3.3.2) the inundation water temperature used in the present investigation was 95°C as opposed to a temperature of 97°C used by Ben Boudinar. This lower water temperature may have caused the condensate layer around the active tube to have become slightly sub-cooled. This slightly cooler layer of condensate may have reduced the amount of heat being transferred by firstly reducing the heat flux and secondly by causing more steam to condense on the condensate layer itself, which would in turn thicken the condensate film and increase resistance to the transfer of heat.

Although this slight difference in the inundation water temperature was discussed as a possible source of error it was believed that the effect exerted on the OHTC was minor in comparison to the effects of non-condensable gases and the previously mentioned errors in the condensate mass flow evaluation carried out by Ben Boudinar.

It should be noted that the results of the previously discussed 2-start roped tube comparison were subject to the same possible sources of error that were mentioned with respect to both the plain and 6-start roped tubes. Non-condensable gases, such as air, may have been present during the 2-start tube experiments but based on the results it was believed that there was not a significant enough concentration of these gases to have caused a reduction in heat transfer.

The fluctuations in the inundation water flow rate and the temperature difference in the "condensate" water may have increased the performance of the OHTC for the 2-start tubes instead of decreasing the amount of heat transfer as shown for the plain and 6-start roped tubes. It was discussed in section (4.3.1) that as the steam velocity was increased the OHTC was also enhanced and that the highest OHTC values were found for the tubes with the heaviest condensate loading (i.e. 2-start tubes). With an increased amount of condensate located on the 2-start tubes, as a result of the above mentioned reasons, comparatively more condensate would be removed by the steam flowing at 0.51m/s than from the plain or 6-start tubes which had smaller condensate loadings. This larger amount of condensate removed from the 2-start tube would have reduced the film thickness caused a greater amount of heat to be transferred.

Once the results of the present investigation had been compared with the previous inundation data, the OHTC information was then compared to theoretically evaluated results. This comparison was used to determine how well the modified computer programs simulated the effects of both inundation and vapour shear on plain and roped tubes and was discussed in section (5.2.2).

5.2.2 Theoretical and Experimental Results

In the computer programs written by Ben Boudinar^[39], a number of expression (eqns (1.31), (1.33), (1.38) and (1.40)) were included that were capable of evaluating the amount of heat transferred by an inundated tube in a condenser tube bundle. Through a comparison with experimental data, Ben Boudinar determined that the theoretical expression that provided the closest agreement with the measured results was Kern's^[24] equation, eqn. (1.38).

With Kern's equation and the results of the theoretical and experimental vapour shear data comparison (section (4.3.2)) combinations of equations were devised in an attempt to theoretically evaluate the effects of vapour shear and inundation on both plain and roped tubes. The combinations of equations used in the theoretical simulations are shown in Table 10.

TABLE 10: Combinations of equations used to simulate the effects of vapour shear and inundation on condenser tube bundles

Tube Type	Water-side h.t.c. Eqn.	Condensing-side h.t.c. Eqn.	Inundation Eqn.
Plain	Dittus-Boelter	Berman	Kerns
2-start	Seider-Tate	Fuks	Kerns
6-start	Seider-Tate	Shekriladze	Kerns

When the results from the plain tube experiments were compared with the theoretically evaluated data, as shown in Figure 47, the agreement between the two data sets was determined to be very good. A maximum deviation of just -7% was found for the top tube and minimum deviations of +0% were found for both the 2nd and 8th tubes in the bundle. The magnitude of the

deviations between the two sets of data was very similar to those of the vapour shear data comparison shown in Table 4, and were well within the $\pm 15\%$ error band for the experiment results discussed in section (4.4).

After the successful outcome of the plain tube data comparison, which demonstrated the validity of the vapour shear and inundation computer model, the roped tube program was used to predict the performance of both 2-start and 6-start roped tube bundles.

With respect to the 2-start roped tube comparison, as shown in Figure 48, the theoretical data was found to underestimate the experimental results. This underprediction extended to every tube in the bundle, shown in Table 11, and the averaged deviation from the experimental results was found to be approximately -14%.

TABLE 11: Percentage deviation of the theoretical data from the experimental 2-start roped tube bundle results.

Tube	% Deviation
1	-11
2	-16
3	-14
4	-16
5	-15
6	-15
7	-14
Average deviation	-14.4

Similar results to those of the 2-start tubes were discovered during the 6-start roped tube data comparison, as shown in Figure 49. The computer generated data also underpredicted the experimental results for all of the tubes in the bundle, shown in Table 12. However, the averaged deviation of the two sets of data was found to be approximately -11%, which was less than the averaged difference between the 2-start tube data.

TABLE 12: Percentage deviation of the theoretical data from the experimental 6-start roped tube bundle results.

Tube	% Deviation
1	-14
2	-11
3	-13
4	-11
5	-12
6	-13
7	-10
8	-10
9	-8
Average deviation	-11.3

It was believed that the theoretical underpredictions of the roped tube experimental data, shown in Figures 48 and 49, may be explained in terms of the roped tube theory and the conditions inside the test condenser.

With respect to the experimental conditions inside the test condenser, it was observed that as the flow rate of inundation or "condensate" water was increased the mode through which it drained toward the dummy and active tubes changed. At very low flow rates the "condensate" water drained from the inundation tube to the other tubes in the bundle in the form of droplets. As the flow rate was increased the drainage mode changed to a combination of droplets and thin streams of inundation water. Finally, at high inundation water flow rates the "condensate" water was observed to flow continuously in thick streams from several locations on the inundation tube towards the other tubes.

The drainage mode of the "condensate" water through the tube bundle (as described above) was believed to have had a great impact upon the experimentally obtained OHTC results. In the areas of the active tube directly affected by a stream of inundation water the thickness of the condensate film would be greater. This difference in the thickness of the condensate layer would result in areas along the length of the tube that had heavy condensate loadings and other locations where the condensate loading was much lighter. In this manner areas with high and low local heat transfer coefficients could have been established, resulting in enhanced tube performance similar to the method discussion in section (1.2.2.1).

The drainage mode of the condensate and the higher steam velocity (0.51m/s) may have further increased the experimentally obtained OHTC values by causing the falling condensate to splash between the tubes in the bundle. If the condensate splashed between tubes, some tubes would receive more condensate and others would receive less causing more heat to be transferred^[30]. Also it has been shown that as condensate splashes onto inundated condenser tubes it can cause turbulent or wavy flow^[5,23] which also increases heat transfer.

The underpredictions of the experimentally obtained OHTC data may also be explained in terms of the theory used in the roped tube program. In the roped tube theory discussed in section (1.2.3.2) Baghernejad made a number of assumptions. Assumptions (1) and (4) neglect the beneficial affects of surface tension, which were shown by Gregorig^[42] to be fundamental to the enhanced performance of roped tubes in comparison to plain tubes.

However, assumption (4) may have been the largest single contributing factor towards the underprediction of the experimentally obtained OHTC results. It has previously been shown^[17] that the condensate layer around the circumference of a tube was not constant. This was confirmed by observation during the course of the experiments. The inundation water flowing from the inundation tube to the active tube and the steam velocity caused the condensate film to be thicker in various locations along the length of the condenser tube, and to splash between the tubes which would have contributed to an uneven distribution of condensate.

As a result of the comparisons between the data from the vapour shear and inundation experiments and both previous inundation test results and theoretical data a number of conclusions were drawn, as discussed in section (5.3).

5.3 Conclusions from the Vapour Shear and Inundation Experiments

The following conclusions were based on the results of the theoretical and experimental investigations carried out using various condenser tube bundles.

- 1) Condensate inundation was found to decrease the OHTC performance of the plain, 2-start and 6-start tubes.

- 2) High steam velocity (0.51m/s) reduced the effect of inundation and improved the OHTC performance of a bundle of 2-start roped tubes. The above results were not conclusively shown for similar bundles of plain and 6-start roped tubes.

- 3) The order of performance of the tubes with respect to OHTC when subjected to the effects of high vapour velocity and condensate inundation were, from highest to lowest, 2-start, 6-start and plain tubes respectively.

- 4) The performance of the roped tubes with respect to OHTC was superior to the equivalent plain tube.

- 5) Using previously developed theory it was possible to simulate the performance of condenser tube bundles within the following error ranges:
 - i) plain tubes +0% to -7%
 - ii) 2-start tubes -11% to -16%
 - iii) 6-start tubes -8% to -14%

Chapter 6

General Conclusions

6.1 Conclusions

In the first part of the experimental programme, the vapour shear tests showed that as the velocity of the steam increased so did the OHTC performance of both the plain and roped tubes. A comparison of the experimental results showed that the OHTC performance of both the 2-start and the 6-start roped tubes was superior to that of the equivalent plain tube. These tests also revealed that the geometry (i.e. staggered and in-line bundle configurations) of the plain and enhanced tubes had little effect on the amount of heat transferred.

The data from the multi-tube experiments confirmed the results of previous tests in that condensate inundation was clearly shown to reduce the amount of heat transferred by both plain and roped tubes. The effect of inundation was then shown to be reduced and the OHTC improved for a bundle of 2-start roped tubes through the use of a higher steam velocity (0.51m/s). This result was not conclusively shown for similar bundles of plain and 6-start roped tubes and reasons for this behaviour have been discussed.

In addition to the experimental work, the modification and operation of two computer programs, used to predict the performance of condenser tubes subjected to vapour shear and the combined effects of vapour shear and inundation, was discussed. The theoretical results were compared with the measured experimental data and very good agreement was found for the plain tube simulations. The predictions for the roped tubes were judged less

successful and reasons for this outcome have been analysed and discussed in the preceding chapter.

6.2 Recommendations for Future Work

The results of the experiments performed in the present investigation have provided a useful starting point into the effect steam velocity has on the performance of roped condenser tubes. It should be noted however, that the tests were carried out under a specific set of conditions and that only two types of enhanced tubes were used.

In order to more fully understand the effect of vapour velocity on enhanced tubes further experimental and theoretical developments are required. Tests should be carried out using a variety of commonly used types of roped tubes in order to build up a body of knowledge. This experimental data should then be used to develop semi-empirical theory similar to that of Kern's, for tube bundles, and Shekrladze, for the effects of steam velocity, as a precursor to more theoretical equations.

Other possible areas of future development lie in the study of non-condensable gases and water-side tube fouling. By combining the effects of vapour shear, inundation, non-condensable gases and water-side tube fouling very important information could be gained that would very closely approximate the actual operating conditions of industrial condensers. It was also believed that experiments of this nature should be carried out using relatively large banks of tubes at sub-atmospheric conditions so that the simulations are as realistic as possible.

REFERENCES

1. Nusselt, W. 'Die Oberflächen-Kondensation des Wasserdampfes', Z. VD. I., 60, 541-546 and 569-575, 1916.
2. Rohsenow, W.H., Webber, J.H. and Ling, A.T. 'Effect of vapour velocity on laminar and turbulent film condensation', Trans. ASME 78, 1637-1643, 1956.
3. Fuks, S.N. 'Heat transfer with condensation of steam flowing in a horizontal tube bundle', Teploenergetika, 4(1), 35-39, 1957: English translation NEL 1041, National Engineering Laboratory, East Kilbride.
4. Chung, P.M. 'Film condensation with and without body force in boundary layer flow of vapour over a flat plate', NASA Tech. Note, D790, 1961.
5. Berman, L.D. and Tumanov, Y.A. 'Investigation of the heat transfer in the condensation of moving steam on a horizontal tube', Teploenergetika, 9(10), 77-83, 1962: English translation RTS 2593, National Lending Library.
6. Silver, R.S. 'An approach to a general theory of surface condensers', Trans. I.Mech.E. P14/64, 1964.
7. Berman, L.D. 'An approximate method of calculating heat exchange with vapour condensate on a horizontal tube bundle', Teploenergetika, 11(3), 74-78, 1964.
8. Shekrladze, I.G. and Gomelauri, V.I. 'Theoretical study of laminar film condensation of flowing vapour', Int. J. Heat Mass Transfer, 9, 581-591, 1966.
9. Fujii, T., Uehara, H. and Kurata, C. 'Laminar filmwise condensation of flowing vapour on a horizontal cylinder', Int. J. Heat Mass Transfer, 15, 236-246, 1972.
10. Shekrladze, I.G. Inzh-Fiz.zh, 32(2), 1977.
11. Berman, L.D. 'Influence of vapour velocity on heat transfer with filmwise condensation on a horizontal tube', Teploenergetika, 26(5), 16-20, 1979.

12. Kutateladze, S.S., Gogonin, N.I., Dorokhov, A.R., Sosunov, V.I. 'Film condensation of flowing vapour on a bundle of plain horizontal tubes', *Teploenergetika* 26(5), 12-15, 1979.
13. Marto, P.J., Nunn, R.H. 'Power condenser heat transfer technology' 193-225, Hemisphere Publishing Corp., 1981.
14. Lee, W.C. and Rose, J.W. 'Film condensation on a horizontal tube-effect of vapour velocity'. 7th Int. Ht. Transf. Conf., Munich, Paper CS17, 1982.
15. Rose, J.W. 'Effect of pressure gradient in forced convection film condensation on a horizontal tube', *Int. J. Heat Mass Transfer*, Vol. 27, No. 1, 39-47, 1984.
16. Uehara, H. and Dilao, C.O. 'Overall heat transfer coefficients of horizontal tube type condenser', *Proceedings 2nd Int. Symp. Condensers and Condensation*, Bath, 175-184, 1990.
17. Jakob, M. 'Heat transfer', Vol. 1, J. Wiley and Sons Inc., 1949.
18. Young, F.L. and Wohlenberg, W.J. 'Condensation of saturated freon-12 vapour on a bank of horizontal tubes', *Trans. ASME*, 64, 787-794, 1942.
19. Short, G.E. and Brown, H.E. 'Condensation of vapours on vertical banks of horizontal tubes', *I.Mech.E. Proc. General Discussion Heat Transfer*, 27-31, 1951.
20. Bromley, L.A. 'Effect of heat capacity of condensate', *Industrial and Engineering Chemistry*, Vol. 44, No. 12, 2966-2969, 1952.
21. Rohsenow, W.M. 'Heat transfer and temperature distribution in laminar-film condensation', *Trans. ASME*, 78, 1645-1648, 1956.
22. Cunningham, J. and Homes, A. 'The effect of air on condensation on a roped tube', *Desalination*, 38, 65-74, 1981.
23. Labuntsov, D.A. 'Heat transfer on film condensation of pure vapours on vertical surfaces and horizontal pipes', *Teploenergetika*, 4(1), 72-79, 1957.
24. Kern, D.Q. 'Mathematical development of loading in horizontal condensers', *J. Am. Chem. Engrs.*, Vol. 4, No. 2, 157-160, 1958.

25. Chen, M.M. 'An analytical study of laminar film condensation', Trans. ASME, Vol. 83, 48-60, 1961.
26. Grant, I.D.R. and Osment, B.D.J. 'The effect of condensate drainage on condenser performance', NEL Report No. 350, 1968.
27. Nobbs, D.W. 'The effect of downward vapour velocity and inundation on the condensation rates on horizontal tubes and tube banks', PhD dissertation, University of Bristol, 1975.
28. Nobbs, D.W. and Mayhew, Y.R. 'Effect of downward vapour velocity and inundation on condensation rates on horizontal tube banks', NEL Report No. 619, 39-54, 1976.
29. Bergles, A.E., Blumenkrantz, A.R. and Taborek, J. 'Performance evaluation criteria for enhanced heat transfer surfaces', Proc. of 5th Int. Ht. Trans. Conf., Vol. 2, 239-243, 1974.
30. Eissenberg, D.M. and Bogue, D. 'Tests of an enhanced horizontal tube condenser under conditions of horizontal steam cross flow', 4th Int. Ht. Transf. Conf., Paris, Paper HE2.1.
31. Withers, J.G. and Young, E.H. 'Steam condensing on vertical rows of horizontal corrugated and plain tubes', Ind. and Eng. Chem. Process Design and Dev., 10(1), 19-30, 1971.
32. Catchpole, J.P. and Drew, B.C.H. 'Evaluation of some shaped tubes for steam condensers', NEL Report No. 619, 68-83, 1976.
33. Cunningham, J. and Milne, H.K. 'The effect of helix angle on the performance of roped tubes', 6th Int. Ht. Transf. Conf., Toronto, Vol. 2, 601-605, 1978.
34. Mimura, K. and Isozaki, A. 'Heat transfer and pressure drop of corrugated tubes', Desalination, 22, 131-139, 1977.
35. Mehta, M.H. and Rao, M.R. 'Heat transfer and frictional characteristics of spirally enhanced tubes for horizontal condensers', Advances in Enhanced Heat Transfer, ASME, New York, 11-21, 1979.

36. Marto, P.J., Reilly, D.J. and Fenner, J.H. 'An experimental comparison of enhanced heat transfer condenser tubing', *Advances in Enhanced Heat Transfer*, ASME, New York, 1-10, 1979.
37. Sethumadhavan, R. and Rao, M.R. 'Turbulent flow friction and heat transfer characteristics of single and multistart spirally enhanced tubes', *J. of Heat Transfer*, Vol. 108, 55-61, 1986.
38. Baghernejad, M., 'Condensate inundation in horizontal roped tube bundles', PhD dissertation, University of Glasgow, 1987.
39. Ben Boudinar, M. 'Effect of condensate inundation on roped tubes', MSc dissertation, University of Glasgow, 1988.
40. Cunningham, J. and Ben Boudinar, M. 'The effect of condensate inundation on the performance of roped tubes', unpublished.
41. Cunningham, J. and Baghernejad, M. 'The effect of vapour shear and condensate drainage in condensers using roped tubes', *desalination*, 45, 135-142, 1983.
42. Gregorig, R. 'Zeitschrift fur angewandte', *Mathematikund Physik* 5, 36-49, 1954 (Translation by D.K. Edwards, UCLA)
43. Webb, R.L. 'A generalised procedure for the design and optimisation of fluted Gregorig condensing surfaces', *J. of Heat Transfer*, Vol. 101, 335-339, 1979.
44. Pearce, D.L. 'Prospects for spirally-roped condenser tubes' Powergen Division, CEGB.
45. Gogonin, I.I. and Dorokhov, A.R., *Zh. Prikl. Mekh. Tekh. Fiz*, 1971(2).
46. Sugawara, S., Michiyoshi, T. and Mimamiyona, T. 'The condensation of vapour flowing normal to a horizontal pipe', *Proc. 6th Japan Nat. Congr. Appl. Mech.* 385-388, 1956.
47. Denny, V.E. and Mills, A.F. 'Laminar film condensation of a flowing vapour on a horizontal cylinder at normal gravity', *J. of Heat Transfer*, Vol. 91, 495-501, 1969.

48. Aoune, A. and Burnside, B.M. 'Vapour shear effects on tubes in a horizontal row in downwards condensing flow', Proceedings 2nd Int. Symp. Condensers and Condensation, Bath, 461-472, 1990.
49. Nicol, A.A. and Wallace, D.J. 'The influence of vapour shear force on condensation on a cylinder', Multi-phase Flow Systems, I.Chem.E. Symp. Ser. No. 38, Vol. 1, Paper D3, 1974.
50. Heat Exchanger Institute; Standards for Steam Surface Condensers, 6th Ed. (1970).
51. Katz, D.L. and Geist, J.M. 'Condensation on six finned tubes in a vertical row', Trans. ASME, 70, 907, 1948.
52. 'YIM heat exchanger tubes: design data for horizontal roped tubes in steam condensers', Technical Memorandum 3, Leeds, 1976.
53. Withers, J.G., Young, E.H. and Lambert, W.B. 'Heat transfer characteristics of corrugated tubes in steam condensing applications', Chem. Engng. Symp. Series, No. 174, Vol. 14, 15-24, 1978.
54. Hilarionos, P., 'Computer design of surface condensers', Final Year Honours Project, Department of Mechanical Engineering, University of Glasgow, 1986.
55. Rogers, G.F.C. and Mayhew, Y.R. 'Thermodynamic and transport properties of fluids - SI units', 4th edition, Basil Blackwell Publishers.
56. Van der Hegge Zijnen, B.G. 'Flow through uniformly tapped pipes', Appl. Sci. Res., Vol. A3, 144-163.

APPENDIX A

DERIVATION OF THE OUTER TUBE WALL TEMPERATURE EXPRESSION

To obtain an expression that was dependant on the terms T_{wi} and dT , it was necessary to begin with the following two equations:

$$dX = \frac{dQ}{\pi D_i \alpha_i (T_{wi} - T_{cw})} \quad (2.13)$$

and

$$dQ = \frac{2\pi \lambda_{tw} dX}{\ln\left(\frac{r_o}{r_i}\right)} (T_{wo} - T_{wi}) \quad (2.10)$$

Eqn (2.13) was then substituted into (2.10)

$$dQ = \frac{2\pi \lambda_{tw}}{\ln\left(\frac{r_o}{r_i}\right)} \frac{dQ}{\pi D_i \alpha_i (T_{wi} - T_{cw})} (T_{wo} - T_{wi})$$

$$dQ = \frac{2\pi \lambda_{tw} dQ T_{wo}}{\ln\left(\frac{r_o}{r_i}\right) \pi D_i \alpha_i (T_{wi} - T_{cw})} - \frac{2\pi \lambda_{tw} dQ T_{wi}}{\ln\left(\frac{r_o}{r_i}\right) \pi D_i \alpha_i (T_{wi} - T_{cw})}$$

$$\frac{2\pi \lambda_{tw} T_{wo}}{\ln\left(\frac{r_o}{r_i}\right) \pi D_i \alpha_i (T_{wi} - T_{cw})} - \frac{2\pi \lambda_{tw} T_{wi}}{\ln\left(\frac{r_o}{r_i}\right) \pi D_i \alpha_i (T_{wi} - T_{cw})} = 0$$

$$\pi D_i \alpha_i (T_{wi} - T_{cw}) = \frac{2\pi \lambda_{tw} T_{wo}}{\ln\left(\frac{r_o}{r_i}\right)} - \frac{2\pi \lambda_{tw} T_{wi}}{\ln\left(\frac{r_o}{r_i}\right)}$$

$$D_i \alpha_i (T_{wi} - T_{cw}) = \frac{2 \lambda_{tw} T_{wo}}{\ln\left(\frac{r_o}{r_i}\right)} - \frac{2 \lambda_{tw} T_{wi}}{\ln\left(\frac{r_o}{r_i}\right)}$$

$$D_i \alpha_i T_{wi} - D_i \alpha_i T_{cw} = \frac{2 \lambda_{tw} T_{wo}}{\ln\left(\frac{r_o}{r_i}\right)} - \frac{2 \lambda_{tw} T_{wi}}{\ln\left(\frac{r_o}{r_i}\right)}$$

$$D_i \alpha_i T_{wi} + \frac{2 \lambda_{tw} T_{wo}}{\ln\left(\frac{r_o}{r_i}\right)} = \frac{2 \lambda_{tw} T_{wi}}{\ln\left(\frac{r_o}{r_i}\right)} + D_i \alpha_i T_{cw}$$

$$T_{wi} \left[D_i \alpha_i + \frac{2 \lambda_{tw}}{\ln\left(\frac{r_o}{r_i}\right)} \right] = D_i \alpha_i T_{cw} + \frac{2 \lambda_{tw} T_{wo}}{\ln\left(\frac{r_o}{r_i}\right)} \quad (2.14)$$

Then Eqn (2.13) was substituted into Eqn (2.11)

$$dQ = \alpha_o A_o (T_s - T_{wo}) \quad (2.11)$$

$$dQ = dX \pi D_i \alpha_i (T_{wi} - T_{cw}) = \alpha_o A_o (T_s - T_{wo}) = \alpha_o \pi D_o dX (T_s - T_{wo})$$

$$\therefore dX \pi D_i \alpha_i (T_{wi} - T_{cw}) = \alpha_o \pi D_o dX (T_s - T_{wo})$$

$$D_i \alpha_i (T_{wi} - T_{cw}) = \alpha_o D_o (T_s - T_{wo})$$

$$T_{wi} - T_{cw} = \frac{\alpha_o D_o}{\alpha_i D_i} (T_s - T_{wo})$$

$$T_{wi} = \frac{\alpha_o D_o}{\alpha_i D_i} (T_s - T_{wo}) + T_{cw} \quad (2.15)$$

Eqn. (2.15) was then substituted into Eqn. (2.14) to find an expression for T_{wo}

$$\therefore \left[\frac{\alpha_o D_o}{\alpha_i D_i} (T_s - T_{wo}) + T_{cw} \right] \left[\alpha_i D_i + \frac{2 \lambda_{tw}}{\ln\left(\frac{r_o}{r_i}\right)} \right] = \alpha_i D_i T_{cw} + \frac{2 \lambda_{tw} T_{wo}}{\ln\left(\frac{r_o}{r_i}\right)}$$

$$\begin{aligned} \frac{\alpha_o D_o}{\alpha_i D_i} (T_s - T_{wo}) \alpha_i D_i + \frac{\alpha_o D_o}{\alpha_i D_i} (T_s - T_{wo}) \frac{2 \lambda_{tw}}{\ln\left(\frac{r_o}{r_i}\right)} + T_{cw} \alpha_i D_i + \frac{2 \lambda_{tw} T_{cw}}{\ln\left(\frac{r_o}{r_i}\right)} \\ = \alpha_i D_i T_{cw} + \frac{2 \lambda_{tw} T_{wo}}{\ln\left(\frac{r_o}{r_i}\right)} \end{aligned}$$

$$\alpha_o D_o (T_s - T_{wo}) + \frac{\alpha_o D_o}{\alpha_i D_i} (T_s - T_{wo}) \frac{2 \lambda_{tw}}{\ln\left(\frac{r_o}{r_i}\right)} + \frac{2 \lambda_{tw} T_{cw}}{\ln\left(\frac{r_o}{r_i}\right)} = \frac{2 \lambda_{tw} T_{wo}}{\ln\left(\frac{r_o}{r_i}\right)}$$

$$\begin{aligned} \alpha_o D_o T_s - \alpha_o D_o T_{wo} + \frac{\alpha_o D_o}{\alpha_i D_i} (T_s) \frac{2 \lambda_{tw}}{\ln\left(\frac{r_o}{r_i}\right)} - \frac{\alpha_o D_o}{\alpha_i D_i} \frac{2 \lambda_{tw}}{\ln\left(\frac{r_o}{r_i}\right)} T_{wo} + \frac{2 \lambda_{tw} T_{cw}}{\ln\left(\frac{r_o}{r_i}\right)} \\ = \frac{2 \lambda_{tw} T_{wo}}{\ln\left(\frac{r_o}{r_i}\right)} \end{aligned}$$

$$\begin{aligned} \alpha_o D_o T_s + \frac{\alpha_o D_o}{\alpha_i D_i} \frac{2 \lambda_{tw}}{\ln\left(\frac{r_o}{r_i}\right)} T_s + \frac{2 \lambda_{tw} T_{cw}}{\ln\left(\frac{r_o}{r_i}\right)} = \alpha_o D_o T_{wo} + \frac{\alpha_o D_o 2 \lambda_{tw}}{\alpha_i D_i \ln\left(\frac{r_o}{r_i}\right)} T_{wo} \\ + \frac{2 \lambda_{tw} T_{wo}}{\ln\left(\frac{r_o}{r_i}\right)} \end{aligned}$$

The entire expression was then multiplied by $\frac{1}{\alpha_0 D_o}$

$$\therefore T_s + \frac{2 \lambda_{tw}}{\alpha_i D_i \ln\left(\frac{r_o}{r_i}\right)} T_s + \frac{2 \lambda_{tw} T_{cw}}{\alpha_o D_o \ln\left(\frac{r_o}{r_i}\right)} = T_{wo} + \frac{2 \lambda_{tw} T_{wo}}{\alpha_i D_i \ln\left(\frac{r_o}{r_i}\right)} + \frac{2 \lambda_{tw} T_{wo}}{\alpha_o D_o \ln\left(\frac{r_o}{r_i}\right)}$$

$$T_s \left(1 + \frac{2 \lambda_{tw}}{\alpha_i D_i \ln\left(\frac{r_o}{r_i}\right)}\right) + \frac{2 \lambda_{tw} T_{cw}}{\alpha_o D_o \ln\left(\frac{r_o}{r_i}\right)} = T_{wo} \left(1 + \frac{2 \lambda_{tw}}{\alpha_i D_i \ln\left(\frac{r_o}{r_i}\right)}\right) + \frac{2 \lambda_{tw} T_{wo}}{\alpha_o D_o \ln\left(\frac{r_o}{r_i}\right)}$$

$$\text{Let } G1 = \frac{2 \lambda_{tw}}{D_o \ln\left(\frac{r_o}{r_i}\right)} \quad \text{and } G2 = \left(1 + \frac{2 \lambda_{tw}}{\alpha_i D_i \ln\left(\frac{r_o}{r_i}\right)}\right)$$

$$\therefore T_s G2 + \frac{T_{cw}}{\alpha_o} G1 = T_{wo} G2 + \frac{T_{wo}}{\alpha_o} G1$$

$$T_s G2 + \frac{T_{cw}}{\alpha_o} G1 = T_{wo} \left(G2 + \frac{G1}{\alpha_o}\right)$$

$$\alpha_o T_s G2 + T_{cw} G1 = T_{wo} (\alpha_o G2 + G1)$$

$$T_{wo} = \frac{\alpha_o T_s G2 + T_{cw} G1}{\alpha_o G2 + G1} \quad (2.18)$$

Now it was necessary to find an alternate form of α_o that did not contain the term T_{wo} .

Therefore eqn. (1.30) was substituted into (1.4)

$$\alpha_o = 0.725 \left(\frac{g \lambda_f^3 \rho_f (\rho_f - \rho_g) h_{fg}}{\mu_f D_o (T_s - T_{wo})} \right)^{1/4} \quad (1.4)$$

$$h_{fg}' = h_{fg} + 3/8 C_{pf} (T_s - T_{wo}) = h_{fg} \left(X_f + \frac{0.68 C_{pf} (T_s - T_{wo})}{h_{fg}} \right)$$

$$\alpha_o = 0.725 \left(\frac{g \lambda_f^3 \rho_f (\rho_f - \rho_g) \left(h_{fg} \left(X_f + \frac{0.68 C_{pf} (T_s - T_{wo})}{h_{fg}} \right) \right)}{\mu_f D_o (T_s - T_{wo})} \right)^{1/4}$$

$$\alpha_o = 0.725 \left(\frac{g \lambda_f^3 \rho_f (\rho_f - \rho_g) \left(X_f h_{fg} + \frac{0.68 h_{fg} C_{pf} (T_s - T_{wo})}{h_{fg}} \right)}{\mu_f D_o (T_s - T_{wo})} \right)^{1/4}$$

$$\alpha_o = 0.725 \left(\frac{g \lambda_f^3 \rho_f (\rho_f - \rho_g) X_f h_{fg} + g \lambda_f^3 \rho_f (\rho_f - \rho_g) (0.68) C_{pf} (T_s - T_{wo})}{\mu_f D_o (T_s - T_{wo})} \right)^{1/4}$$

$$\alpha_o = 0.725 \left(\frac{g \lambda_f^3 \rho_f (\rho_f - \rho_g) X_f h_{fg}}{\mu_f D_o (T_s - T_{wo})} + \frac{g \lambda_f^3 \rho_f (\rho_f - \rho_g) (0.68) C_{pf} (T_s - T_{wo})}{\mu_f D_o (T_s - T_{wo})} \right)^{1/4}$$

$$\alpha_o = 0.725 \left(\frac{g \lambda_f^3 \rho_f (\rho_f - \rho_g) X_f h_{fg}}{\mu_f D_o (T_s - T_{wo})} + \frac{g \lambda_f^3 \rho_f (\rho_f - \rho_g) (0.68) C_{pf}}{\mu_f D_o} \right)^{1/4}$$

At this point it was assumed that ρ_g was small in comparison to ρ_f and that $X_f=1.0$

$$\alpha_o = 0.725 \left(\frac{g \lambda_f^3 \rho_f^2 h_{fg}}{\mu_f D_o (T_s - T_{wo})} + \frac{g \lambda_f^3 \rho_f^2 (0.68) C_{pf}}{\mu_f D_o} \right)^{1/4}$$

$$\text{Let } P = \frac{\rho_f^2 g \lambda_f^3}{\mu_f D_o} \quad RA = 0.68 C_{pf} \quad \Delta T = T_s - T_{wo}$$

Therefore

$$\alpha_o = 0.725 \left(\frac{P h_{fg}}{\Delta T} + RA \right)^{1/4} \quad (2.19)$$

With eqn. (2.18) and eqn. (2.19) it was now possible to find the final expression for T_{wo} .

$$T_{wo} = \frac{T_{cw} G1 + \alpha_o T_s G2}{\alpha_o G2 + G1} \quad (2.18)$$

$$T_{wo}(\alpha_o G2 + G1) = T_{cw} G1 + \alpha_o T_s G2$$

$$T_{wo} \alpha_o G2 + T_{wo} G1 = T_{cw} G1 + \alpha_o T_s G2$$

$$T_{wo} \alpha_o G2 + T_{wo} G1 - T_{cw} G1 - \alpha_o T_s G2 = 0$$

$$T_{wo} \alpha_o G2 - \alpha_o T_s G2 + T_{wo} G1 - T_{cw} G1 = 0$$

$$\alpha_o G2 (T_{wo} - T_s) + T_{wo} G1 - T_{cw} G1 = 0$$

The above expression for α_o , eqn. (2.19) was then used to determine the final expression $f(T_{wo})$

$$f(T_{wo}) = 0.725 \left(\frac{p h_{fg}}{\Delta T} + RA \right)^{1/4} G2 (T_{wo} - T_s) + T_{wo} G1 - T_{cw} G1 = 0 \quad (2.22)$$

In order to evaluate T_{wo} with the Newton-Raphson iterative method the derivative of eqn. (2.22) was required. Start with the derivative of eqn. (2.19) which was used in eqn. (2.22).

$$\alpha_o = 0.725 \left(\frac{p h_{fg} X_f}{\Delta T} + RA \right)^{1/4}$$

$$\text{Let PR1} = \frac{p h_{fg} X_f}{\Delta T}$$

The derivative of PR1 was

$$\frac{d}{dT} = p h_{fg} X_f \Delta T^{-2}$$

$$\text{Let PR2} = \frac{p h_{fg} X_f}{\Delta T^2}$$

With PR1 and PR2 the derivative of α_0 was now possible.

$$\therefore \frac{d \alpha_0}{dT} = \left(\frac{1}{4}\right)(0.725) \left(\frac{p h_{fg} X_f}{\Delta T} + RA\right)^{1/4 - 1} \left(\frac{p h_{fg} X_f}{\Delta T^2}\right)$$

$$\frac{d \alpha_0}{dT} = 0.181 \left(\frac{p h_{fg} X_f}{\Delta T} + RA\right)^{-3/4} \left(\frac{p h_{fg} X_f}{\Delta T^2}\right)$$

$$\frac{d \alpha_0}{dT} = 0.181 \text{ PR2} \left(\text{PR1} + RA\right)^{-3/4}$$

Now that $\frac{d \alpha_0}{dT}$ has been obtained $f'(T_{wo})$ could be calculated.

Therefore, the function and the first derivative of T_{wo} were found to be as follows:

$$\therefore f(T_{wo}) = 0.725 \left(\frac{p h_{fg}}{\Delta T} + RA\right)^{1/4} G2 (T_{wo} - T_s) + T_{wo} G1 - T_{cw} G1$$

$$\therefore f'(T_{wo}) = \frac{d \alpha_0}{dT} G2 (T_{wo} - T_s) + \alpha_0 G2 + G1 \quad (2.23)$$

APPENDIX B

DERIVATION OF THE INNER TUBE WALL TEMPERATURE EXPRESSION

To begin the derivation of the $f(T_{wi})$ and $f'(T_{wi})$ terms necessary for the Newton-Raphson method, eqns. (2.14) and (2.15) needed to be rearranged. Thus,

$$T_{wi} = \frac{\alpha_o D_o}{\alpha_i D_i} (T_s - T_{wo}) + T_{cw} \quad (2.15)$$

$$T_{wi} - T_{cw} = \frac{\alpha_o D_o}{\alpha_i D_i} (T_s - T_{wo})$$

$$\frac{\alpha_i D_i}{\alpha_o D_o} (T_{wi} - T_{cw}) = T_s - T_{wo}$$

$$T_{wo} = T_s - \frac{\alpha_i D_i}{\alpha_o D_o} (T_{wi} - T_{cw})$$

$$T_{wo} = T_s - \frac{\alpha_i D_i}{\alpha_o D_o} T_{wi} + \frac{\alpha_i D_i}{\alpha_o D_o} T_{cw} \quad (2.25)$$

and

$$T_{wi} \left(D_i \alpha_i + \frac{2 \lambda_{tw}}{\ln\left(\frac{r_o}{r_i}\right)} \right) = D_i \alpha_i T_{cw} + \frac{2 \lambda_{tw} T_{wo}}{\ln\left(\frac{r_o}{r_i}\right)} \quad (2.14)$$

$$T_{wi} \left(1 + \frac{2 \lambda_{tw}}{D_i \alpha_i \ln\left(\frac{r_o}{r_i}\right)} \right) = T_{cw} + \frac{2 \lambda_{tw} T_{wo}}{D_i \alpha_i \ln\left(\frac{r_o}{r_i}\right)} \quad (2.14)$$

$$\text{Let } G2 = 1 + \frac{2 \lambda_{tw}}{D_i \alpha_i \ln\left(\frac{r_o}{r_i}\right)}$$

$$\therefore T_{wi} G2 = T_{cw} + \frac{2 \lambda_{tw} T_{wo}}{D_i \alpha_j \ln\left(\frac{r_o}{r_i}\right)} \quad (2.26)$$

Eqn. (2.25) was then substituted into eqn. (2.26)

$$\therefore T_{wi} G2 = T_{cw} + \frac{2 \lambda_{tw}}{D_i \alpha_j \ln\left(\frac{r_o}{r_i}\right)} \left(T_s - \frac{\alpha_j D_i}{\alpha_o D_o} T_{wi} + \frac{\alpha_j D_i}{\alpha_o D_o} T_{cw} \right)$$

$$T_{wi} G2 = T_{cw} + \frac{2 \lambda_{tw} T_s}{D_i \alpha_j \ln\left(\frac{r_o}{r_i}\right)} - \frac{2 \lambda_{tw} \alpha_j D_i T_{wi}}{\alpha_j D_i \alpha_o D_o \ln\left(\frac{r_o}{r_i}\right)} + \frac{2 \lambda_{tw} \alpha_j D_i T_{cw}}{D_i \alpha_j D_o \alpha_o \ln\left(\frac{r_o}{r_i}\right)}$$

$$T_{wi} G2 = T_{cw} + \frac{2 \lambda_{tw} T_s}{D_i \alpha_j \ln\left(\frac{r_o}{r_i}\right)} - \frac{2 \lambda_{tw} T_{wi}}{\alpha_o D_o \ln\left(\frac{r_o}{r_i}\right)} + \frac{2 \lambda_{tw} T_{cw}}{D_o \alpha_o \ln\left(\frac{r_o}{r_i}\right)}$$

$$T_{wi} G2 = T_{cw} + \frac{2 \lambda_{tw} T_s}{D_i \alpha_j \ln\left(\frac{r_o}{r_i}\right)} + \frac{2 \lambda_{tw}}{\alpha_o D_o \ln\left(\frac{r_o}{r_i}\right)} (T_{cw} - T_{wi})$$

$$\text{Let } G1 = \frac{2 \lambda_{tw}}{D_o \ln\left(\frac{r_o}{r_i}\right)}$$

$$\therefore T_{wi} G2 = T_{cw} + \frac{2 \lambda_{tw} T_s}{D_i \alpha_j \ln\left(\frac{r_o}{r_i}\right)} + \frac{G1}{\alpha_o} (T_{cw} - T_{wi})$$

$$T_{wi} G2 = T_{cw} + \frac{2 \lambda_{tw} T_s}{D_i \alpha_j \ln\left(\frac{r_o}{r_i}\right)} + \frac{G1}{\alpha_o} T_{cw} - \frac{G1}{\alpha_o} T_{wi}$$

$$T_{wi} G2 + \frac{G1}{\alpha_0} T_{wi} = \frac{2 \lambda_{tw} T_s}{D_i \alpha_i \ln\left(\frac{r_o}{r_i}\right)} + T_{cw} + \frac{G1}{\alpha_0} T_{cw}$$

$$T_{wi} \left(G2 + \frac{G1}{\alpha_0} \right) = \frac{2 \lambda_{tw} T_s}{D_i \alpha_i \ln\left(\frac{r_o}{r_i}\right)} + T_{cw} \left(1 + \frac{G1}{\alpha_0} \right)$$

$$\text{Let } G2 - 1 = \frac{2 \lambda_{tw}}{D_i \alpha_i \ln\left(\frac{r_o}{r_i}\right)}$$

$$\therefore T_{wi} \left(G2 + \frac{G1}{\alpha_0} \right) = (G2 - 1) T_s + T_{cw} \left(1 + \frac{G1}{\alpha_0} \right)$$

$$\therefore T_{wi} \left(G2 + \frac{G1}{\alpha_0} \right) - T_{cw} \left(1 + \frac{G1}{\alpha_0} \right) - T_s (G2 - 1) = 0 \quad (2.27)$$

Therefore, the function and derivative of T_{wi} were found to be:

$$f(T_{wi}) = T_{wi} \left(G2 + \frac{G1}{\alpha_0} \right) - T_{cw} \left(1 + \frac{G1}{\alpha_0} \right) - T_s (G2 - 1) \quad (2.28)$$

$$f'(T_{wi}) = G2 + \frac{G1}{\alpha_0} \quad (2.29)$$

APPENDIX C

POLYNOMIALS FOR PREDICTING THE PROPERTIES OF WATER

A) Density: ρ in [kg/m³]

$$\rho = 1003.7 - 0.174 \frac{[T]}{[^{\circ}\text{C}]} - 0.00277 \frac{[T]^2}{[^{\circ}\text{C}]}$$

$$15 \leq \frac{[T]}{[^{\circ}\text{C}]} < 100$$

B) Viscosity: μ in [kg/ms]

$$\frac{1}{\mu} = 560.4 + 19.21 \frac{[T]}{[^{\circ}\text{C}]} + 0.139 \frac{[T]^2}{[^{\circ}\text{C}]} - 3.382 \frac{[T]^3}{[^{\circ}\text{C}]} \times 10^{-4}$$

$$0.01 < \frac{[T]}{[^{\circ}\text{C}]} < 100$$

C) Specific Heat: C_p in [kJ/kg °C]

$$C_p = 4.215 - 2.229 \frac{[T]}{[^{\circ}\text{C}]} \times 10^{-3} + 3.772 \frac{[T]^2}{[^{\circ}\text{C}]} \times 10^{-5} -$$

$$1.536 \frac{[T]^3}{[^{\circ}\text{C}]} \times 10^{-7}$$

$$0.01 < \frac{[T]}{[^{\circ}\text{C}]} < 100$$

D) Thermal Conductivity: λ in [kW/m °C]

$$\lambda = 5.707 \times 10^4 + 1.78 \frac{[T]}{[^\circ\text{C}]} \times 10^{-6} -$$

$$6.781 \frac{[T]^2}{[^\circ\text{C}]} \times 10^{-9}$$

$$15 < \frac{[T]}{[^\circ\text{C}]} < 100$$

APPENDIX D

THE PLAIN TUBE PROGRAM

```
C*****
C   - THE BASIC PROCEDURE USED IS KNOWN AS THE POINTWISE
C   HEAT EXCHANGER RATING METHOD.
C   - THIS PROGRAM EVALUATES THE DIFFERENT PARAMETERS OF
C   HEAT TRANSFER FOR A VERTICAL ARRAY OF HORIZONTAL PLAIN TUBES
C   WITH STEAM CONDENSING WITH THE FOLLOWING CHARACTERISTICS :
C   * DOWNWARD STEAM FLOW OVER VERTICAL ARRAY OF HORIZONTAL TUBES.
C   * STAGNANT OR LOW STEAM VELOCITY.
C   * STEAM SATURATED THROUGHOUT.
C   * ABSCENCE OF NON-CONDENSABLE GASES.
C*****
C   ****DEFINITION OF DATA SYMBOLS****
C*****
C DT10: INITIAL GUESS FOR COOLING WATER TEMP. RISE ALONG INCREMENT DXG
C TW10: INITIAL GUESS FOR INNER TUBE WALL TEMP.
C TW01: INITIAL GUESS FOR OUTER TUBE WALL TEMP.
C CI:PARAMETER THAT DECIDES WHICH CORRELATION
C     IS USED FOR THE ESTIMATION OF THE WATER-SIDE
C     HEAT TRANSFER COEFFICIENT, THAT IS:
C   CI=1.0: DITTUS-BOELTER EQUATION
C   CI=2.0: SIEDER-TATE EQUATION
C   CI=3.0: ALLAN AND ECKERT EQUATION
C COR : PARAMETER THAT DECIDES WHICH CORRELATION IS
C       USED FOR THE ESTIMATION OF THE CONDENSATE H.T.C
C       WHEN CONSIDERING THE TUBES BELOW THE TOP ONE:
C   COR=1.0: FUKS CORRELATION
C   COR=2.0: GRANT AND OSMENT CORRELATION
C   COR=3.0: NUSSELT CORRELATION
C   COR=4.0: KERN'S CORRELATION
C DI:INSIDE TUBE DIAMETER
C DO:OUTSIDE TUBE DIAMETER
C DXG:INCREMENTAL LENGTH
C OTL:TUBE LENGTH
C NTB:NUMBER OF TUBES CONSIDERED IN A VERTICAL ARRAY
C TWK: THERMAL CONDUCTIVITY OF TUBE MATERIAL
C CBL:CONDENSER BOX LENGHT
C CBW:CONDENSER BOX WIDTH
C COVV:PARAMETER WHICH DETERMINES THE CORRELATION USED
C     TO CALCULATE THE H.T.C WITH THE EFFECTS OF
C     VAPOUR VELOCITY INCLUDED
C   COVV=1.0: FUKS EQN
C   COVV=2.0: SHEKRILADZE EQN
C   COVV=3.0: BERMAN EQN
C   COVV=4.0: BERMAN AND TUMANOV EQN
C EQD:BUNDLE WIDTH
C VV:VAPOUR VELOCITY
C PST:STEAM PRESSURE
C XF: DRYNESS FRACTION OF STEAM.
C EPS:CONVERGENCE CRITERION FOR DIFFERENT ITERATIONS
C NPTS:NUMBER OF DIFFERENT SETS OF INPUT DATA VARIABLES
C T1(I):INLET COOLING WATER TEMP.
C VICW(I):COOLING WATER VELOCITY
C*****
C   ****DEFINITION OF SYMBOLS USED****
C*****
C AO:OUTSIDE SURFACE AREA OF TUBE
C AI:INSIDE SURFACE AREA OF TUBE
C MI: NUMBER OF INCREMENTS(SECTIONS) PER TUBE
C HFG: LATENT HEAT OF VAPOURISATION
C G: ACCELERATION OF GRAVITY
C TI(L,M):INLET CW TEMP. FOR THE L.th INCREMENT AND M.th TUBE
C DT(L,M):CW TEMP RISE FOR '.....'
C TO(L,M):OUTLET CW TEMP.FOR'.....'
C TWI(L,M):INNER TUBE TEMP FOR '.....'
C TWO(L,M):OUTER TUBE TEMP FOR '.....'
C HW(L,M):WATER-SIDE H.T.COEFF. FOR'.....'
C HF(L,M):CONDENSATE H.T.COEFF. FOR'.....'
C OHTC(L,M):OVERALL H.T.COEFF. FOR'.....'
```

```
C MCW(L,M):COOL. WATER FLOWRATE FOR '
C DQ(L,M):HEAT LOAD FOR '
C DMC(L,M):CONDENSATE FLOWRATE FOR '
C TCW(L,M):MEAN COOL.WATER TEMP. FOR'
C TAW(L,M):MEAN BULK COOL. WATER TEMP. FOR'
C THT(L,M): TERM USED FOR SUMMATION OF INCREMENTAL HEAT LOADS ALONG TUBE
C LENGTH
C TACP(L,M): 'CONDENSATE RATE '
C AOH (L,M):'OHTC '
C AWC(L,M):'WATERSIDE H.T.C '
C ACF(L,M):'CONDENSING SIDE H.T.C '
C TIT (L,M): 'INNER TUBE WALL TP '
C TOT(L,M): 'OUTER TUBE WALL TP '
C STACP(L,M):CONDENSATE LOAD ON THE L.th INCREMENT OF THE M.th TUBE
C TERM USED FOR CALCULATION OF CONDENSING h.t.c FOR TUBES BELOW
C TOP ONE.
C SUM(L,M): INCREMENTAL LENGTH SUMMATION ALONG ENTIRE TUBE LENGTH
C ( AS TO TELL THE PROGRAM WHEN TO STOP )
C THT1(I,MI+1,M):TOTAL HEAT LOAD FOR M.th TUBE AND I.th INLET CONDITION
C TO1(I,MI+1,M):OUTLET CW TEMP FOR'
C TACP1(I,MI+1,M):CONDENSATE FLOWRATE'
C AOHTC(I,MI+1,M):AVERAGE OVERALL H.T.C'
C AWTC(I,MI+1,M):AVERAGE WATERSIDE H.T.C'
C ACFC(I,MI+1,M):AVERAGE CONDENSATE H.T.C'
C TIT1(I,MI+1,M):AVERAGE INNER TUBE WALL TEMP'
C TOT1(I,MI+1,M):AVERAGE OUTER TUBE WALL TEMP'
C THTF(I,MI+1,M):TOTAL CONDENSER HEAT LOAD
C TO1CF(I,MI+1,M):AVERAGE CONDENSER OUTLET COOL. WATER TEMP.
C TACPF(I,MI+1,M):TOTAL CONDENSER CONDENSATE MASS-FLOWRATE
C AOHTCF(I,MI+1,M):AVERAGE CONDENSER OVERALL H.T.COEFF.
C AWTCF(I,MI+1,M):AVERAGE CONDENSER WATER-SIDE H.T.COEFF.
C ACFCF(I,MI+1,M):AVERAGE CONDENSER CONDENSATE H.T.COEFF.M
C***** DECLARATION OF ARRAY VARIABLES *****
REAL TI(25,25),DT(25,25),TO(25,25),TW1(25,25),
* TW0(25,25),HW(25,25),MCW(25,25),DQ(25,25),
* DMC(25,25),TCW(25,25),HF(25,25),OHTC(25,25),
* TAW(25,25),DETW(25,25),ZTW(25,25),
* STACP(25,25),
* CETW(25,25),TB(25,25),THT(25,25),TACP(25,25),
* AOH(25,25),AWC(25,25),ACF(25,25),SUM(25,25),CPFT(25,25),
* CPTW(25,25),THT1(25,25,25),TO1(25,25,25),
* TACP1(25,25,25),ACFC(25,25,25),
* AOHTC(25,25,25),AWTC(25,25,25),
* TCF(25,25),ACFCF(25,25,25),
* THTF(25,25,25),TO1F(25,25,25),TACPF(25,25,25),
* AOHTF(25,25,25),AWTF(25,25,25),ACFF(25,25,25),
* TO1CF(25,25,25),AOHTCF(25,25,25),AWTCF(25,25,25),
* TIT1(25,25,25),TOT1(25,25,25),TIT(25,25),TOT(25,25)
DIMENSION T1(25),V1CW(25),A1(13),B1(13),C(36),D(36),E(36),F(36)
REAL HFG,G,PI,TS1,DHFG,XF,CBL,CBW,EQD,VV
REAL TT
INTEGER M,L,MI
C ***** INPUT DATA *****
READ(8,1) DT10,TW10,TW01,CI
READ(8,2) DI,DO,DXG,OTL
READ(8,3) NTB,TWK,PST,XF
READ(8,4) EPS,NPTS,COR
READ(8,5) CBL,CBW,COVV,VV
READ(8,6) (T1(I),V1CW(I),I=1,NPTS)
READ(8,7) (A1(I),B1(I),I=1,13)
READ(8,8) (C(I),D(I),E(I),F(I),I=1,36)
1 FORMAT(2X,F4.2,2X,F5.2,2X,F5.2,2X,F3.1)
2 FORMAT(2X,F5.3,2X,F5.3,2X,F7.5,2X,F5.3)
3 FORMAT(2X,I2,2X,F5.3,2X,F4.2,2X,F4.2)
4 FORMAT(2X,F6.4,2X,I2,2X,F3.1)
5 FORMAT(2X,F5.3,2X,F5.3,2X,F3.1,2X,F6.3)
6 FORMAT(2X,F5.2,2X,F5.3)
```

```
8      FORMAT(2X,F5.2,2X,F5.1,2X,F6.4,2X,F6.1)
C*****
C      G1: FACTOR USED IN THE ITERATIVE PROCEDURE
C      FOR CALCULATING TW1 AND TW0
C      G1=2.*TWK/(DO*LOG(DO/DI))
C      STEAM ASSUMED TO BE SATURATED
C      INTERPOLATION OF THE STEAM PROPERTIES FROM THE
C      GIVEN STEAM PRESSURE
C      CALL VPR(T,PST,C,D,E,F,TS1,DEV,HFG)
C      CALL VVIS(TS1,A1,B1,ZV)
C      CALCULATION OF BUNDLE WIDTH
C      EQD=(DO+(2.0*(1.25*DO))+(2.0*(DO/2.0)))*CBL
C      G=9.81
C      PI=3.14159
C      AI=PI*DI*DXG
C      AO=PI*DO*DXG
C      DC=DO/(0.01*DI)
C      MI: NUMBER OF TUBE INCREMENTS CONSIDERED
C      MI=OTL/DXG
C*****
C      ***** CALCULATIONS OF PROCESS VARIABLES *****
C*****
C      DO 91 I=1,NPTS
C      CALCULATIONS FOR FIRST TUBE
C      M=1
C      SET INITIAL VALUE OF PARAMETERS TO BE CALCULATED
C      EQUAL ZERO
C      L=1
C      THT(L,M)=0
C      TACP(L,M)=0
C      AOH(L,M)=0
C      AWC(L,M)=0
C      ACF(L,M)=0
C      SUM(L,M)=0
C      TIT(L,M)=0
C      TOT(L,M)=0
C      INCREMENTAL CALCULATIONS FOR TOP TUBE
C      DO 10 L=2,MI+1
C      IF(L.EQ.2) GOTO 9
C      GOTO 11
9      TI(L,M)=T1(I)
C      GOTO 12
11     TI(L,M)=TO(L-1,M)
12     TA=TI(L,M)
C      CALL TAR(DT10,TA,TS1,TB,TW1F,TW0F,HFF,HWF,DTF,AI,AO,EPS,G1,
C      * TW10,TW01,DI,DO,VICW(I),TWK,HFG,A,B,G,M,CI,OTL,XF,DC,
C      * COVV,DEV,VV,ZV,EQD)
C      DT(L,M)=DTF
C      TO(L,M)=TI(L,M)+DT(L,M)
C      TW1(L,M)=TW1F
C      TW0(L,M)=TW0F
C      HW(L,M)=HWF
C      SAI=PI*(DI**2.)/4.
C      TCW(L,M)=TI(L,M)+(DT(L,M)/2.)
C      TAW(L,M)=(TCW(L,M)+TW1(L,M))/2.
C      CALL ETA1(TAW(L,M),DE,Z,CP,CE)
C      DETW(L,M)=DE
C      CPTW(L,M)=CP
C      MCW(L,M)=SAI*DETW(L,M)*VICW(I)
C      DQ(L,M)=MCW(L,M)*CPTW(L,M)*DT(L,M)
C      TCF(L,M)=(TS1+TW0(L,M))/2.
C      CALL ETA1(TCF(L,M),DE,Z,CP,CE)
C      CPFT(L,M)=CP
C      DHFG: CORRECTED LATENT HEAT OF VAPOURISATION
C      DHFG=XF*HFG+((3./8.)*CPFT(L,M)*(TS1-TW0(L,M)))
C      DMC(L,M)=DQ(L,M)/DHFG
C      STACP(L,M)=DMC(L,M)
C      HFC(L,M)=HFC
```

```

OHTC(L,M)=1./((DO/(DI*HW(L,M)))+( ((DO/2.)*LOG(DO/DI))/TWK)+
* 1./HF(L,M))
THT(L,M)=THT(L-1,M)+DQ(L,M)
TACP(L,M)=TACP(L-1,M)+DMC(L,M)
AOH(L,M)=AOH(L-1,M)+(DXG*OHTC(L,M))
AWC(L,M)=AWC(L-1,M)+(DXG*HW(L,M))
ACF(L,M)=ACF(L-1,M)+(DXG*HF(L,M))
TIT(L,M)=TIT(L-1,M)+TW1(L,M)
TOT(L,M)=TOT(L-1,M)+TWO(L,M)
SUM(L,M)=SUM(L-1,M)+DXG
10 CONTINUE
C CALCULATION OF THE FINAL VARIABLES CHARACTERISTICS FOR TOP TUBE
THT1(I,MI+1,M)=THT(MI+1,M)
TO1(I,MI+1,M)=TO(MI+1,M)
TACP1(I,MI+1,M)=TACP(MI+1,M)
AOHTC(I,MI+1,M)=AOH(MI+1,M)/SUM(MI+1,M)
AWTC(I,MI+1,M)=AWC(MI+1,M)/SUM(MI+1,M)
ACFC(I,MI+1,M)=ACF(MI+1,M)/SUM(MI+1,M)
TIT1(I,MI+1,M)=TIT(MI+1,M)/MI
TOT1(I,MI+1,M)=TOT(MI+1,M)/MI
C CALCULATIONS FOR THE TUBES BELOW THE TOP ONE.
DO 20 M=2,NTB
K=M
L=1
THT(L,M)=0
TACP(L,M)=0
AOH(L,M)=0
AWC(L,M)=0
ACF(L,M)=0
SUM(L,M)=0
TIT(L,M)=0
TOT(L,M)=0
DO 30 L=2,MI+1
IF(L.EQ.2) GOTO 51
GOTO 52
51 TI(L,M)=T1(I)
GOTO 53
52 TI(L,M)=TO(L-1,M)
C EVALUATION OF CONDENSING h.t.c FOR TUBES BELOW THE TOP ONE
53 IF(COR.EQ.1.0) GOTO 22
GOTO 23
22 HF(L,M)=HF(L,1)*((1+(STACP(L,M-1)/DMC(L,M-1)))*(-0.07))
GOTO 29
23 IF(COR.EQ.2.0) GOTO 24
GOTO 25
24 HF(L,M)=HF(L,1)*((1+(STACP(L,M-1)/DMC(L,M-1)))*(-0.223))
GOTO 29
25 IF(COR.EQ.3.0) GOTO 26
GOTO 27
26 HF(L,M)=HF(L,1)*((M**0.75)-((M-1)**0.75))
GOTO 29
27 IF(COR.EQ.4.0) GOTO 28
GOTO 29
28 HF(L,M)=HF(L,1)*((M**(5./6.))-((M-1)**(5./6.)))
29 CONTINUE
HFF=HF(L,M)
TIA=TI(L,M)
CALL RAT(DT10,TIA,TS1,TB,TW1F,TWOF,HFF,HWF,DTF,AI,AO,EPS,
* G1,TW10,TW01,DI,DO,VICW(I),TWK,HFG,A,B,G,M,CI,OTL,XF,DC)
DT(L,M)=DTF
TO(L,M)=TI(L,M)+DT(L,M)
TW1(L,M)=TW1F
TWO(L,M)=TWOF
HW(L,M)=HWF
SAI=PI*(DI**2.)/4.
TCW(L,M)=TI(L,M)+(DT(L,M)/2.)
TAW(L,M)=(TCW(L,M)+TW1(L,M))/2.
CALL ETAL(TAW(L,M),DT(L,M),DO,DI,DXG,EF)

```

```
DETW(L,M)=DE
ZTW(L,M)=Z
CPTW(L,M)=CP
CETW(L,M)=CE
MCW(L,M)=SAI*DETW(L,M)*VICW(I)
DQ(L,M)=MCW(L,M)*CPTW(L,M)*DT(L,M)
TCF(L,M)=(TS1+TW0(L,M))/2.
CALL ETA1(TCF(L,M),DE,Z,CP,CE)
CPFT(L,M)=CP
DHFG=XF*HFG+((3./8.)*CPFT(L,M)*(TS1-TW0(L,M)))
DMC(L,M)=DQ(L,M)/DHFG
HF(L,M)=HFF
OHTC(L,M)=1./(((DO/(DI*HW(L,M))))+(((DO/2.)*LOG(DO/DI))/TWK)+
* 1./HF(L,M))
THT(L,M)=THT(L-1,M)+DQ(L,M)
TACP(L,M)=TACP(L-1,M)+DMC(L,M)
AOH(L,M)=AOH(L-1,M)+(DXG*OHTC(L,M))
AWC(L,M)=AWC(L-1,M)+(DXG*HW(L,M))
ACF(L,M)=ACF(L-1,M)+(DXG*HF(L,M))
TIT(L,M)=TIT(L-1,M)+TW1(L,M)
TOT(L,M)=TOT(L-1,M)+TW0(L,M)
SUM(L,M)=SUM(L-1,M)+DXG
STACP(L,M)=STACP(L,M-1)+DMC(L,M)
30 CONTINUE
C VALUES OF THE DIFFERENT PARAMETERS AT THE OUTLET
C END OF THE TUBE CONSIDERED
THT1(I,MI+1,M)=THT(MI+1,M)
TO1(I,MI+1,M)=TO(MI+1,M)
TACP1(I,MI+1,M)=TACP(MI+1,M)
AOHTC(I,MI+1,M)=AOH(MI+1,M)/SUM(MI+1,M)
AWTC(I,MI+1,M)=AWC(MI+1,M)/SUM(MI+1,M)
ACFC(I,MI+1,M)=ACF(MI+1,M)/SUM(MI+1,M)
TIT1(I,MI+1,M)=TIT(MI+1,M)/MI
TOT1(I,MI+1,M)=TOT(MI+1,M)/MI
20 CONTINUE
91 CONTINUE
C OUTPUT OF INDIVIDUAL TUBES PERFORMANCE
DO 36 M=1,NTB
WRITE(9,341)M
341 FORMAT(1H,, 'ROW NUMBER M=',2X,I2)
WRITE(9,342)
342 FORMAT(70('*'))
WRITE(9,343)
343 FORMAT(70('*'))
WRITE(9,344)
344 FORMAT(1H,, 'TIN',6X,'TOU',4X,'VCW',5X,'Q',7X,'CFR',7X,'OHTC',6X,
* 'HW',7X,'HF')
WRITE(9,345)
345 FORMAT(70('*'))
WRITE(9,346)
346 FORMAT(1H,, '[C]',6X,'[C]',3X,'[M/S]',4X,'[KW]',3X,'[KG/S]',3X,
* '[KW/MMK]',2X,'[KW/MMK]',3X,'[KW/MMK]')
WRITE(9,347)
347 FORMAT(70('*'))
WRITE(9,348) (T1(I),TO1(I,MI+1,M),VICW(I),THT1(I,MI+1,M),
* TACP1(I,MI+1,M),AOHTC(I,MI+1,M),AWTC(I,MI+1,M),
* ACFC(I,MI+1,M),I=1,NPTS)
348 FORMAT(2X,F5.2,2X,F5.2,2X,F4.2,2X,F7.4,2X,F7.5,2X,F8.5,2X,
* F8.5,2X,F10.5)
WRITE(9,300)
300 FORMAT(40('*'))
WRITE(9,301)
301 FORMAT(1H,, 'TIT',6X,'TOT')
WRITE(9,302)
302 FORMAT(40('*'))
WRITE(9,303)
303 FORMAT(1H,, '[C]',6X,'[C]')
WRITE(9,304)
```

```
304  FORMAT(40('*'))
      WRITE(9,305) (TIT1(I,MI+1,M),TOT1(I,MI+1,M),I=1,NPTS)
305  FORMAT(2X,F6.2,4X,F6.2)
36   CONTINUE
C    CALCULATION OF THE MULTI-TUBE CONDENSER PERFORMANCE
      DO 103 I=1,NPTS
      M=1
      THTF(I,MI+1,M)=0
      TO1F(I,MI+1,M)=0
      TACPF(I,MI+1,M)=0
      AOHTF(I,MI+1,M)=0
      AWTF(I,MI+1,M)=0
      ACFF(I,MI+1,M)=0
      DO 291 M=2,NTB+1
      THTF(I,MI+1,M)=THTF(I,MI+1,M-1)+THT1(I,MI+1,M-1)
      TO1F(I,MI+1,M)=TO1F(I,MI+1,M-1)+TO1(I,MI+1,M-1)
      TACPF(I,MI+1,M)=TACPF(I,MI+1,M-1)+TACP1(I,MI+1,M-1)
      AOHTF(I,MI+1,M)=AOHTF(I,MI+1,M-1)+AOHTC(I,MI+1,M-1)
      AWTF(I,MI+1,M)=AWTF(I,MI+1,M-1)+AWTC(I,MI+1,M-1)
      ACFF(I,MI+1,M)=ACFF(I,MI+1,M-1)+ACFC(I,MI+1,M-1)
291  CONTINUE
      TO1CF(I,MI+1,NTB+1)=TO1F(I,MI+1,NTB+1)/NTB
      AOHTCF(I,MI+1,NTB+1)=AOHTF(I,MI+1,NTB+1)/NTB
      AWTCF(I,MI+1,NTB+1)=AWTF(I,MI+1,NTB+1)/NTB
      ACFCF(I,MI+1,NTB+1)=ACFF(I,MI+1,NTB+1)/NTB
103  CONTINUE
C    OUTPUT OF THE OVERALL TUBE ARRAY PERFORMANCE
      WRITE(9,391)
391  FORMAT(70('*'))
      WRITE(9,392)
392  FORMAT(1H,, 'MULTITUBE CONDENSER RESULTS')
      WRITE(9,394)
394  FORMAT(70('*'))
      WRITE(9,395)
395  FORMAT(1H,, 'TIN',6X,'TOU',4X,'VCW',5X,'Q',7X,'CFR',7X,'OHTC',6X,
*   'HW',7X,'HF')
      WRITE(9,396)
396  FORMAT(70('*'))
      WRITE(9,397)
397  FORMAT(1H,, '[C]',6X,'[C]',3X,'[M/S]',4X,'[KW]',3X,'[KG/S]',3X,
*   '[KW/MMK]',2X,'[KW/MMK]',3X,'[KW/MMK]')
      WRITE(9,398)
398  FORMAT(70('*'))
      WRITE(9,399) (T1(I),TO1CF(I,MI+1,NTB+1),V1CW(I),
*   THTF(I,MI+1,NTB+1),TACPF(I,MI+1,NTB+1),AOHTCF(I,MI+1,NTB+1),
*   AWTCF(I,MI+1,NTB+1),ACFCF(I,MI+1,NTB+1),I=1,NPTS)
399  FORMAT(2X,F5.2,2X,F5.2,2X,F4.2,2X,F9.4,2X,F7.5,2X,F8.5,2X,
*   F8.5,2X,F10.5)
      STOP
      END
```

C*****

```
      SUBROUTINE TAR(DT10, TI, TS1, TB, TW1F, TW0F, HFF, HWF, DTF, AI, AO, EPS, G1,
*   TW10, TW01, DI, DO, V1CW, TWK, HFG, A, B, G, M, CI, OTL, XF, DC,
*   COVV, DEV, VV, ZV, EQD)
C    THIS SUBROUTINE CALCULATES THE FINAL VALUE OF THE COOLING TEMP.
C    RISE THROUGH EACH INCREMENT FOR TOP TUBE.
      DIMENSION DT(1000), TC(1000), DEC(1000), CPC(1000), CWF(1000)
      PI=3.14159
      SAI=PI*((DI**2.)/4.)
      K=1
      DT(K)=DT10
14   CALL BOU(TW10, TW01, TI, TB, TW1F, TW0F, V1CW, DT10, TWK, DI, DO,
*   G1, M, G2F, HWF, HFF, TS1, HFG, A, B, G, CI, OTL, XF, DC,
*   COVV, DEV, VV, ZV, EQD)
      Q=HFF*AO*(TS1-TW0F)
      TC(K)=TI+(DT(K)*Q)
```

```
CALL ETA1(TC(K),DE,Z,CP,CE)
DEC(K)=DE
CPC(K)=CP
CWF(K)=DEC(K)*VICW*SAI
K=K+1
DT(K)=Q/(CWF(K-1)*CPC(K-1))
IF(ABS(DT(K)-DT(K-1)).LT.EPS) GOTO 15
DT10=DT(K)
TW10=TWIF
TW01=TWOF
GOTO 14
15 DTF=DT(K)
RETURN
END
C*****
SUBROUTINE BOU(TW10,TW01,T1,TB,TW1F,TW0F,VICW,DT,TWK,DI,DO,
* G1,M,G2F,HWF,HFF,TS1,HFG,A,B,G,CI,OTL,XF,DC,
* COVV,DEV,VV,ZV,EQD)
C THIS SUBROUTINE CALCULATES THE FINAL VALUES OF BOTH THE INNER AND
C OUTER TUBE WALL TEMP. FOR TOP TUBE USING THE RAPHSON-NEWTON
C ITERATIVE PROCEDURE.
DIMENSION TW1(1000),TWO(1000),HFN(1000),FTWON(1000),GAB(1000),
* FTW1(1000),DFTW1(1000),TD(1000),DHFN(1000),DFTWON(1000),
* PR1(1000),PR2(1000)
REAL HFG,RE,PR,NUD,FT,HW,G2,A,B
REAL DEF,ZF,CPF,CEF
INTEGER M
G=9.81
TB=T1+(DT*0.5)
62 TM=(TB+TW10)/2.0
EPS=0.0001
CALL SAM(TM,TW10,TB,VICW,TWK,RE,PR,G1,NUD,DO,DI,HW,G2,
* CI,OTL,DC)
N=1
TWO(N)=TW01
40 TF=(TS1+TWO(N))/2.
CALL ETA1(TF,DE,Z,CP,CE)
DEN=DE
ZN=Z
CPN=CP
CEN=CE
GAB(N)=TS1-TWO(N)
TD(N)=ABS(GAB(N))
C RAPHSON-NEWTON ITERATIVE PROCEDURE ON OUTER TUBE
C WALL TEMP. 'TWO'.
P=((DEN**2.)*G*(CEN**3.))/(ZN*DO*M)
RA=((3./8.)*CPN*P)
HFN(N)=(0.728)*((P*HFG*(1./TD(N)))+RA)**(0.25)
PR1(N)=(P*HFG*(1./TD(N)))
PR2(N)=(P*HFG*((1./TD(N))**(2.)))
DHFN(N)=(0.182)*((PR1(N)+RA)**(-0.75))*(PR2(N))
FTWON(N)=HFN(N)*(TWO(N)*G2-TS1*G2)+TWO(N)*G1-TB*G1
DFTWON(N)=DHFN(N)*(TWO(N)*G2-TS1*G2)+HFN(N)*G2+G1
N=N+1
TWO(N)=TWO(N-1)-(FTWON(N-1)/ABS(DFTWON(N-1)))
IF((TWO(N)-TWO(N-1)).LT.EPS) GOTO 41
GOTO 40
41 TWOF=TWO(N)
I=1
TW1(I)=TW10
TF1=(TS1+TWOF)/2.
CALL ETA1(TF1,DE,Z,CP,CE)
DEF=DE
ZF=Z
CPF=CP
CEF=CE
X=TS1-TWOF
```

C RAPHSON-NEWTON ITERATIVE PROCEDURE IN ORDER TO ESTIMATE
 C THE INNER TUBE WALL TEMP.'TWI'.

A= 1.+0.2*((CPF**X*(M-1))/HFG)
 B=((DEF**2.)*G*(CEF**3.)*DHFG)/(M*DO*ZF*X)
 HF=0.728*A*(B**0.25)
 HFT=HF
 TT=TWOF

CALL VHT(HFT,COVV,TS1,DEV,HFG,TT,VV,DO,ZV,TWK,EQD,HFF)
 HF=HFF

91 FTW1(I)=TW1(I)*(G2+(G1/HF))-TB*(1.+(G1/HF))-
 * TS1*(G2-1.)

DFTW1(I)=G2+(G1/HF)
 I=I+1

TW1(I)=TW1(I-1)-(FTW1(I-1)/DFTW1(I-1))
 IF(ABS(TW1(I)-TW1(I-1)).LT.EPS) GOTO 61
 TP=(TB+TW1(I))/2.

CALL SAM(TP,TW1(I),TB,VICW,TWK,RE,PR,G1,NUD,DO,DI,HW,G2,
 * CI,OTL,DC)

GOTO 91

61 IF(ABS(TW1(I)-TW10).LT.EPS) GOTO 63
 TW10=TW1(I)

GOTO 62

63 TW1F=TW1(I)

G2F=G2

HWF=HW

HFF=HF

RETURN

END

C*****
 SUBROUTINE SAM(TX,TR,TB,VICW,TWK,RE,PR,G1,NUD,DO,DI,HW,G2,
 * CI,OTL,DC)

C THIS SUBROUTINE CALCULATES THE WATER-SIDE H.T.COEFF.

REAL HW,G2,VICW,FT,NUD,RETX,RETB,PRTX,PRTB,NI

REAL TX,TR,TB,CL,AP

CALL ETA1(TX,DE,Z,CP,CE)

CPTX=CP

DETX=DE

ZTX=Z

CETX=CE

PRTX=CPTX*ZTX/CETX

RETX=DETX*VICW*DI/ZTX

CALL ETA1(TB,DE,Z,CP,CE)

DETB=DE

ZTB=Z

CPTB=CP

CETB=CE

PRTB=CPTB*ZTB/CETB

RETB=DETB*VICW*DI/ZTB

C CALCULATION OF THE WATERSIDE h.t.c ACCORDING TO

C THE REQUIRED CORRELATION.

IF(CI.EQ.1.) GOTO 121

IF(CI.EQ.2.) GOTO 122

IF(CI.EQ.3.) GOTO 123

GOTO 312

C COLBURN CORRELATION

121 NUD=0.023*(RETB**0.8)*(PRTB**(1./3.))

GOTO 30

122 CALL ETA1(TR,DE,Z,CP,CE)

ZTR=Z

C SIEDER-TATE CORRELATION

NUD=0.027*(RETB**0.8)*(PRTB**0.33)*(ZTB/ZTR)**0.14

GOTO 30

123 CALL ETA1(TR,DE,Z,CP,CE)

ZTR=Z

CL=1. +((0.96*((7/PRTB)**(0.42)))/(OTL/DI))

IF(RETB.LT.62500.) GOTO 9

NI=0.11

```
9 NI=(RETB/(8.7E05))**(0.84)
C ALLAN AND ECKERT CORRELATION
12 NUD=0.00123*CL*RETB*(PRTB**0.42)*(1.+25*(RETB**(-0.27)))*
* ((ZTB/ZTR)**(NI))
30 AP=NUD*CETX/DI
C HW=1./((1./AP)+(1./DC))
HW=AP
G2=(2.*TWK/(DI*HW*LOG(DO/DI)))+1.
312 CONTINUE
RETURN
END
```

```
      SUBROUTINE ETA1(T,DE,Z,CP,CE)
C THIS SUBROUTINE ALLOWS TO OBTAIN THE PHYSICAL PROPERTIES
C OF WATER WHICH ARE WRITTEN IN POLYNOMIAL FORM
C DE:DENSITY
C Z:VISCOSITY
C CP: SPECIFIC HEAT
C CE: THERMAL CONDUCTIVITY
REAL DE,Z,CP,CE
DE=1003.7-0.174*T-0.00277*(T**2.)
Z=1./(560.4+19.21*T+0.139*(T**2.)-3.382E-04*(T**3.))
CP=4.215-2.229E-03*T+3.772E-05*(T**2.)-1.536E-07*(T**3.)
CE=5.707E-04+1.78E-06*T-6.781E-09*(T**2.)
RETURN
END
```

```
      SUBROUTINE RAT(DT10,TI,TS1,TB,TW1F,TWOF,HFF,HWF,DTF,AI,AO,EPS,
* G1,TW10,TW01,DI,DO,V1CW,TWK,HFG,A,B,G,M,CI,OTL,XF,DC)
C THIS SUBROUTINE CALCULATES THE FINAL COOLING WATER TEMP.
C RISE FOR EACH INCREMENT OF THE TUBES BELOW THE TOP TUBE
DIMENSION DT(1000),TCL(1000),CWF(1000),CPCL(1000),
* DECL(1000)
PI=3.14159
SAI=PI*((DI**2.)/4.)
KD=1
573 DT(KD)=DT10
CALL BOUL(TW10,TW01,TI,TB,TW1F,TWOF,V1CW,DT10,TWK,DI,DO,
* G1,M,G2F,HWF,HFF,TS1,HFG,A,B,G,CI,OTL,XF,DC)
DQF=HFF*AO*(TS1-TWOF)
TCL(KD)=TI+(DT(KD)/2.)
CALL ETA1(TCL(KD),DE,Z,CP,CE)
DECL(KD)=DE
CPCL(KD)=CP
CWF(KD)=DECL(KD)*V1CW*SAI
KD=KD+1
DT(KD)=DQF/(CWF(KD-1)*CPCL(KD-1))
IF (ABS(DT(KD)-DT(KD-1)).LT.EPS) GOTO 574
DT10=DT(KD)
TW10=TW1F
TW01=TWOF
GOTO 573
574 DTF=DT(KD)
RETURN
END
```

```
      SUBROUTINE BOUL(TW10,TW01,T1,TB,TW1F,TWOF,V1CW,DT,TWK,DI,DO,
* G1,M,G2F,HWF,HFF,TS1,HFG,A,B,G,CI,OTL,XF,DC)
C THIS SUBROUTINE CALCULATES BOTH THE INNER AND
C OUTER TUBE WALL TEMPERATURES FOR EACH INCREMENT OF
C THE TUBES BELOW THE TOP ONE.
DIMENSION TW1(1000),TW0(1000),FTWON(1000),DFTWON(1000),
* FTW1(1000),DFTW1(1000)
REAL HFG,RE,PR,NUD,FT,HW,G2,A,B
REAL DEF,ZF,CPF,CEF
INTEGER M
```

```
G=9.81
TB=T1+(DT*0.5)
620 TM=(TB+TW10)/2.
EPS=0.0001
CALL SAM(TM,TW10,TB,V1CW,TWK,RE,PR,G1,NUD,DO,DI,HW,G2,
* CI,OTL,DC)
N=1
TWO(N)=TW01
400 FTWON(N)=HFF*G2*TWO(N)+G1*TWO(N)-TB*G1-HFF*TS1*G2
DFTWON(N)=HFF*G2+G1
N=N+1
TWO(N)=TWO(N-1)-(FTWON(N-1)/DFTWON(N-1))
IF(ABS(TWO(N)-TWO(N-1)).LT.EPS) GOTO 410
GOTO 400
410 TWOF=TWO(N)
I=1
TW1(I)=TW10
910 FTW1(I)=TW1(I)*(G2+(G1/HFF))-TB*(1.+(G1/HFF))-
* TS1*(G2-1.)
DFTW1(I)=G2+(G1/HFF)
I=I+1
TW1(I)=TW1(I-1)-(FTW1(I-1)/DFTW1(I-1))
IF(ABS(TW1(I)-TW1(I-1)).LT.EPS) GOTO 610
TP=(TB+TW1(I))/2.
CALL SAM(TP,TW1(I),TB,V1CW,TWK,RE,PR,G1,NUD,DO,DI,HW,G2,
* CI,OTL,DC)
GOTO 910
610 IF(ABS(TW1(I)-TW10).LT.EPS) GOTO 630
TW10=TW1(I)
GOTO 620
630 CONTINUE
TW1F=TW1(I)
G2F=G2
HWF=HW
RETURN
END
```

C*****

```
SUBROUTINE VPRT(PST,C,D,E,F,TS1,DEV,HFG)
C THIS SUBROUTINE INTERPOLATES THE VALUES FOR THE
C SATURATION TEMP,VAPOUR DENSITY,AND THE LATENT
C HEAT OF VAPOURIZATION GIVEN THE SATURATION PRESSURE
REAL PST,C(36),D(36),E(36),F(36),TS1,DEV,HFG
REAL TEMP,VG
INTEGER G,S,N,I
N=36
I=0
IF(PST.LT.C(1)) THEN
G=1
S=2
GOTO 100
ELSE
IF(PST.GT.C(N)) THEN
G=N-1
S=N
GOTO 100
ELSE
GOTO 10
ENDIF
ENDIF
10 I=1
20 IF(I.GT.N) STOP
IF(PST-C(I)) 30,40,50
30 G=I-1
S=I
GOTO 100
40 G=I
S=I+1
```

```
50     I=I+1
      GOTO 20
100    TEMP=(PST-C(G))/(C(S)-C(G))
      TS1=TEMP*(D(S)-D(G))+D(G)
      VG=TEMP*(E(S)-E(G))+E(G)
      HFG=TEMP*(F(S)-F(G))+F(G)
      DEV=1.0/VG
      RETURN
      END
C*****
      SUBROUTINE VVIS(TS1,A1,B1,ZV)
C     THIS SUBROUTINE INTERPOLATES THE VALUES FOR
C     THE DYNAMIC VISCOSITY OF THE VAPOUR GIVEN THE
C     SATURATION TEMPERATURE
      REAL TS1,A1(13),B1(13),ZV,TEMP,BX
      INTEGER F,S,N,I
      N=13
      I=0
      IF(TS1.LT.A1(1)) THEN
        F=1
        S=2
        GOTO 100
      ELSE
        IF(TS1.GT.A1(N)) THEN
          F=N-1
          S=N
          GOTO 100
        ELSE
          GOTO 10
        ENDIF
      ENDIF
10     I=1
20     IF(I.GT.N) STOP
      IF(TS1-A1(I)) 30,40,50
30     F=I-1
      S=I
      GOTO 100
40     F=I
      S=I+1
      GOTO 100
50     I=I+1
      GOTO 20
100    TEMP=(TS1-A1(F))/(A1(S)-A1(F))
      BX=TEMP*(B1(S)-B1(F))+B1(F)
C     ZV=BX E -6
      ZV=(BX)*(10**(-6.0))
      RETURN
      END
C*****
      SUBROUTINE VHT(HFT,COVV,TS1,DEV,HFG,TT,VV,DO,ZV,TWK,EQD,HFF)
C     THIS SUBROUTINE CALCULATES THE CONDENSING h.t.c WHEN THE
C     VAPOUR VELOCITY IS INCLUDED.THREE EQN'S ARE AVAILABLE FOR USE
      REAL HFT,COVV,TS1,DEV,HFG,TT,VV,DO,ZV,TWK,EQD,HFF
      REAL T2,DE,Z,CP,CE,R,A,X,XHF,Y,PR,PI,G,B,C,TEMP,TEMP1
      G=9.81
      T2=(TS1+TT)/2.0
      CALL ETA1(T2,DE,Z,CP,CE)
      IF(COVV.EQ.1.0) GOTO 10
      GOTO 20
C     FUKS EQN
10     A=(HFT*DO)/CE
      X=((VV)**(2.0))*DEV*HFT/(G*CE*DE)
      TEMP=(28.3*HFT)*((X)**(0.08))
      XHF=(TEMP)*((A)**(-0.58))
      GOTO 150
20     IF(COVV.EQ.2.0) GOTO 30
      GOTO 60
```

```
30  Y=HFG/(T2*CP)
    PR=(Z*CP)/CE
    S=(PR*Y)*(((DEV*ZV)/(DE*Z))**(0.5))
    PI=(CE*T2*(VV**(2.0)))/(G*DO*Z*HFG)
    IF(PI.GT.10.0) GOTO 50
    GOTO 40
40  B=1.0+(1.69/(PI*((1.0+S)**(4.0/3.0))))
    C=(1.0+((B)**(0.5)))*(0.5)
    XHF=HFT*(0.833)*(PI**(0.25))*((1.0+S)**(0.333))*C
    GOTO 150
50  XHF=HFT*(1.25)*(PI**(0.25))*((1.0+S)**(0.333))
    GOTO 150
60  IF(COVV.EQ.3.0) GOTO 70
    GOTO 100
C   BERMAN EQN
70  PI=(CE*T2*(VV**2.0))/(G*DO*Z*HFG)
    IF(PI.GT.0.01.AND.PI.LT.20.0) GOTO 80
    GOTO 90
80  XHF=HFT*(1.28+(0.28*LOG(PI)))
    GOTO 150
100 IF(COVV.EQ.4.0) GOTO 110
C   BERMAN AND TUMANOV EQN
110 R=(VV*EQD*DEV)/ZV
    IF(R.GT.6000.0) GOTO 90
    D=(HFT*DO)/CE
    E=(D)**(0.5)
    F=(11.8/E)
    TEMP1=R**(F)
    XHF=HFT*(1.0+((9.5*10**(-3.0))*(TEMP1)))
    GOTO 150
90  PRINT*, 'OUT OF RANGE, CANNOT USE THIS EQN WITH PRESENT DATA'
150 HFF=XHF
    RETURN
    END
```

APPENDIX E

CALIBRATION EQUATIONS FOR THERMOCOUPLES AND FLOWMETERS

1) Calibration of Thermocouples

The following equations were used in the measured data program to refine data recorded by the Orion data logger. The term (T_{DL}) refers to the temperature recorded by the data logger and the term (T_F) refers to the final corrected temperature. All temperatures were measured in degrees celcius ($^{\circ}C$).

A) Thermocouple mounted on insert with windows

$$T_F = -5.8880 \times 10^{-4} [T_{DL}]^2 + 1.0930 [T_{DL}] - 4.2371$$
$$75 \leq T_F \leq 97 (^{\circ}C)$$

B) Thermocouple mounted on insert without windows

$$T_F = 7.4954 \times 10^{-4} [T_{DL}]^2 + 1.1012 [T_{DL}] - 0.3326$$
$$75 \leq T_F \leq 97 (^{\circ}C)$$

C) Cooling water inlet thermocouple

$$T_F = 9.7660 \times 10^{-5} [T_{DL}]^2 + 1.0083 [T_{DL}] - 0.2727$$
$$15 \leq T_F \leq 50 (^{\circ}C)$$

D) Cooling water outlet temperature

$$T_F = 8.6588 \times 10^{-5} [T_{DL}]^2 + 0.9979 [T_{DL}] - 0.0861$$
$$15 \leq T_F < 50 (^{\circ}C)$$

E) Inlet inundation water thermocouple

$$T_F = -6.2395 \times 10^{-4} [T_{DL}]^2 + 1.1012 [T_{DL}] - 4.5699$$
$$75 \leq T_F < 97 (^{\circ}C)$$

F) Condensate water outlet thermocouple

$$T_F = 1.0685 \times 10^{-4} [T_{DL}]^2 + 1.0116 [T_{DL}] - 0.2688$$
$$75 \leq T_F \leq 97 (^{\circ}C)$$

G) Steam inlet thermocouple

$$T_F = -3.6111 \times 10^{-4} [T_{DL}]^2 + 1.0645 [T_{DL}] - 2.9385$$
$$75 \leq T_F \leq 97 \text{ (}^\circ\text{C)}$$

H) Steam outlet temperature

$$T_F = -7.2581 \times 10^{-4} [T_{DL}]^2 + 1.1174 [T_{DL}] - 4.9378$$
$$75 \leq T_F \leq 97 \text{ (}^\circ\text{C)}$$

2) Calibration of Rotameters

A) Cooling water flowmeter

The rotameter used to measure the cooling water flowrate from the main building supply was a Fisher and Porter type FP-1-35-G-10/80 that used float type 1-GNSVT-64. The flowrate was determined with the following equation:

$$\dot{M}_{CW} = -7.6335 \times 10^{-4} [FR]^2 + 1.2159 [FR] - 11.2209$$

where FR was the flow reading from the rotameter measured in % of total flow.

B) Inundation water rotameter

Two identical Fisher and Porter FP-1/4-25-G-5/84 tri flat rotameters with titanium ball floats were used to measure the inundation water flowing from the hot water tank to the inundation tube in the bundle. The flowrate was determined using the following equation

$$\dot{M}_{IN} = -1.041 \times 10^{-4} [FR]^2 + 1854.431 [FR] + 0.7682$$

where FR was the flow reading from the rotameter over the range $0.5 \leq FR \leq 25$ and \dot{M}_{IN} was the mass flow of inundation water in kg/s.

3) Calibration of Steam Nozzle

The mass flow of steam was determined by measuring the pressure drop across a calibrated orifice plate in the steam line with a mercury manometer.

With the pressure drop (ΔP) in centimetres of mercury (Hg) and the following expression the mass flow could be calculated

$$\dot{M}_S = -0.4 + 6.6 \sqrt{\Delta P}$$

where \dot{M}_S was the mass flow of steam in kg/hour.

For the vapour shear experiments the mass flow rate was held at $\Delta P = 14\text{cm}$ which was equal to $6.745 \times 10^{-3} \text{ kg/s}$. During the inundation experiments the mass flow rate was maintained at $\Delta P = 20\text{cm}$ which was equal to $8.09 \times 10^{-3} \text{ kg/s}$.

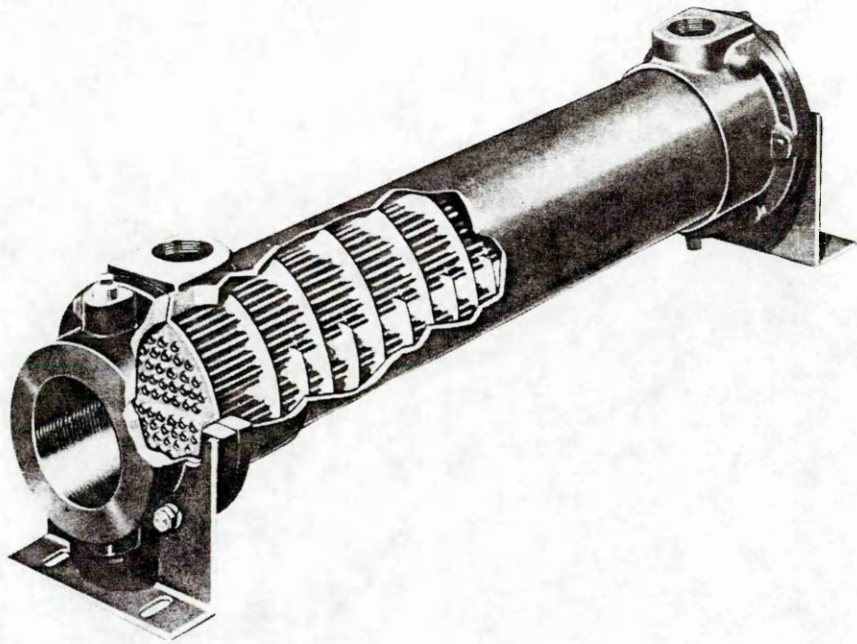


Figure 1: Typical Shell and Tube Type Condenser

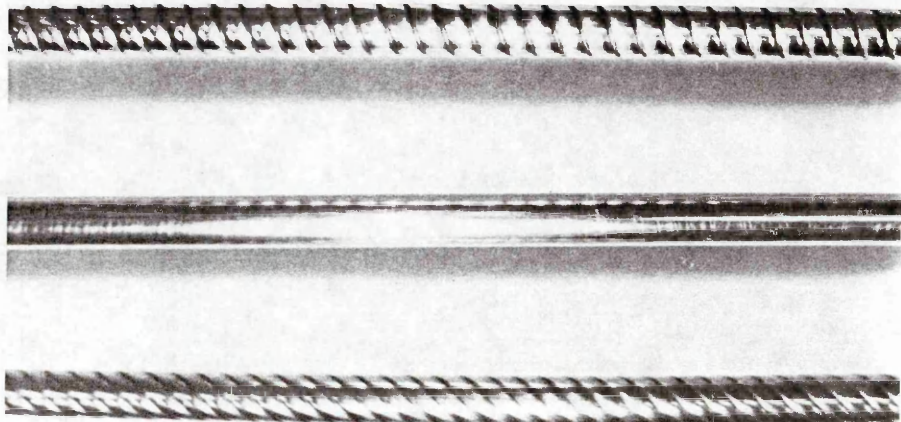


Figure 2: Typical Plain and Roped Condenser Tubes

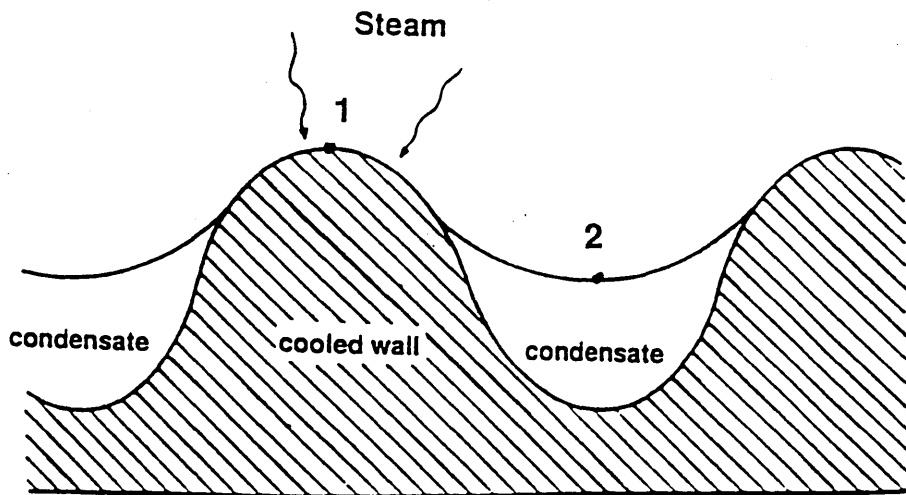


Figure 3: Cross Sectional View of the Profile of a Roped Tube

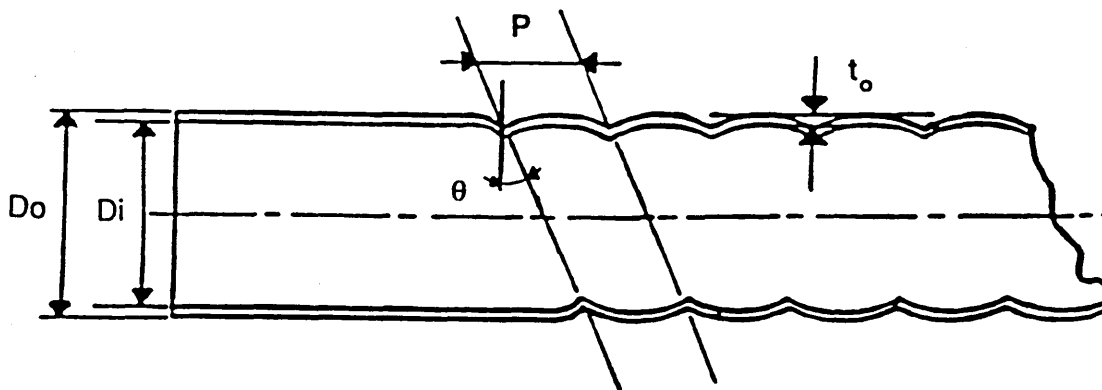


Figure 4: Typical Roped Tube Configuration with the Various Characteristics

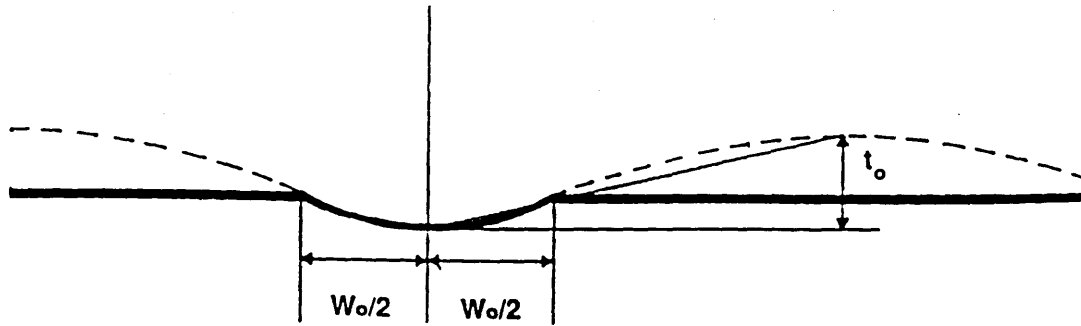


Figure 5: The Assumed Roped Tube Profile

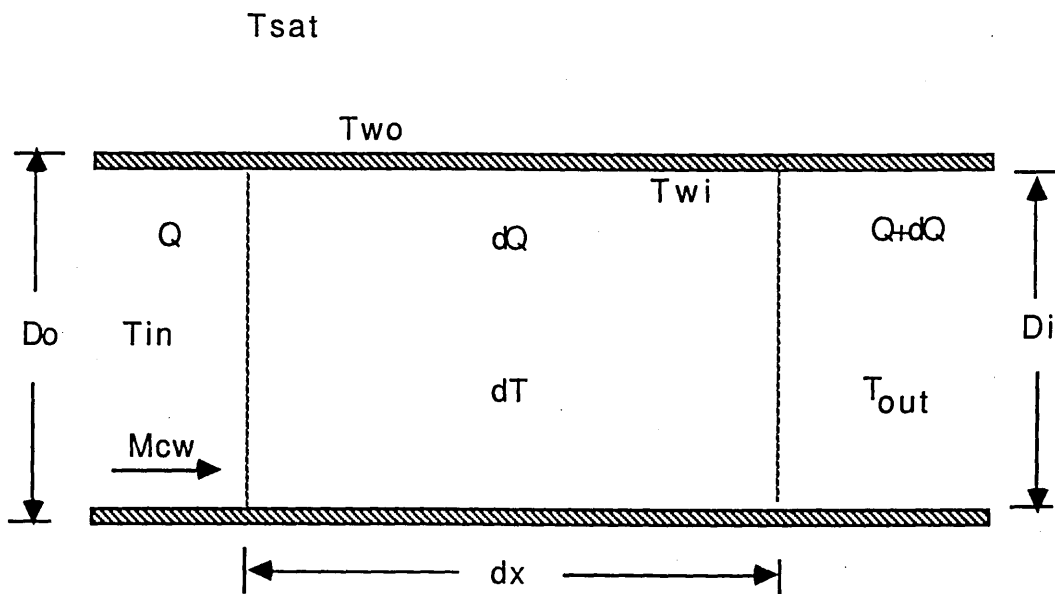


Figure 6: A Typical Tube Increment Used in the Computer Simulation Process

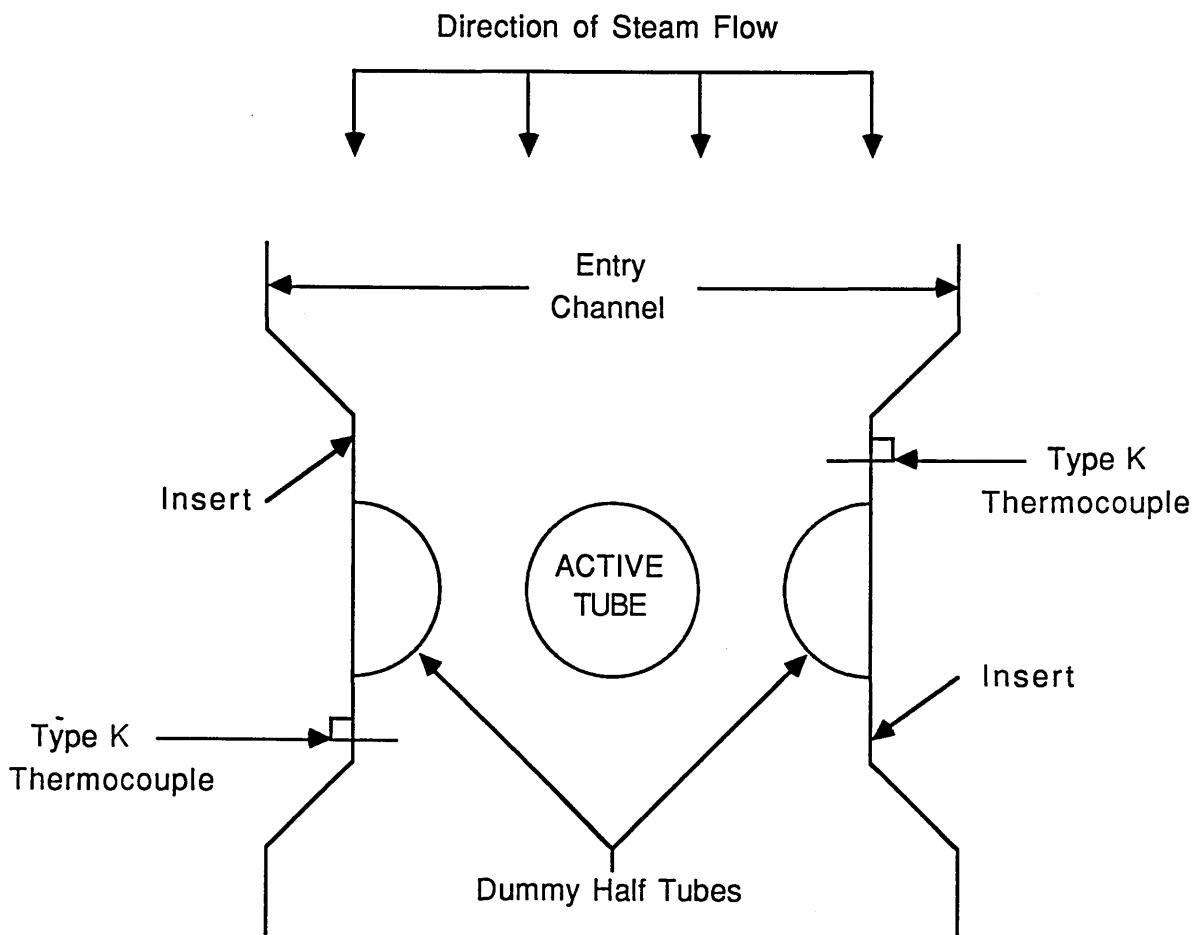


Figure 7: Side View of the Condenser Test Cell

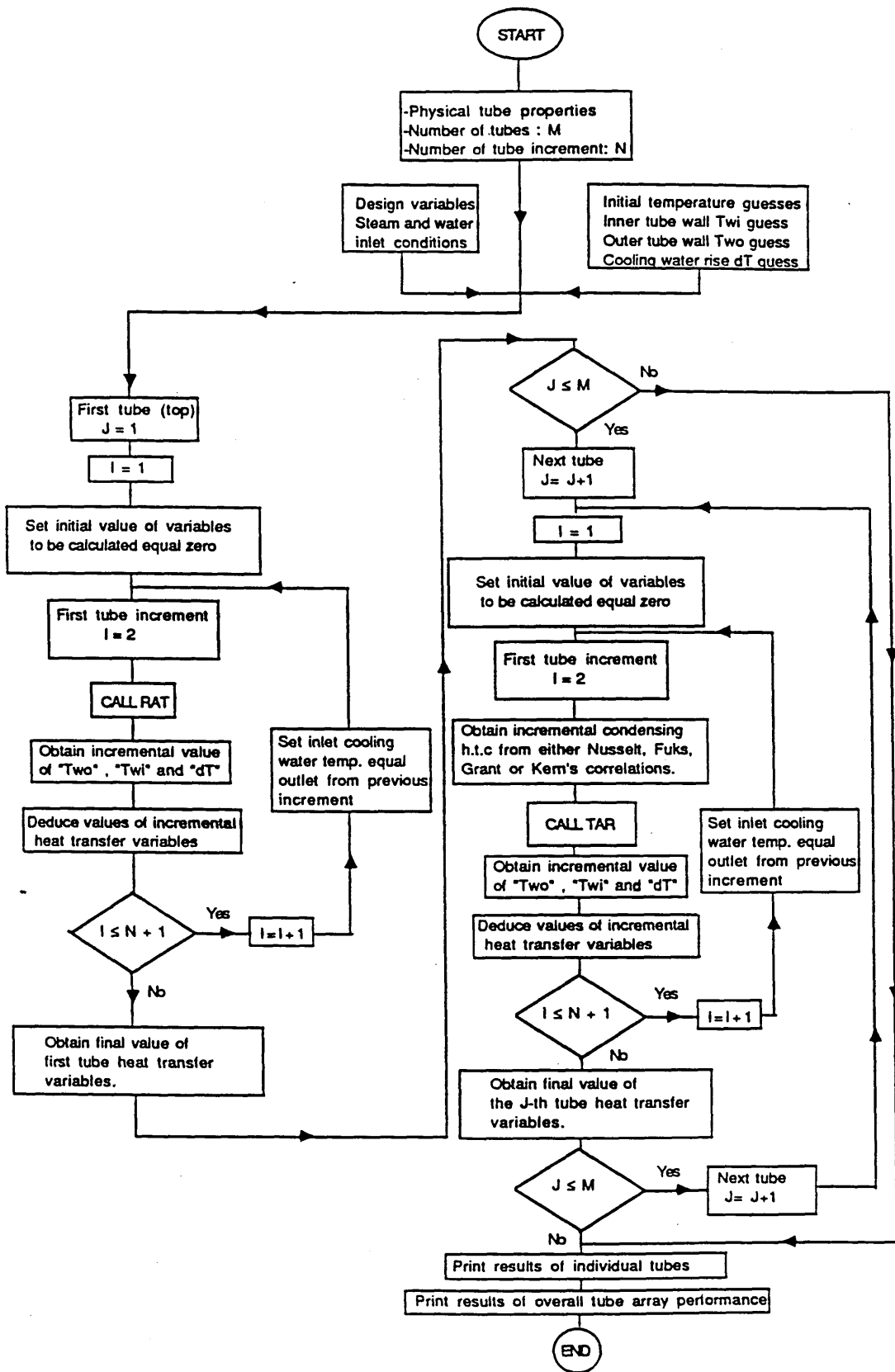
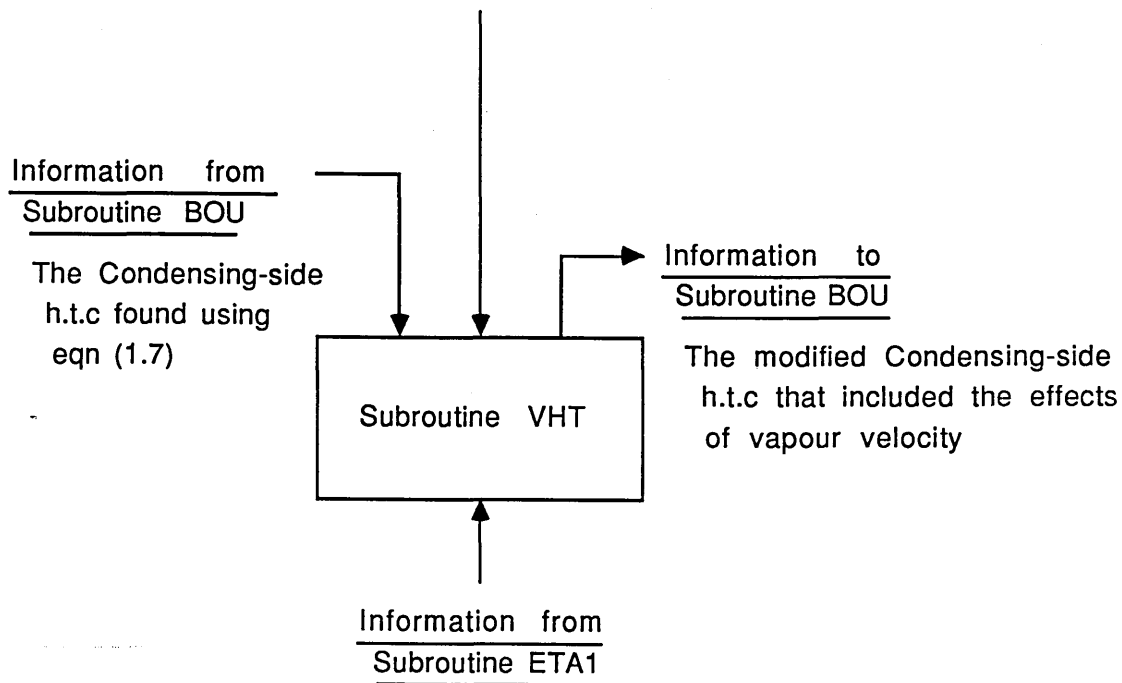


Figure 8:Flow Diagram of the Plain Tube Computer Program

Information from the
Main Line Program

The condensate water temperature, steam temperature, steam density, steam viscosity, steam velocity and the choice of condensing-side equations (COVV)



The Condensing-side h.t.c found using eqn (1.7)

The modified Condensing-side h.t.c that included the effects of vapour velocity

The density, viscosity, specific heat capacity and thermal conductivity of the condensate water

Figure 9: Overview of the Operation of Subroutine VHT

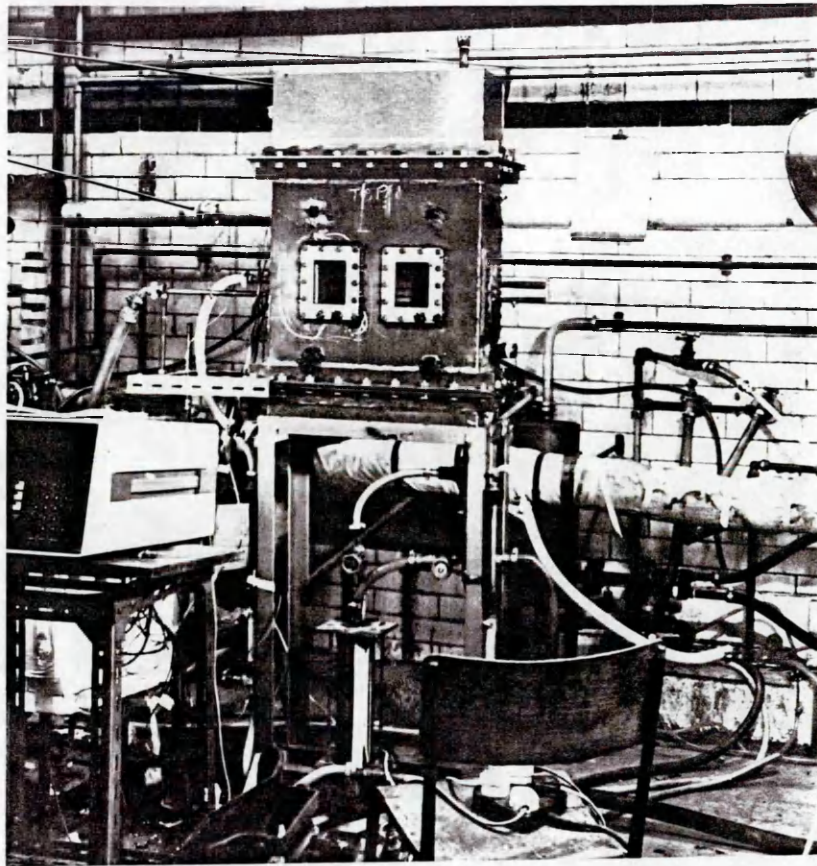


Figure 10: The Assembled Test Condenser Rig

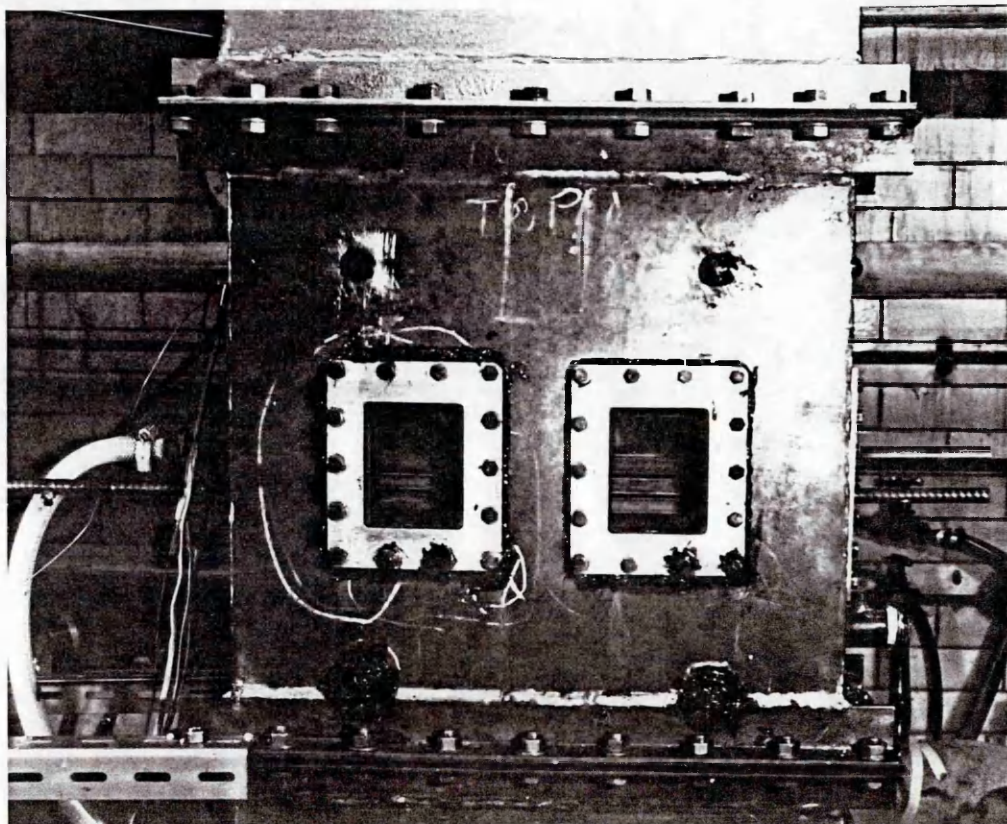


Figure 11: Front View of the Test Condenser

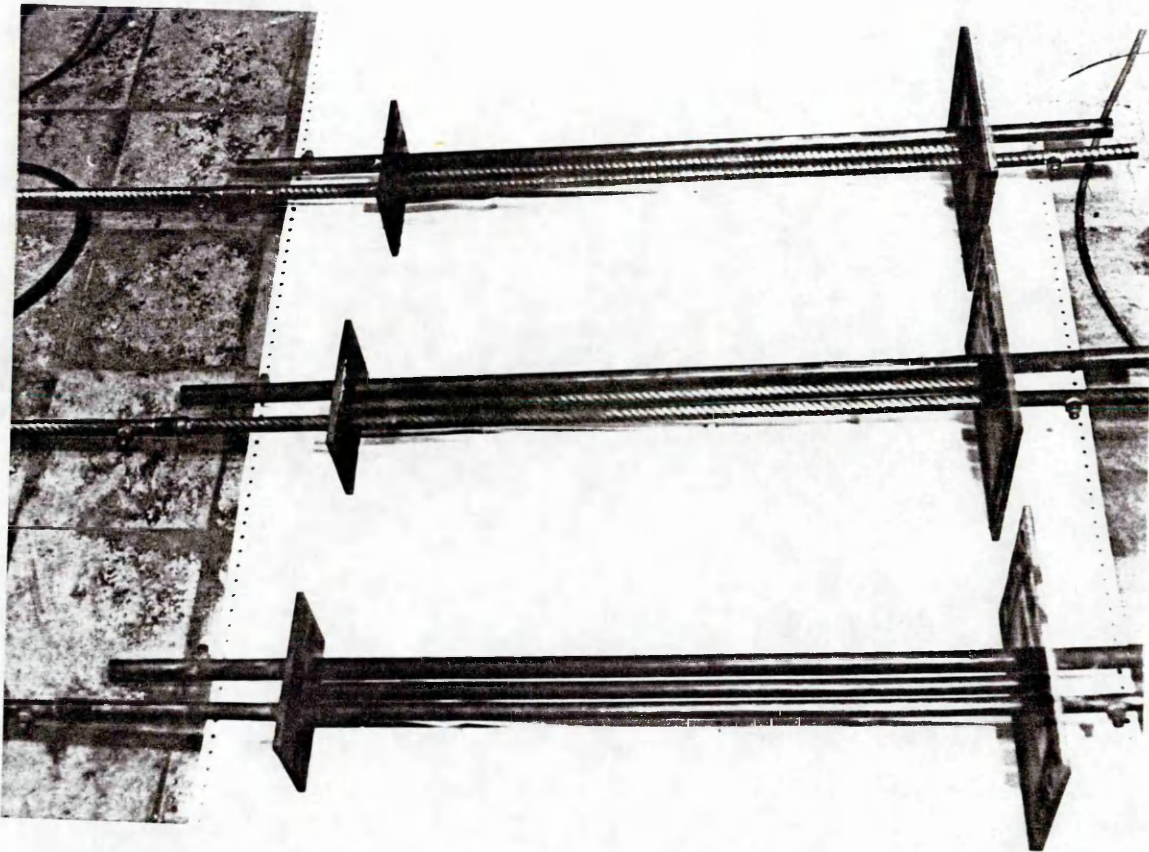


Figure 12:Condenser Tube Bundles

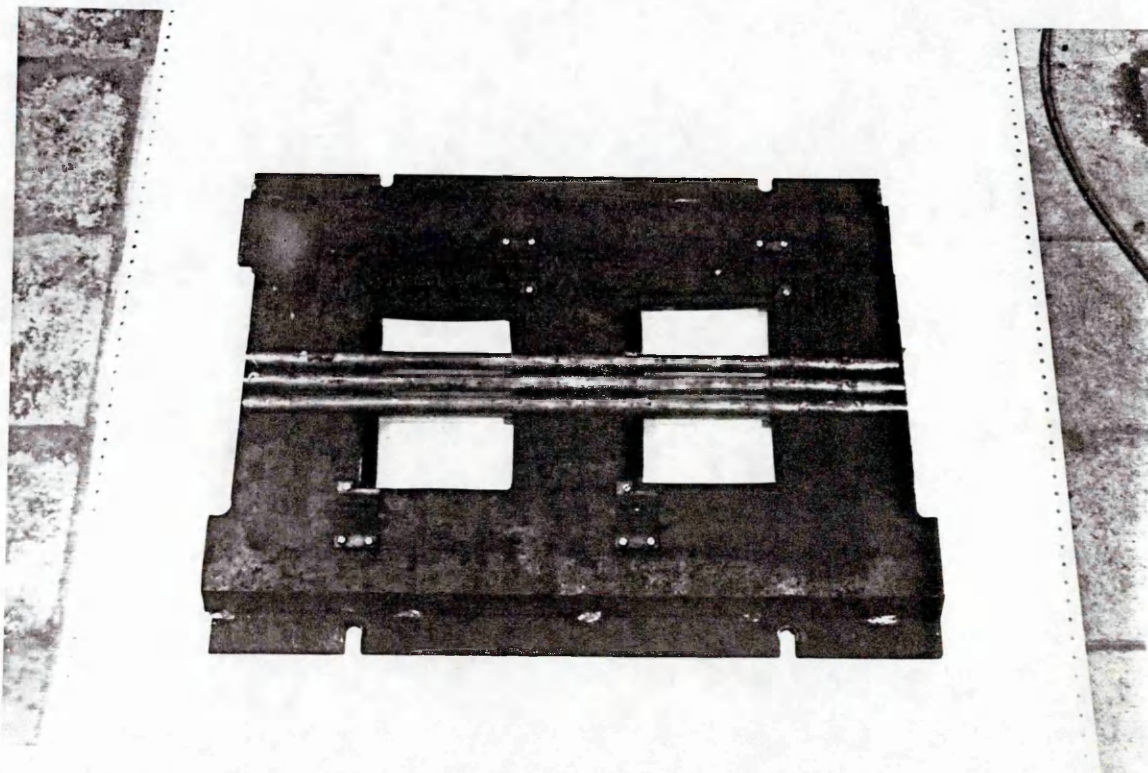


Figure 13:Test Section Insert

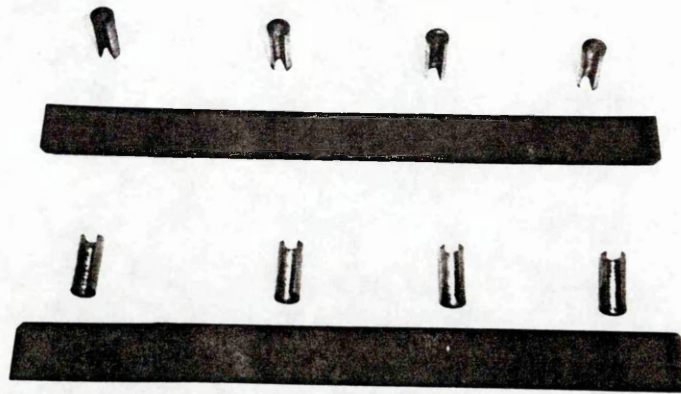


Figure 14: Insert Spacers

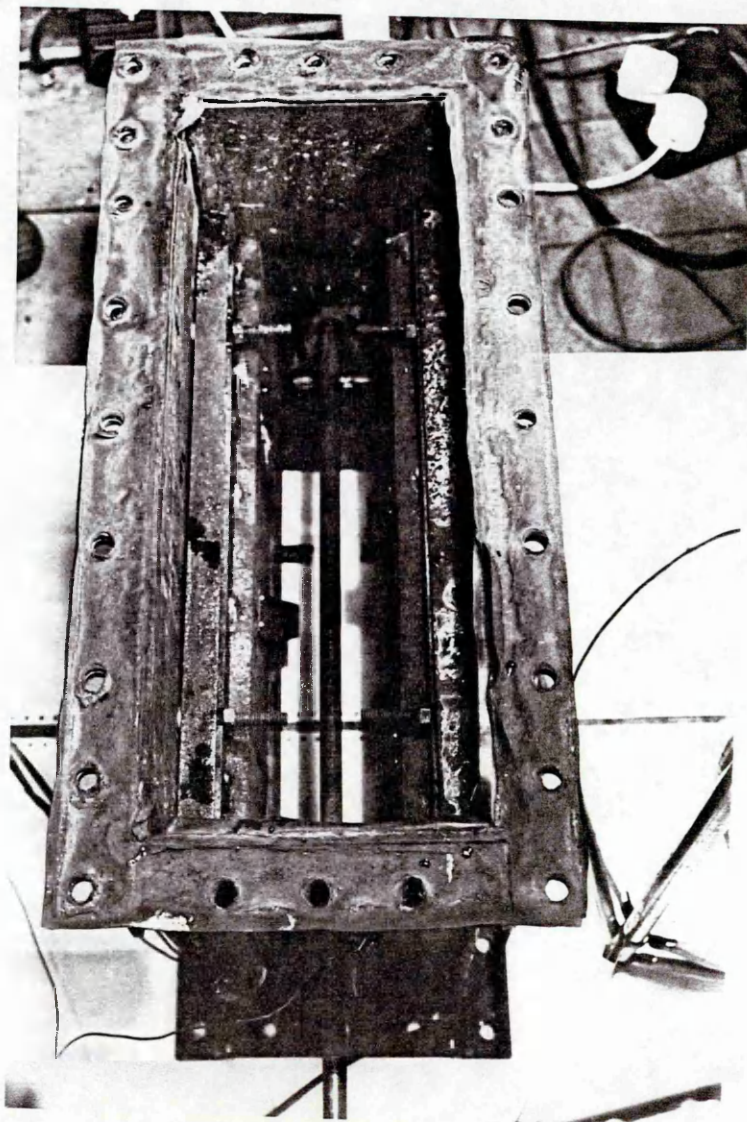


Figure 15: Top View of the Test Condenser

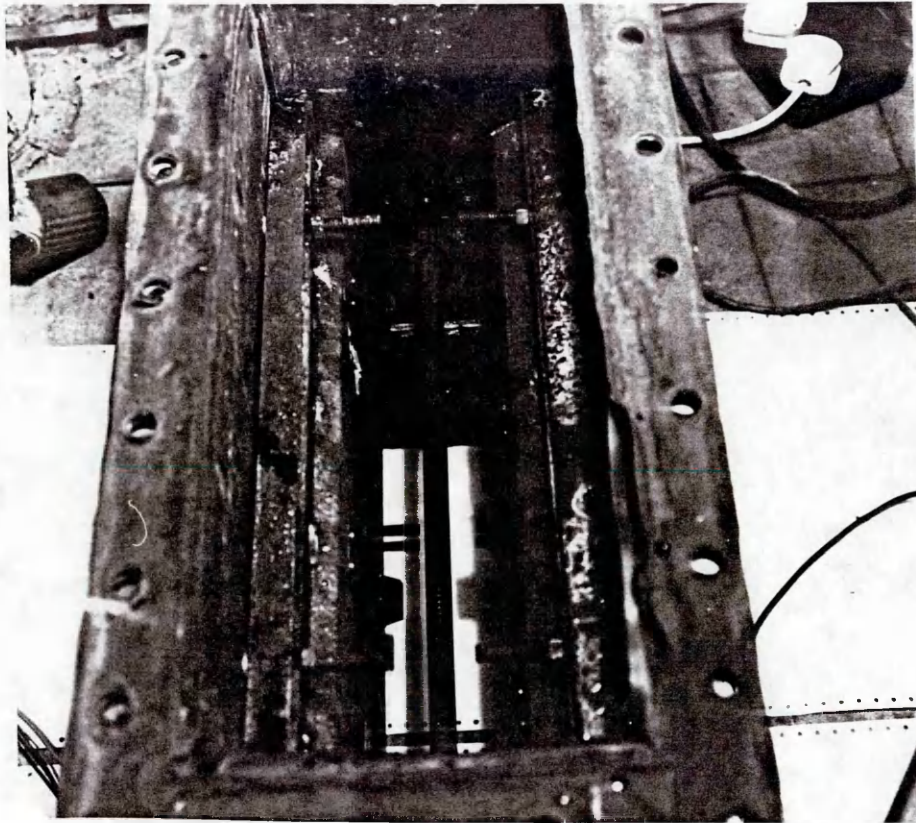


Figure 16:Channel Area Inside the Test Condenser

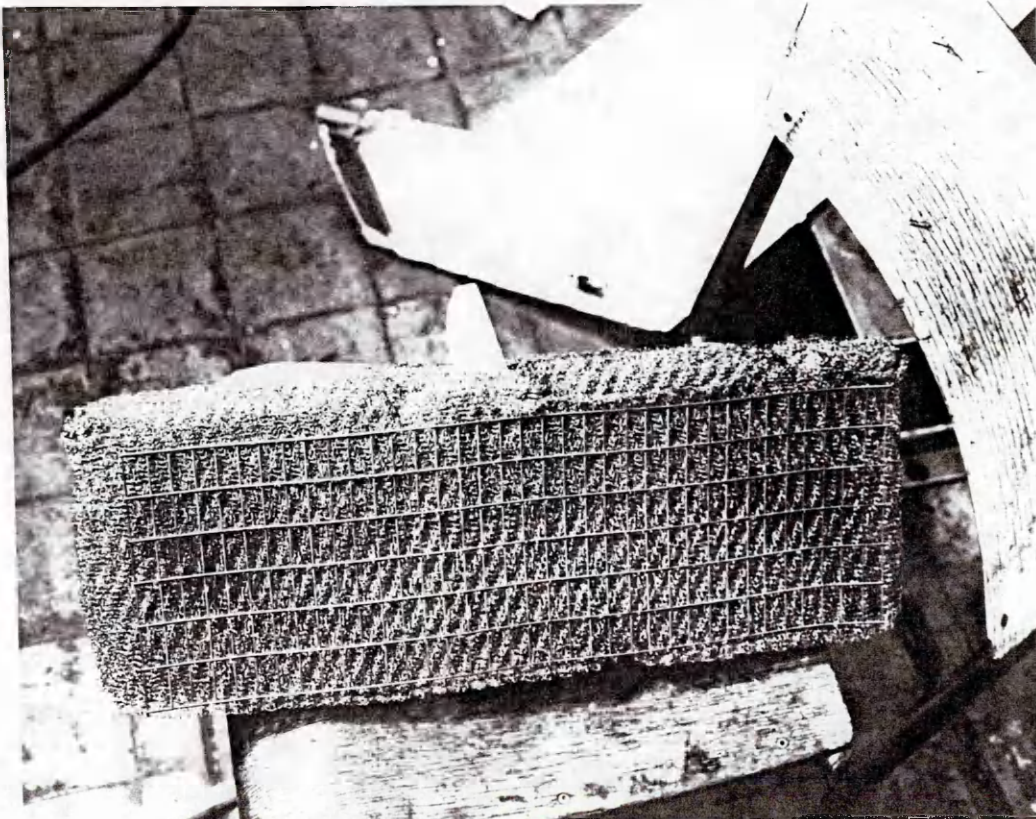


Figure 17:Wire Mesh Strainer

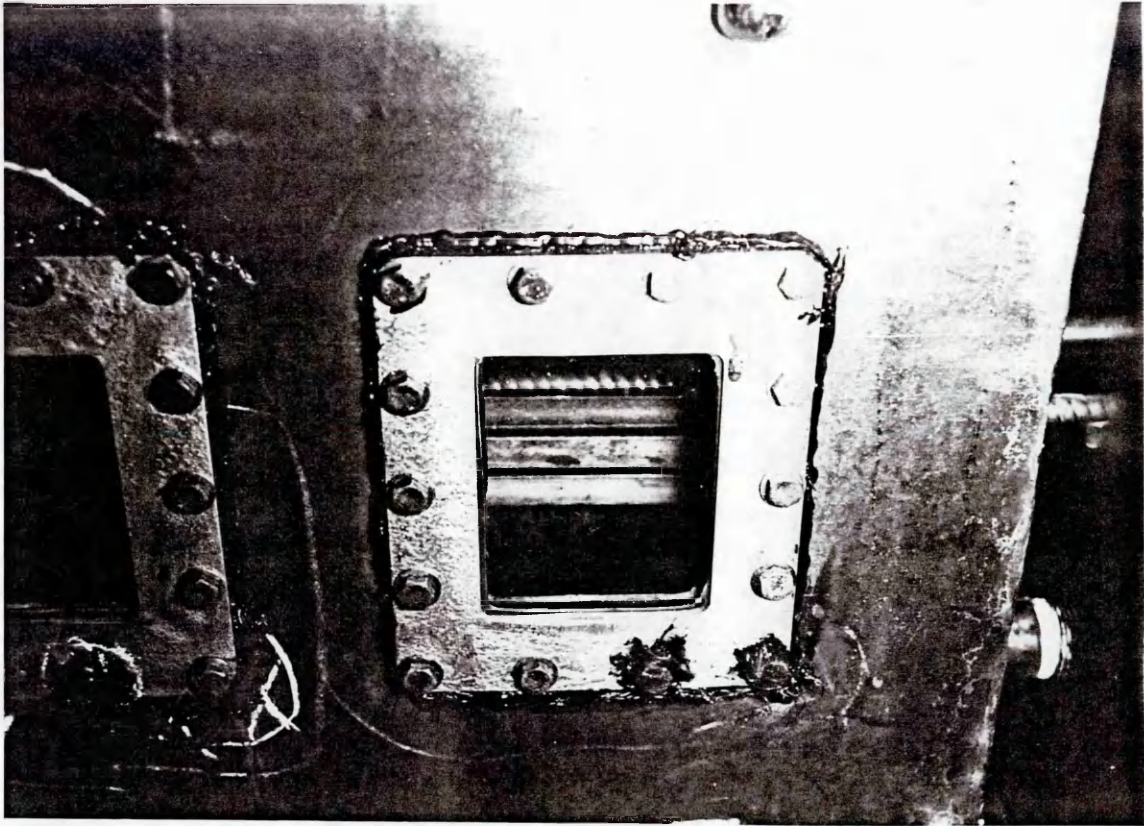


Figure 18: Front View of the Condenser Box Window

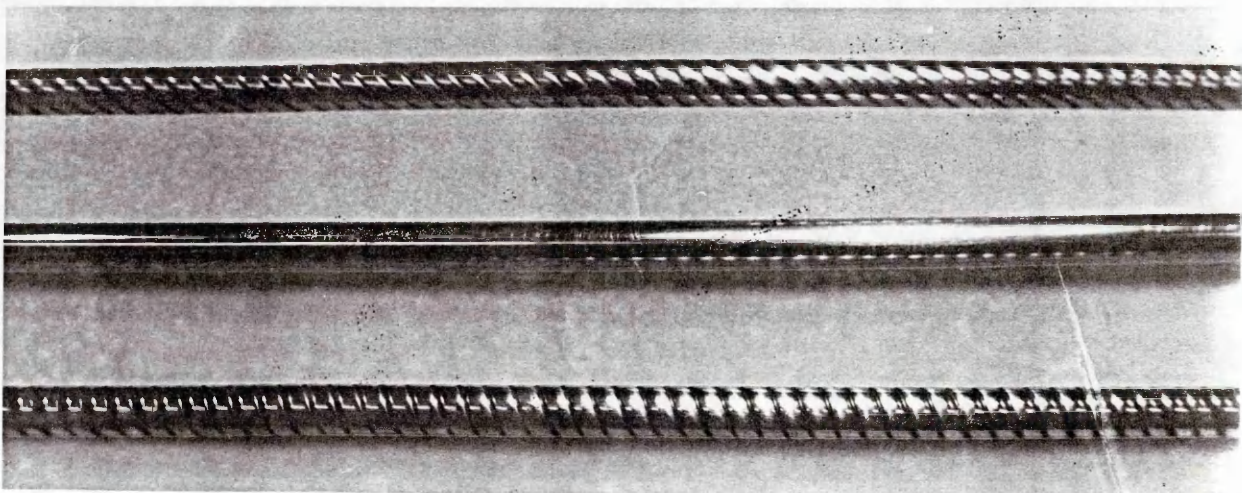


Figure 19: The Condenser Tubes Under Consideration

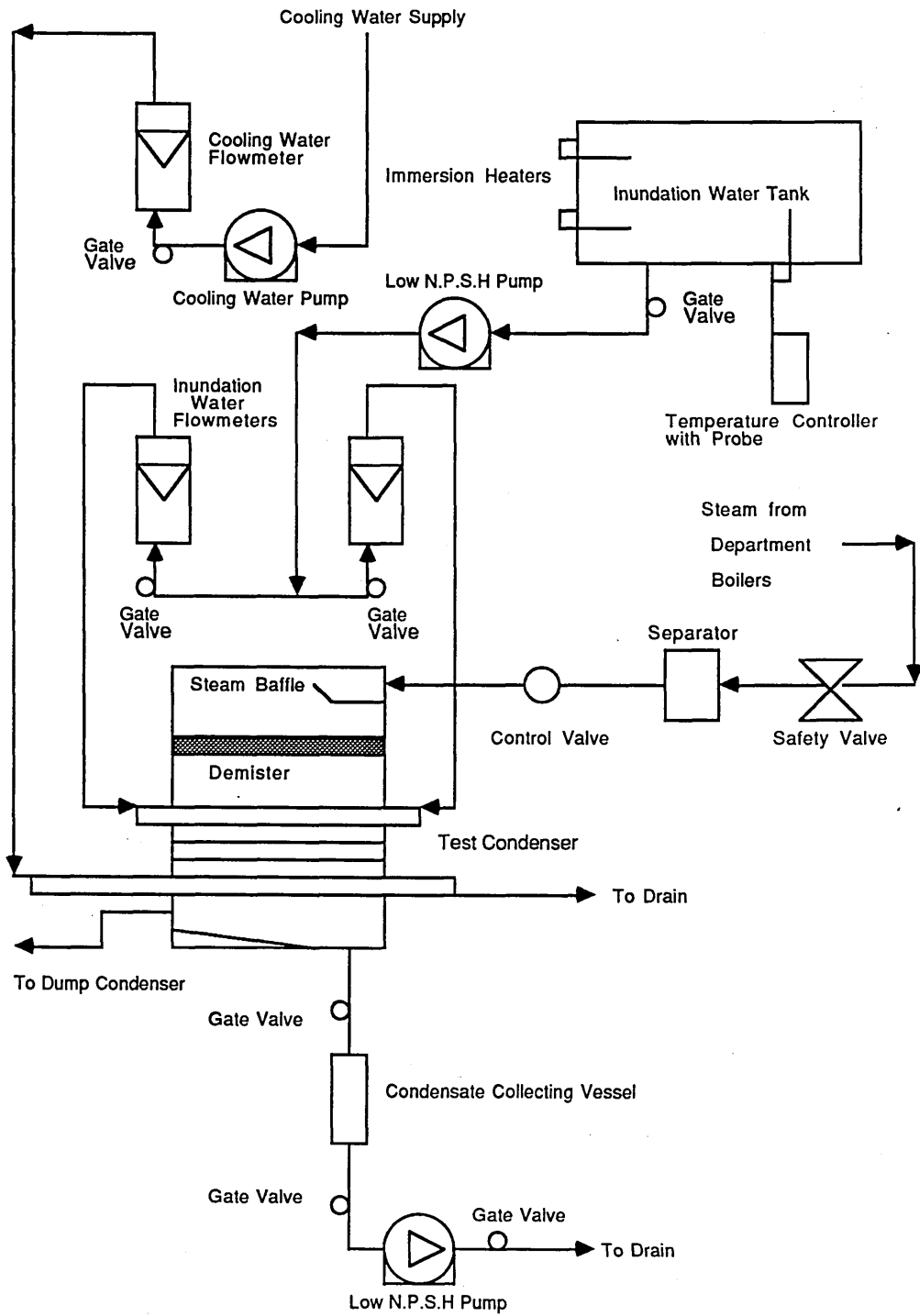


Figure 20: Schematic Diagram of the Experimental Apparatus

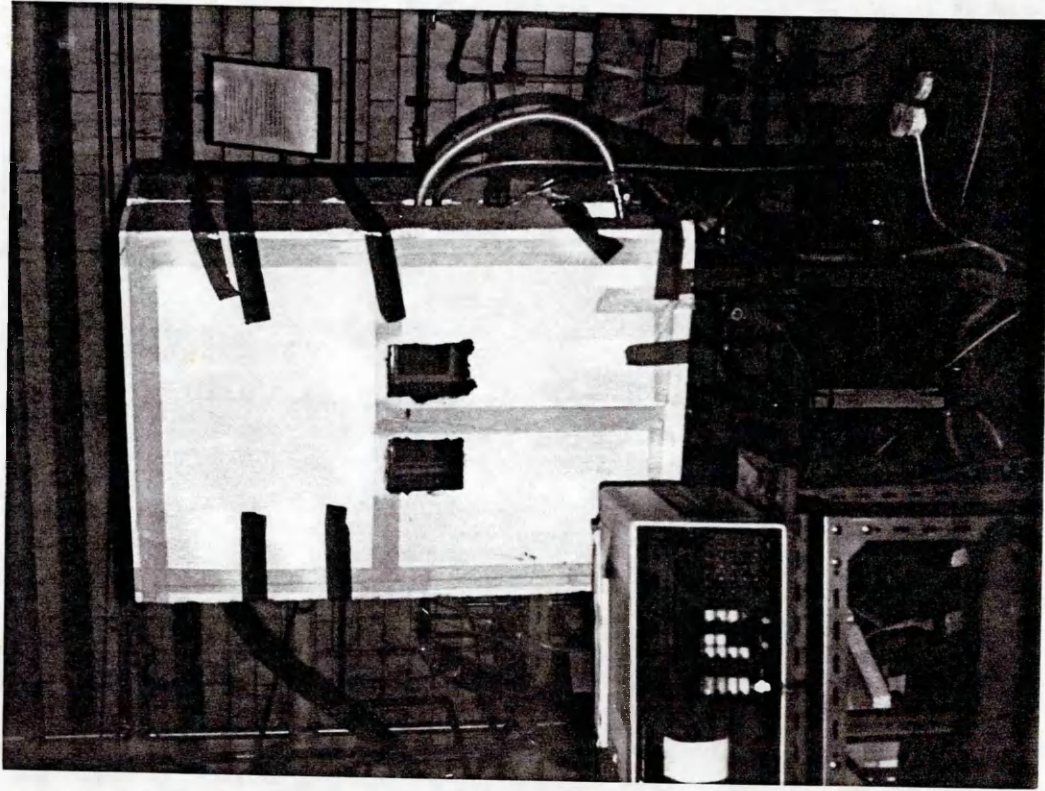


Figure 21: Front View of Test Condenser With Insulation

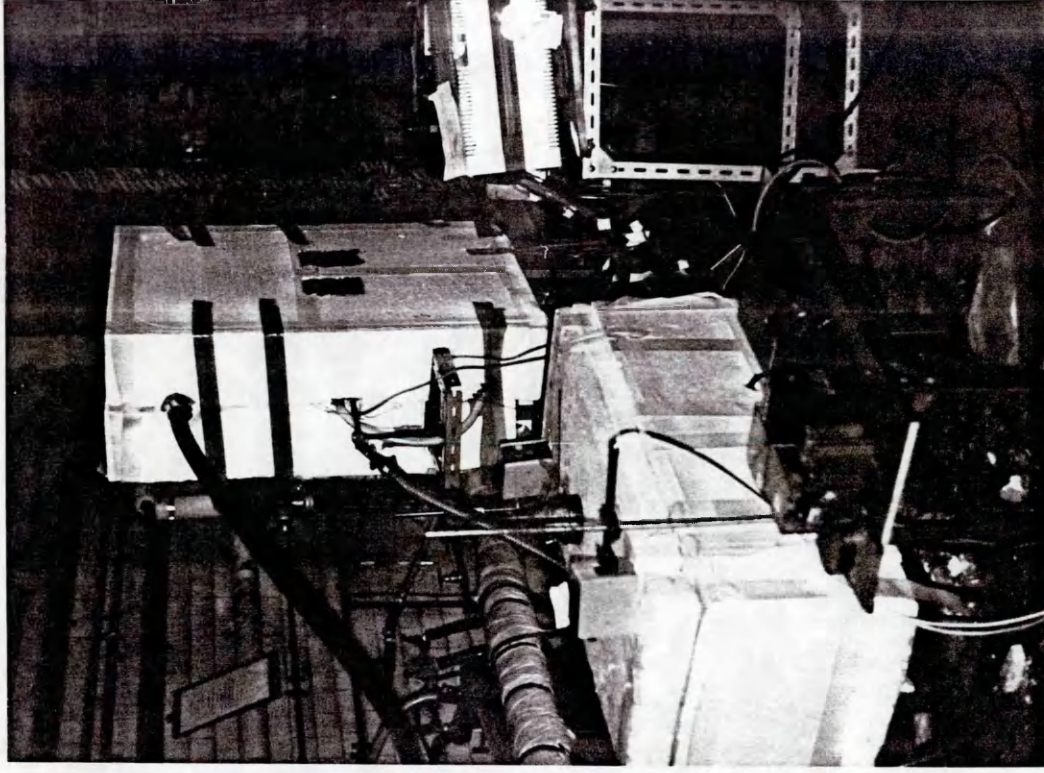


Figure 22: Side View of the Test Condenser and Inundation Tank with Insulation

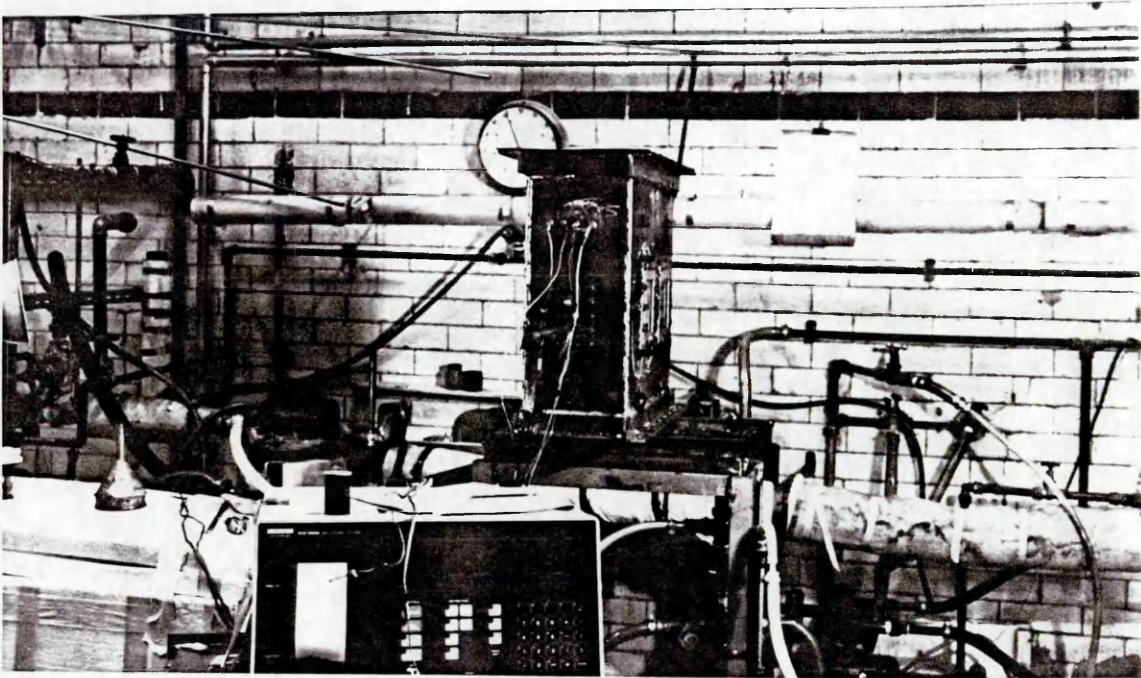


Figure 23:Side View of the Un-assembled Test Condenser

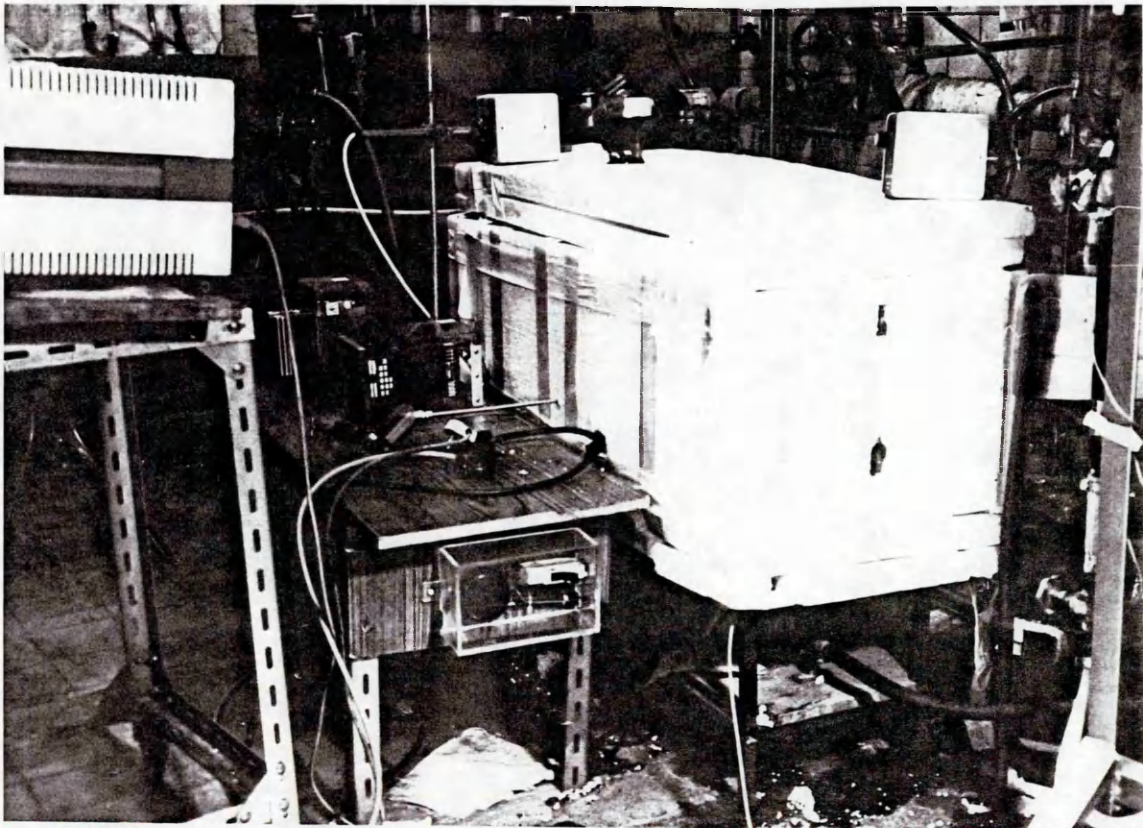


Figure 24:Insulated Condensate Water Tank

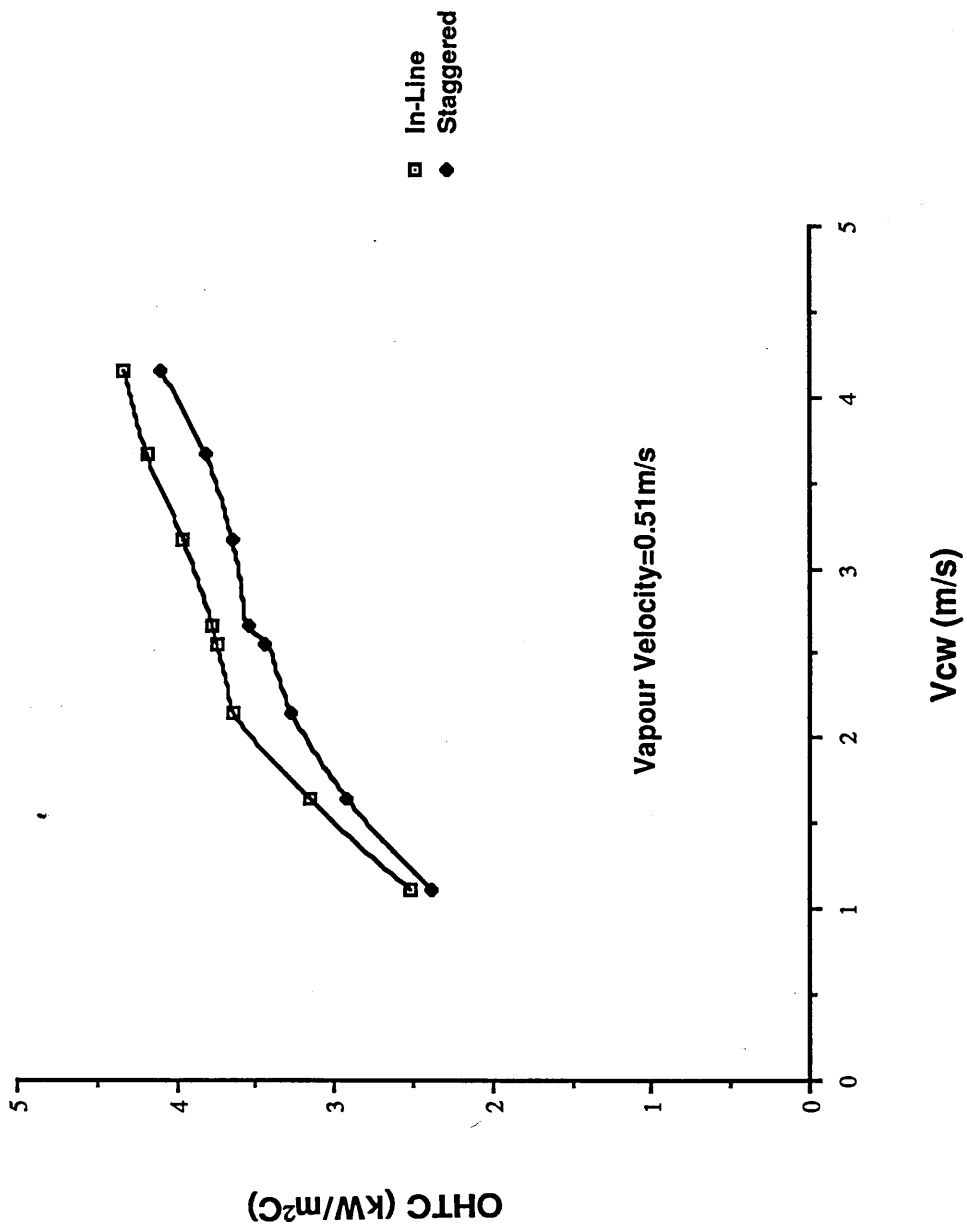


Figure 25:Insert Position Comparison for Plain Tubes

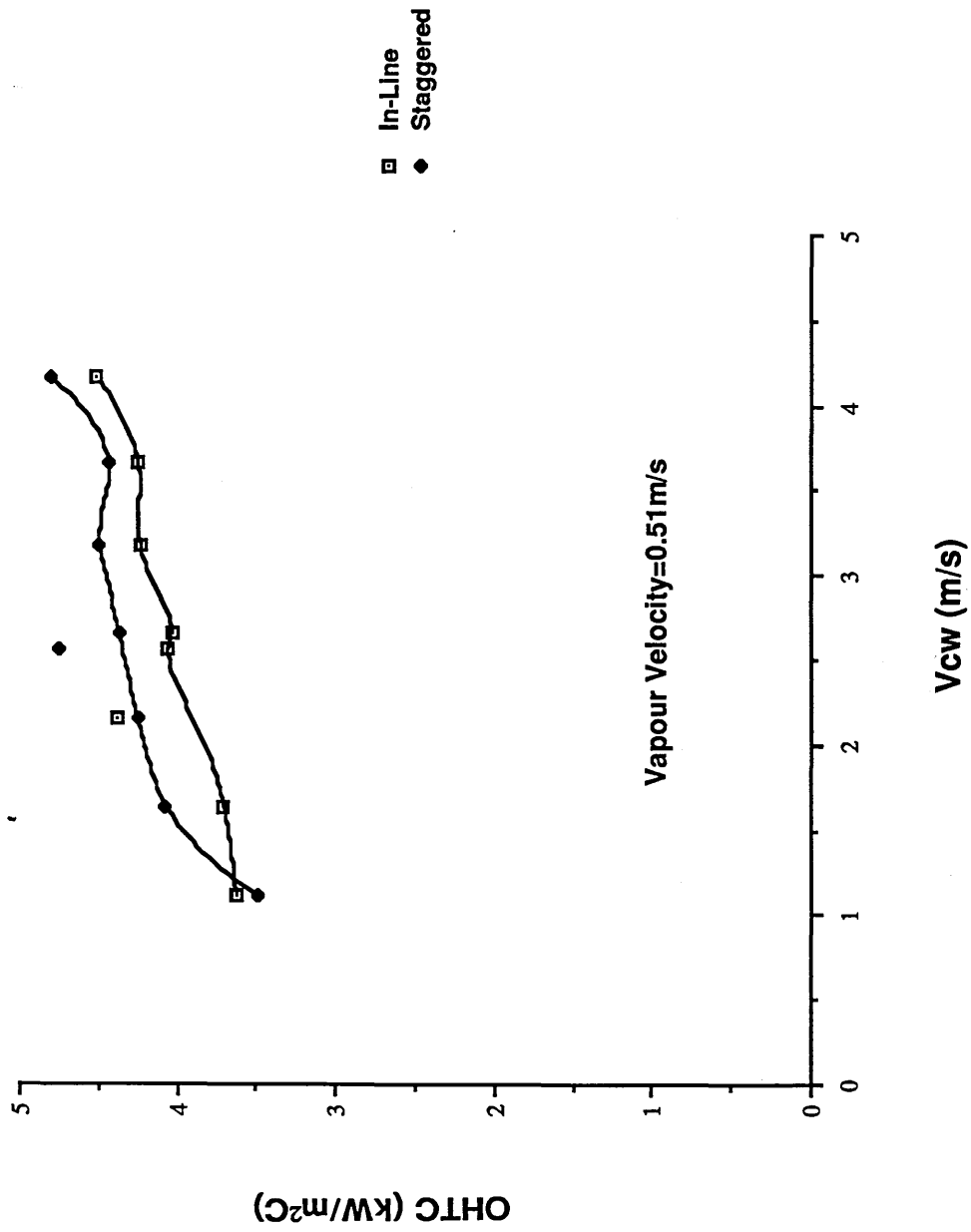


Figure 26: Insert Position Comparison for 6-Start Roped Tubes

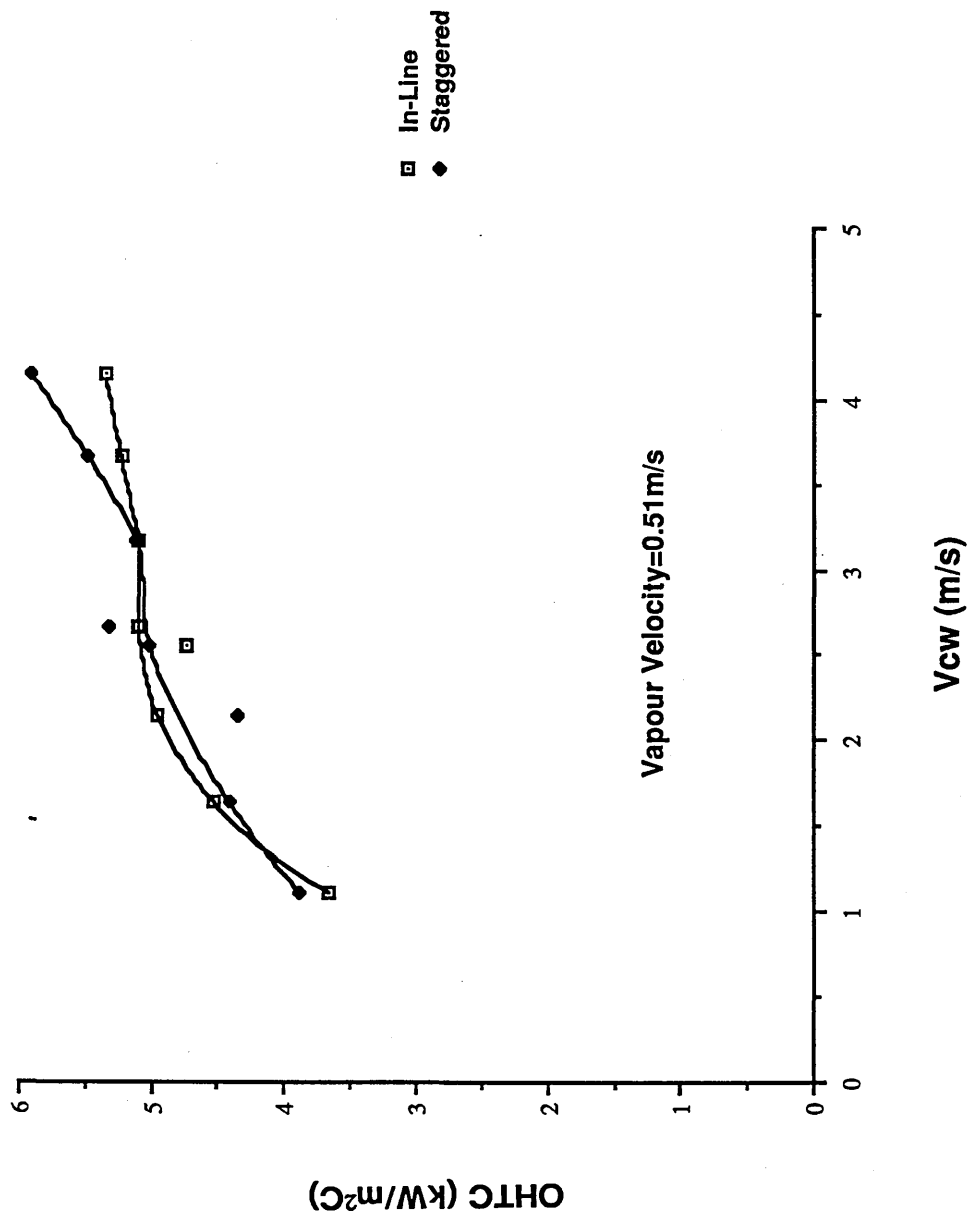


Figure 27:Insert Position Comparison for 2-Start Roped Tubes

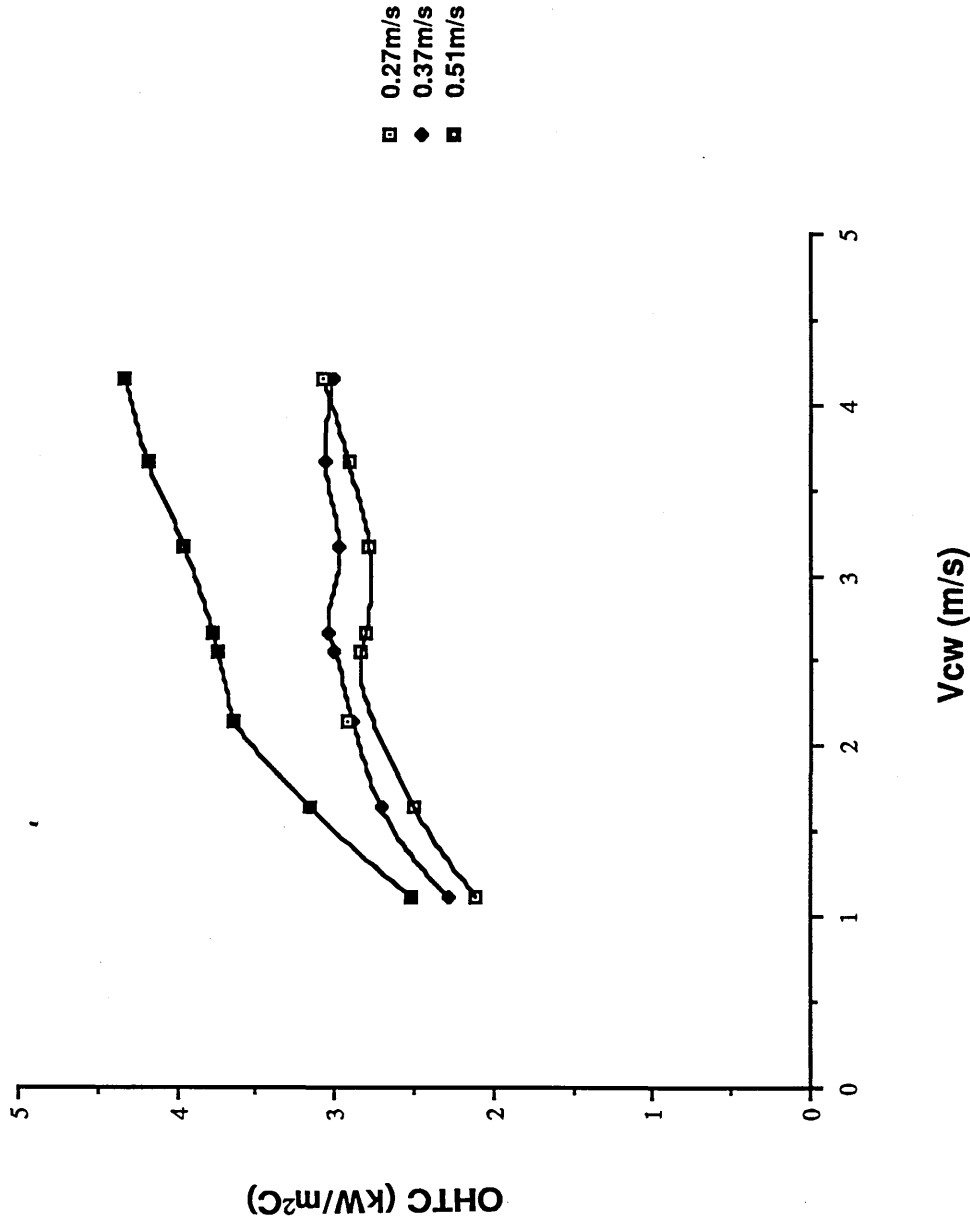


Figure 28: OHTC Performance of Plain Tubes with various Steam Velocities

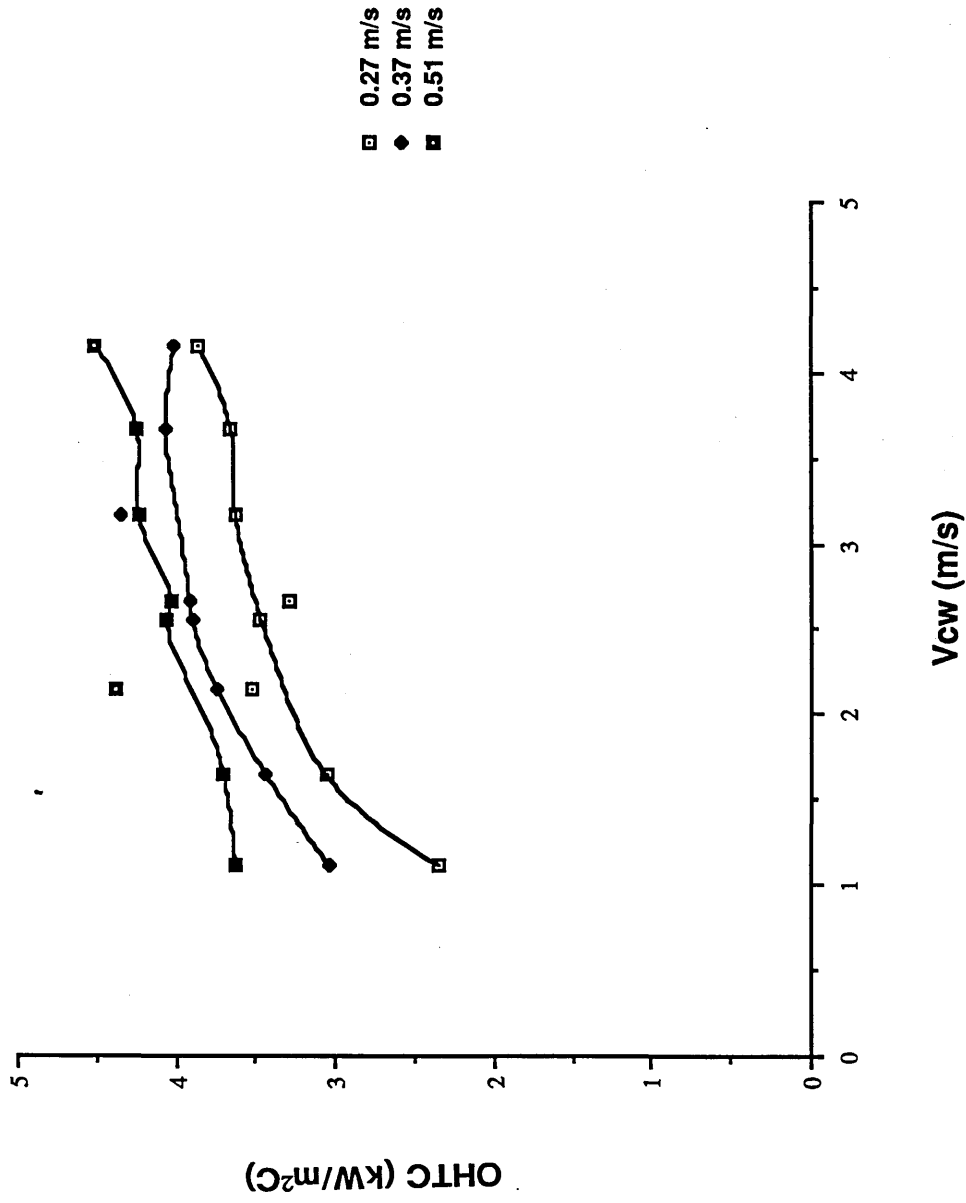


Figure 29: OHTC Performance of 6-Start Tubes with various Steam Velocities

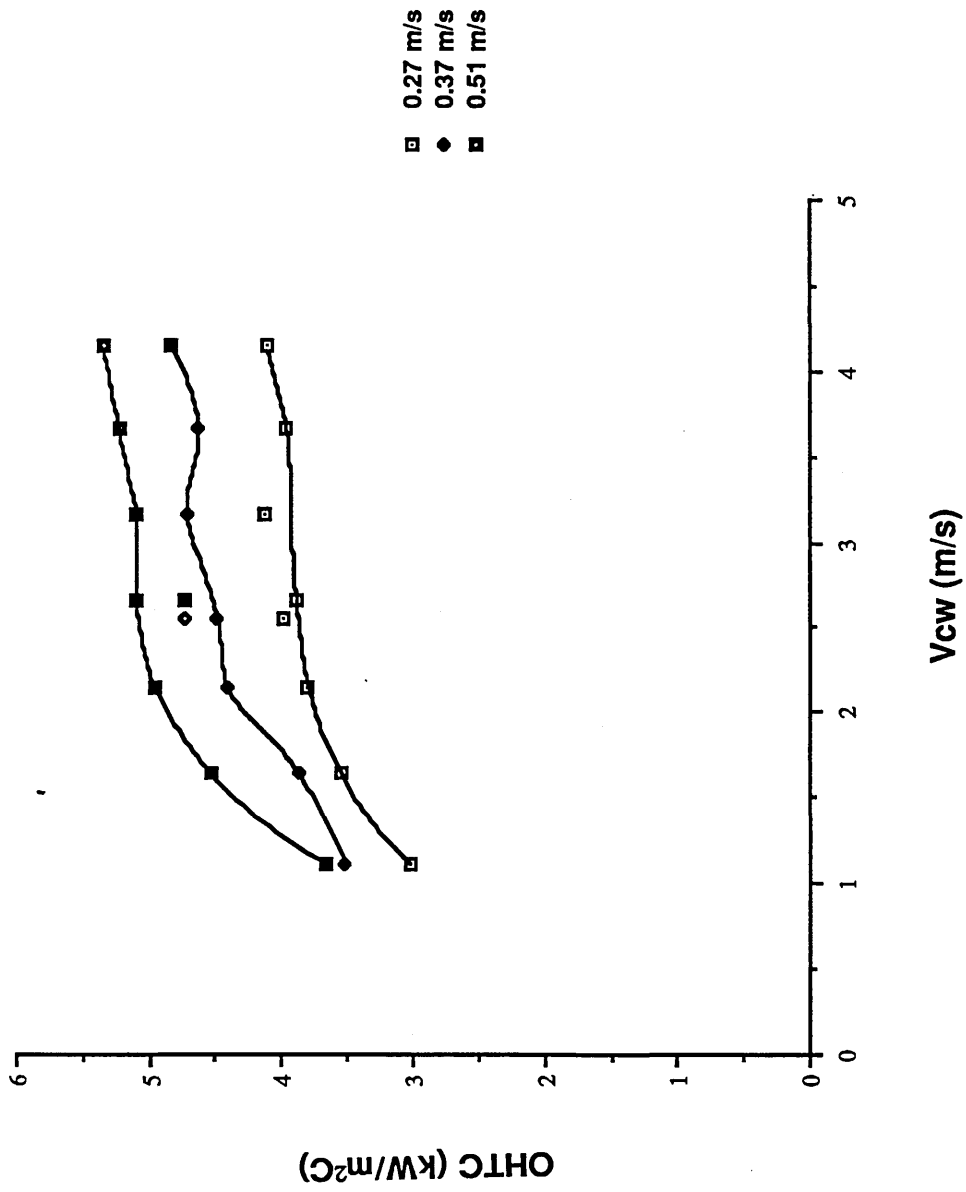


Figure 30: OHTC Performance of 2-Start Tubes with various Steam Velocities

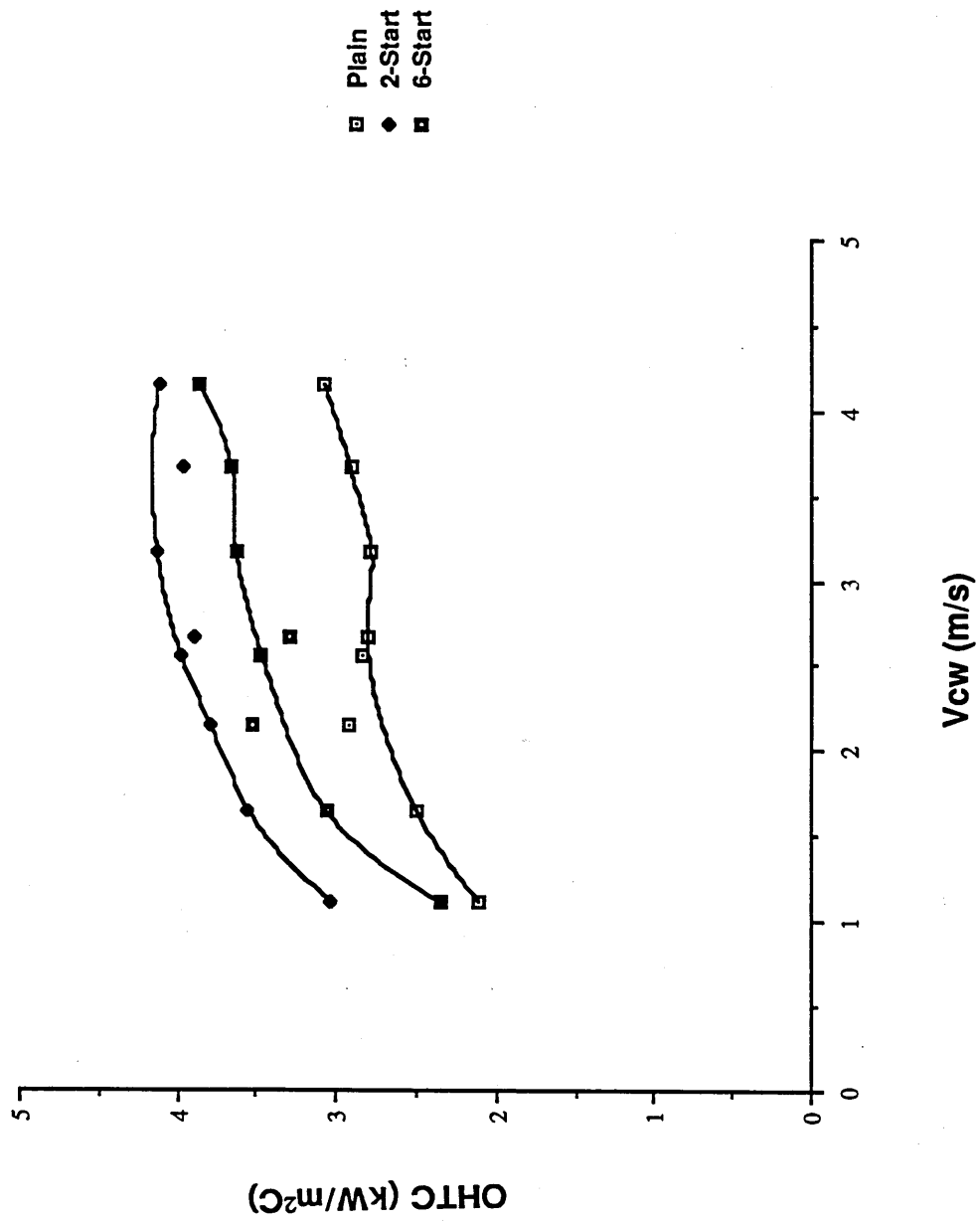


Figure 31:OHTC Performance for a Steam Velocity of 0.27 m/s

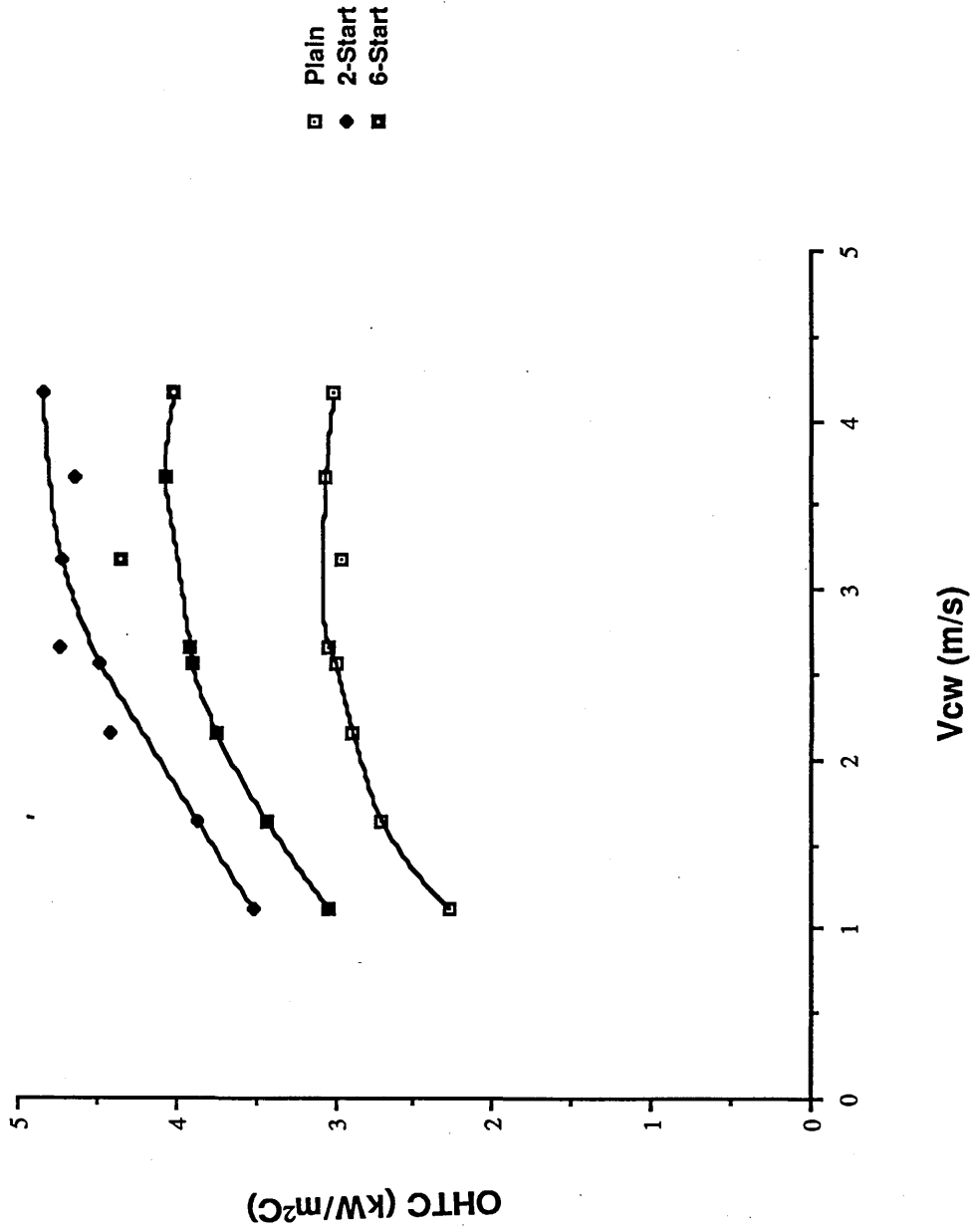


Figure 32:OHTC Performance for a Steam Velocity of 0.37 m/s

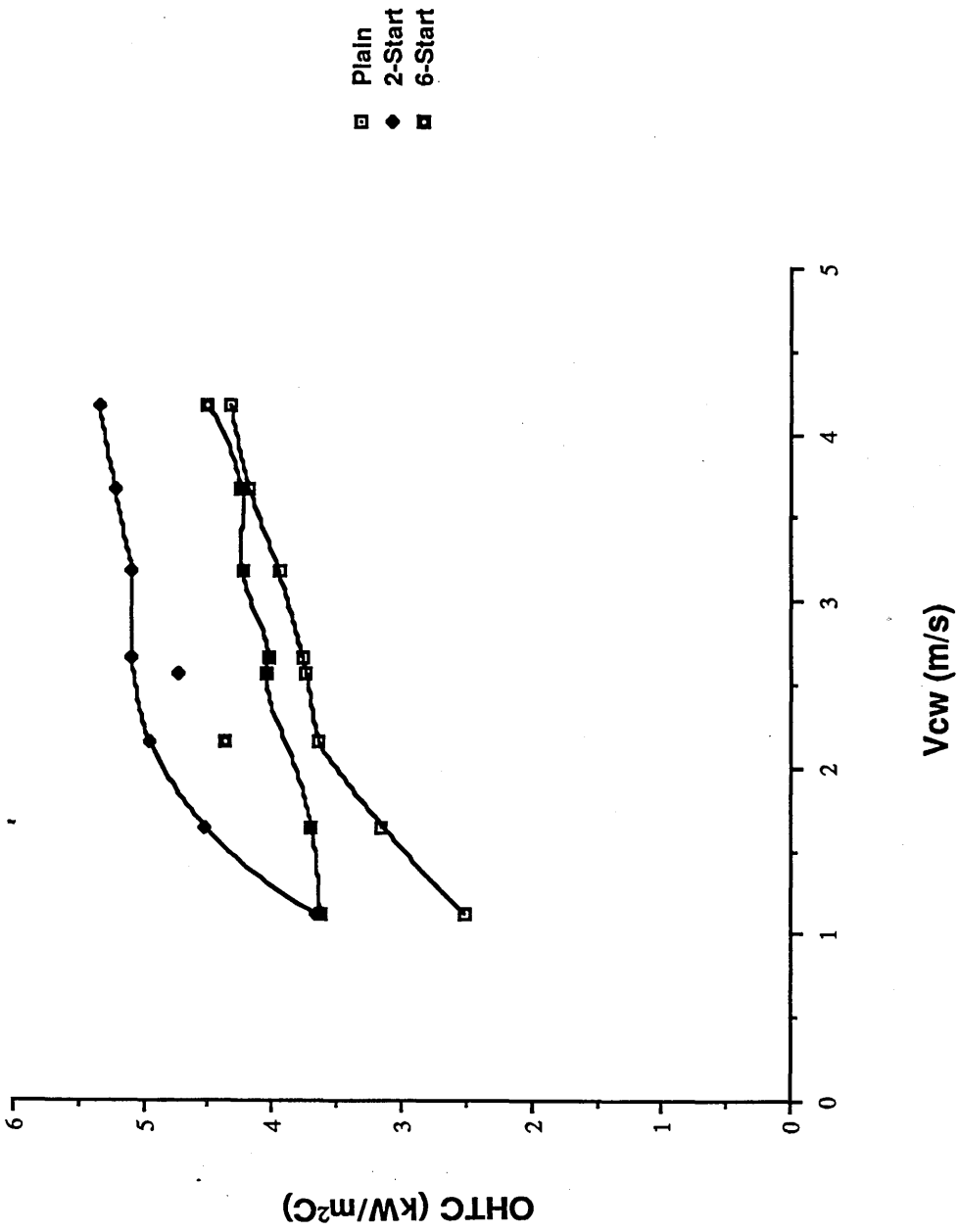


Figure 33:OHTC Performance for a Steam Velocity of 0.51m/s

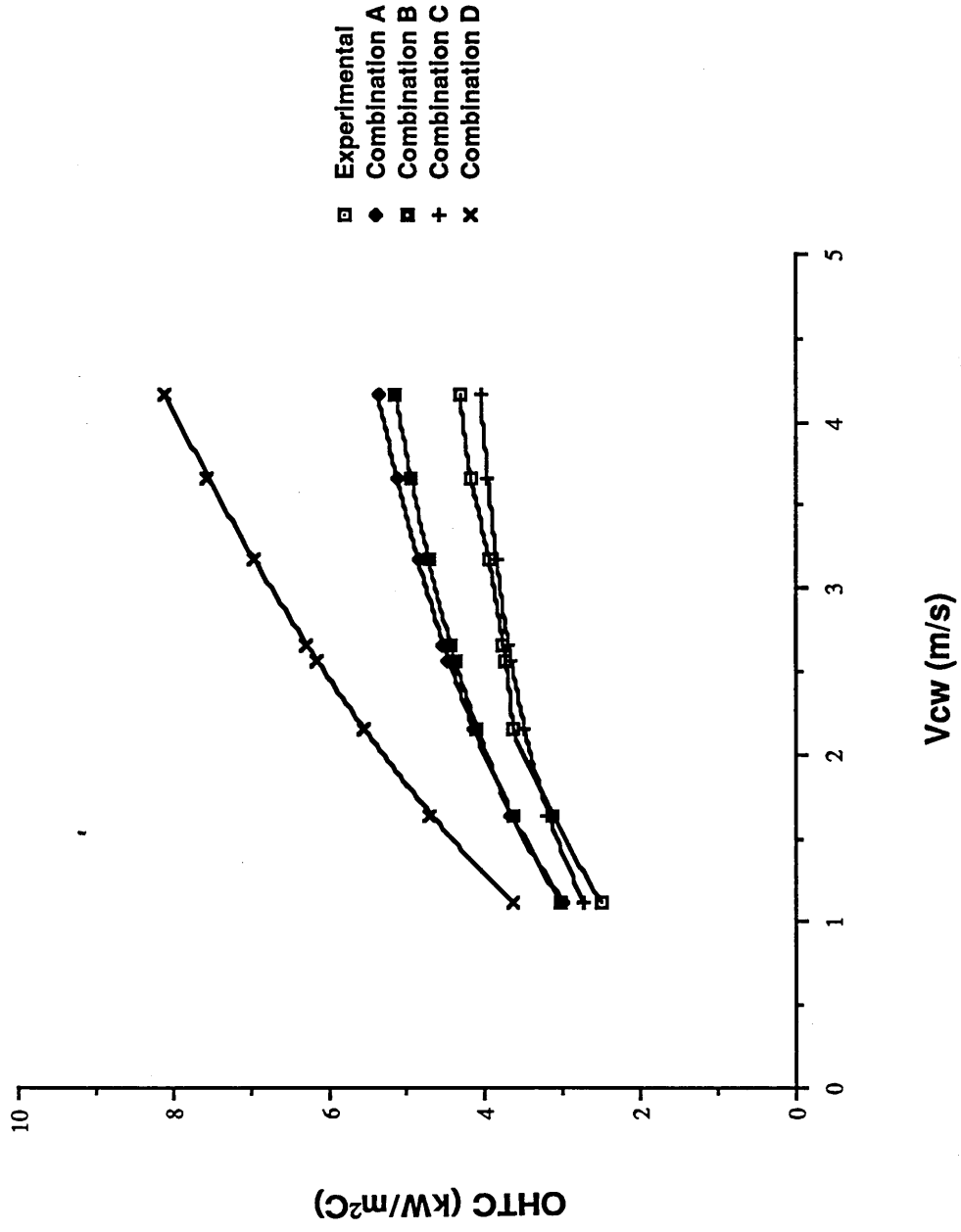


Figure 34: Plain Tube Results Comparison for a Steam Velocity of 0.51m/s

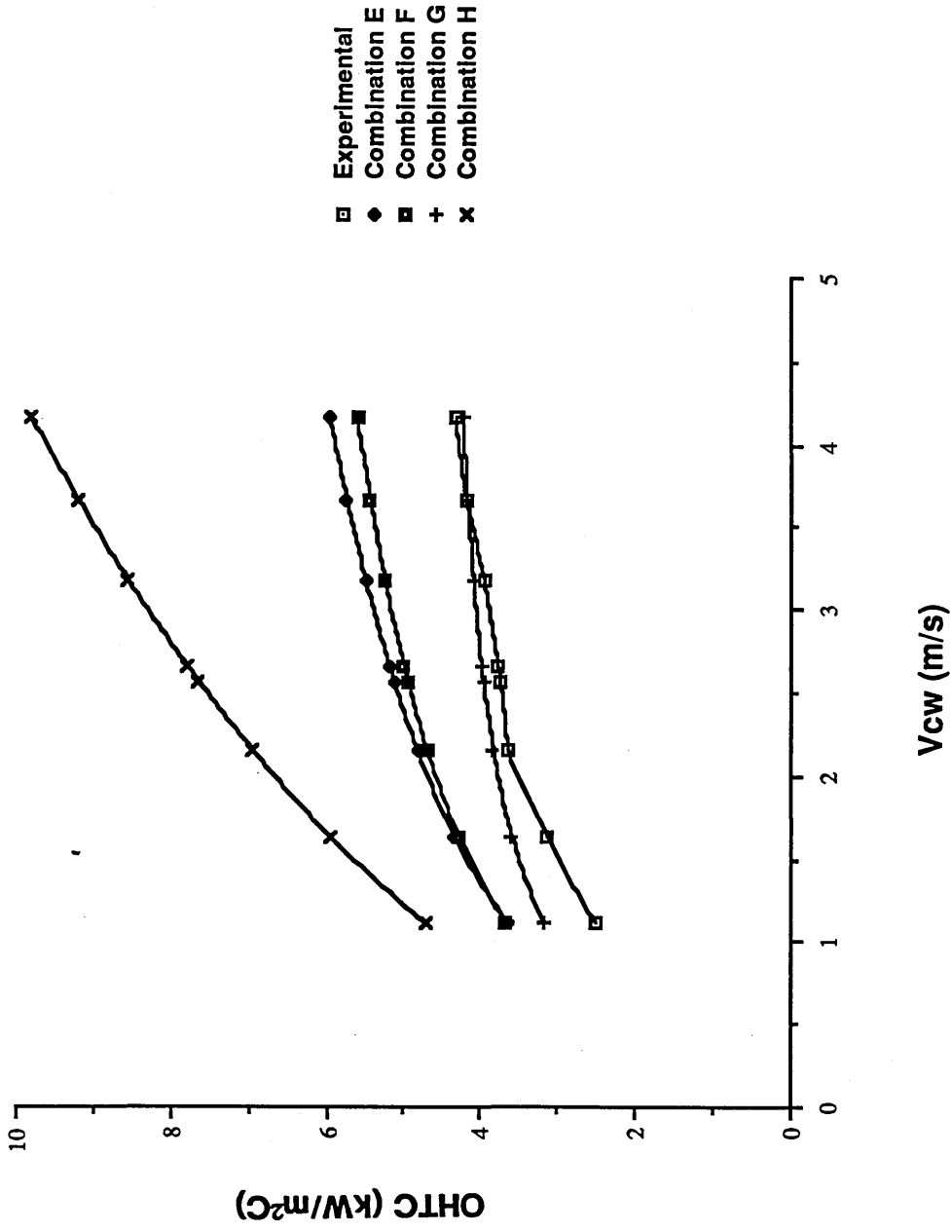


Figure 35: Plain Tube Results Comparison for a Steam Velocity of 0.51 m/s

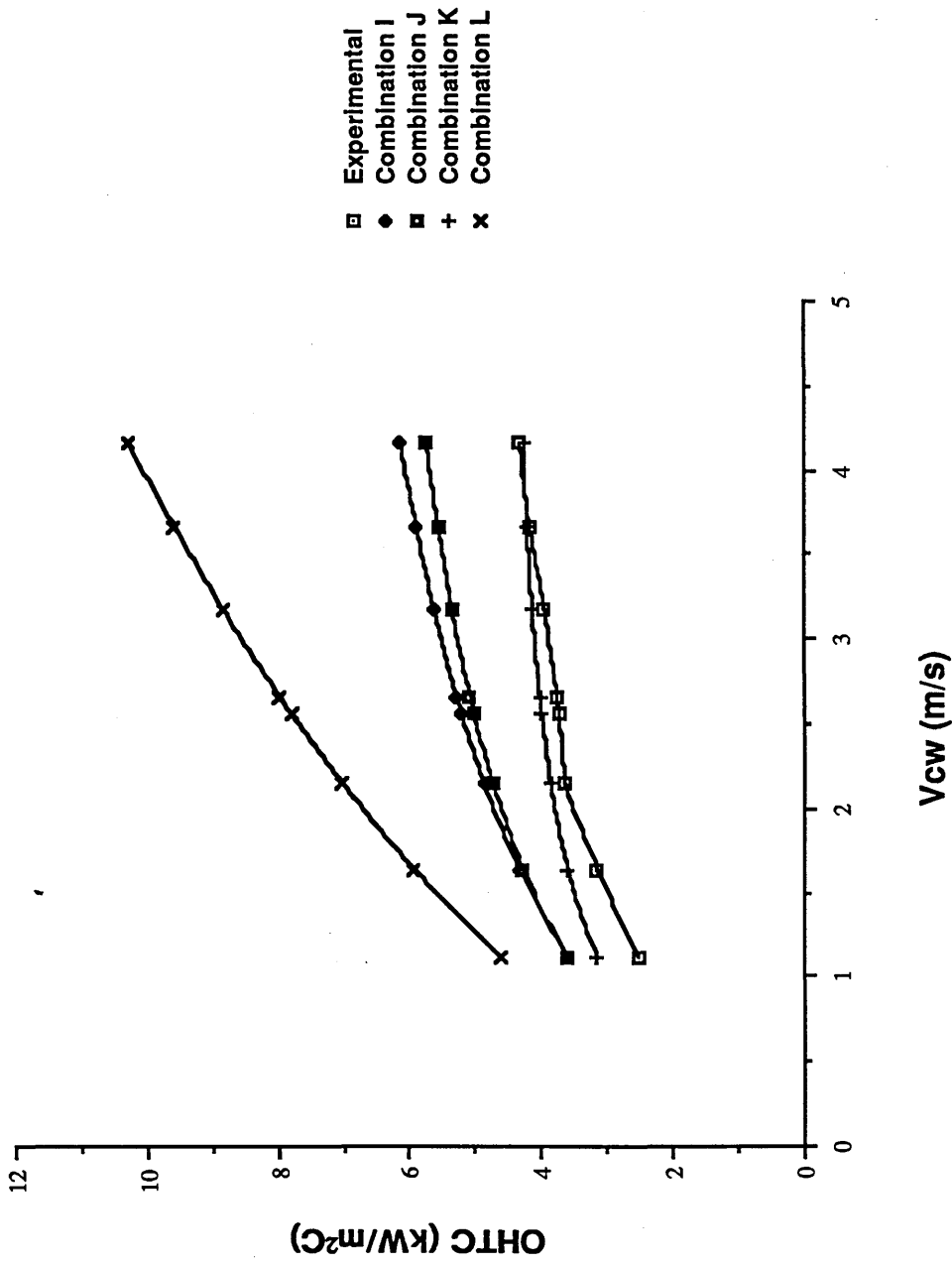


Figure 36: Plain Tube Results Comparison for Steam Velocity of 0.51 m/s

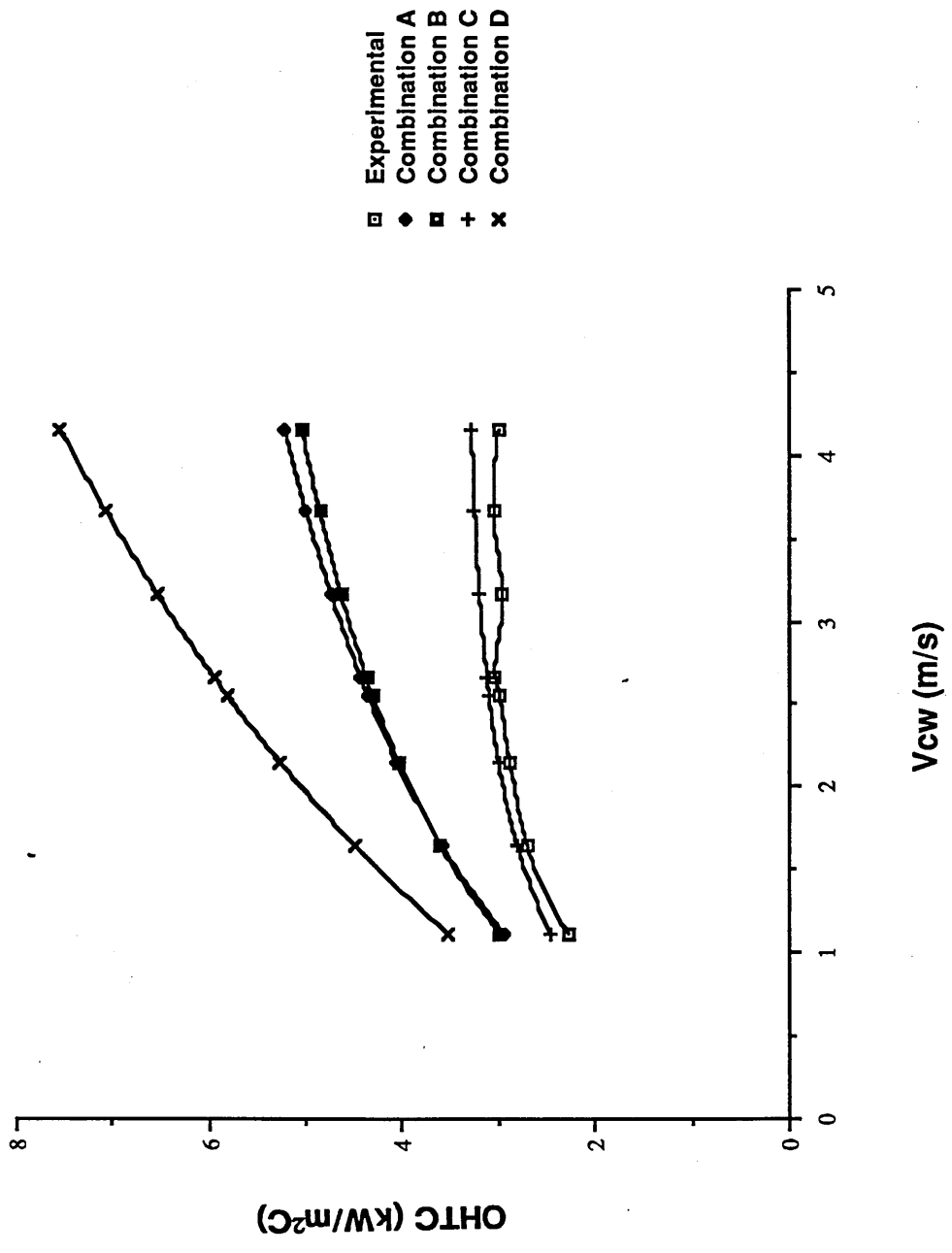


Figure 37: Plain Tube Results Comparison for a Steam Velocity of 0.37m/s

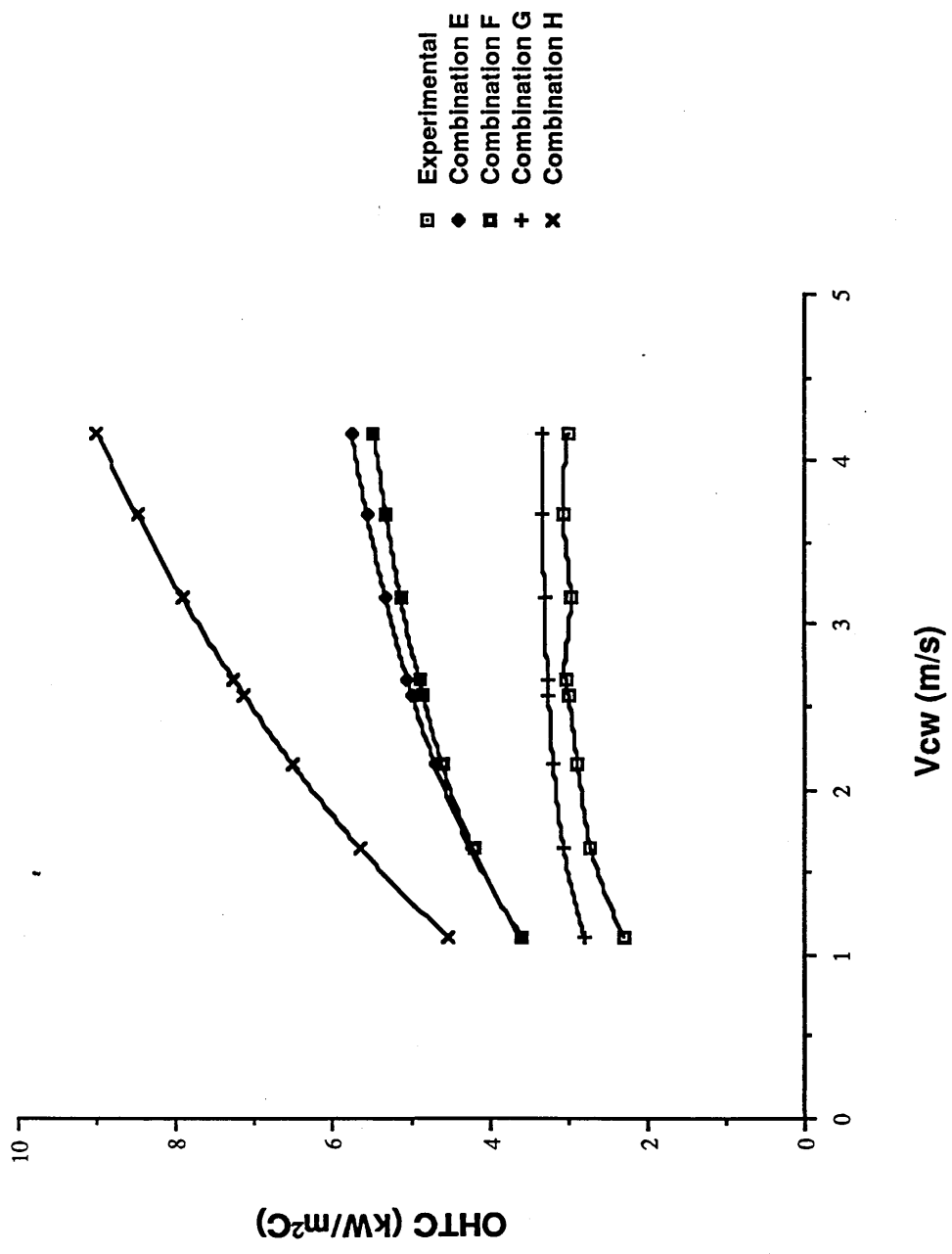


Figure 38: Plain Tube Results Comparison for a Steam Velocity of 0.37m/s

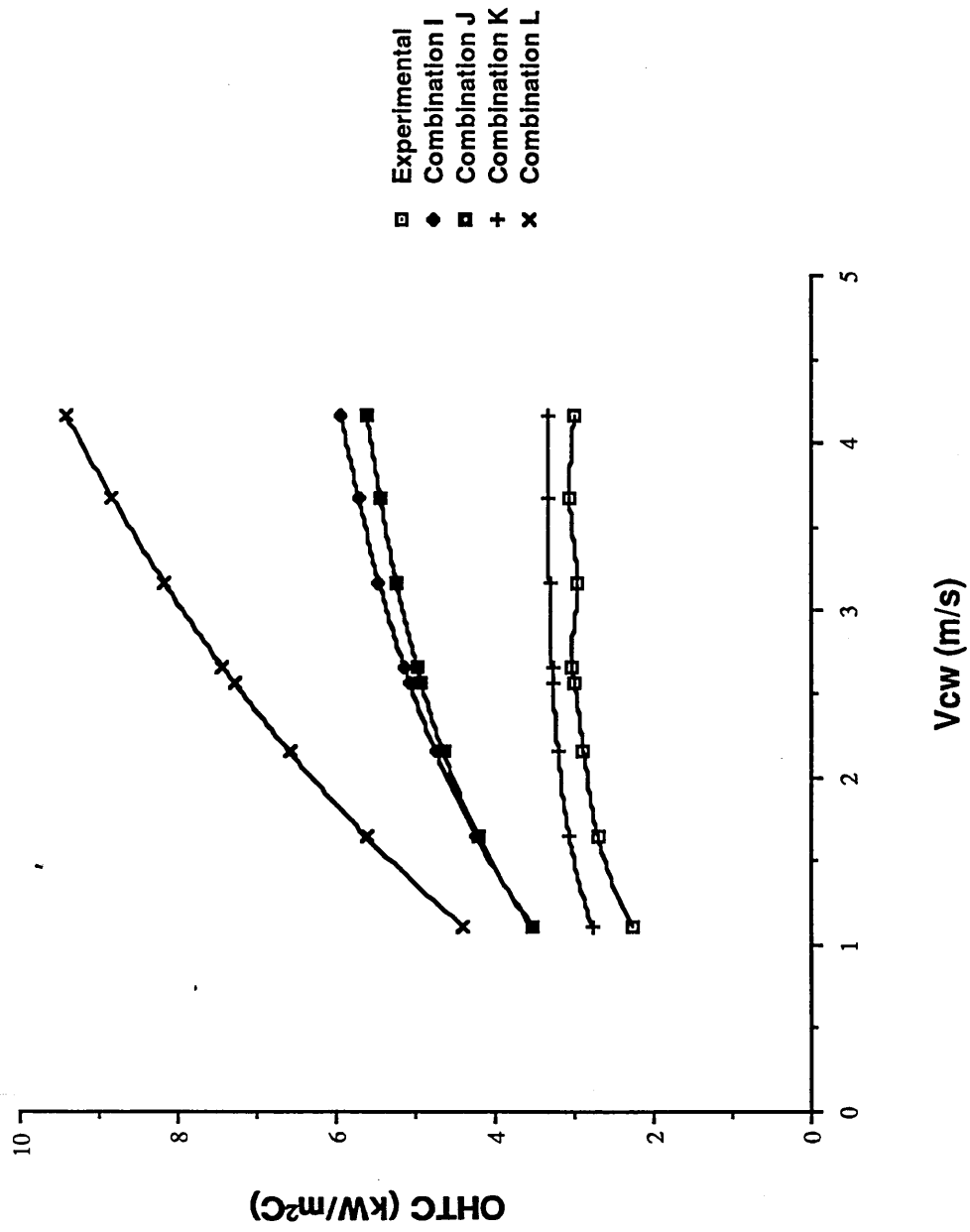


Figure 39: Plain Tube Results Comparison for a Steam Velocity of 0.37 m/s

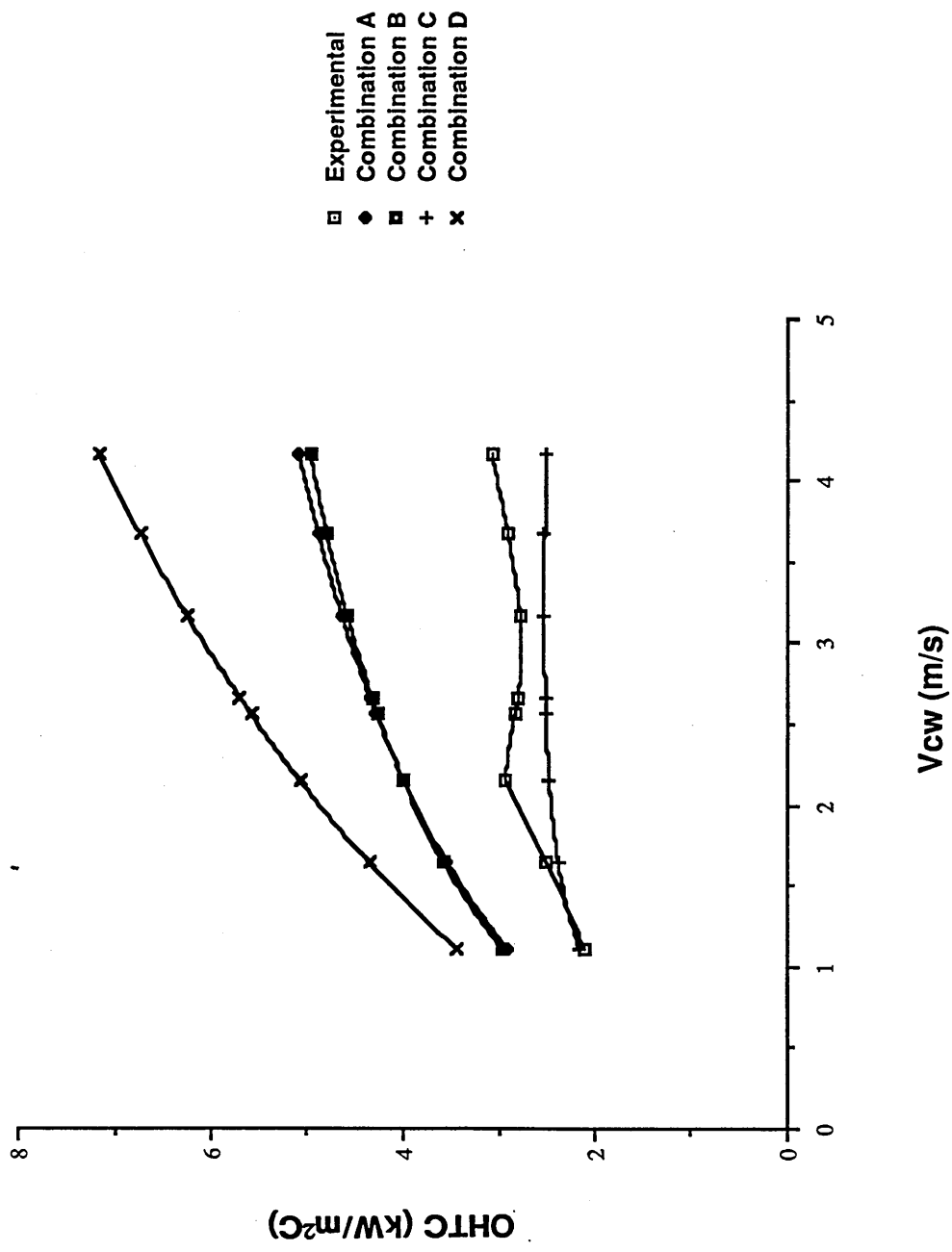


Figure 40: Plain Tube Results Comparison for a Steam Velocity of 0.27 m/s

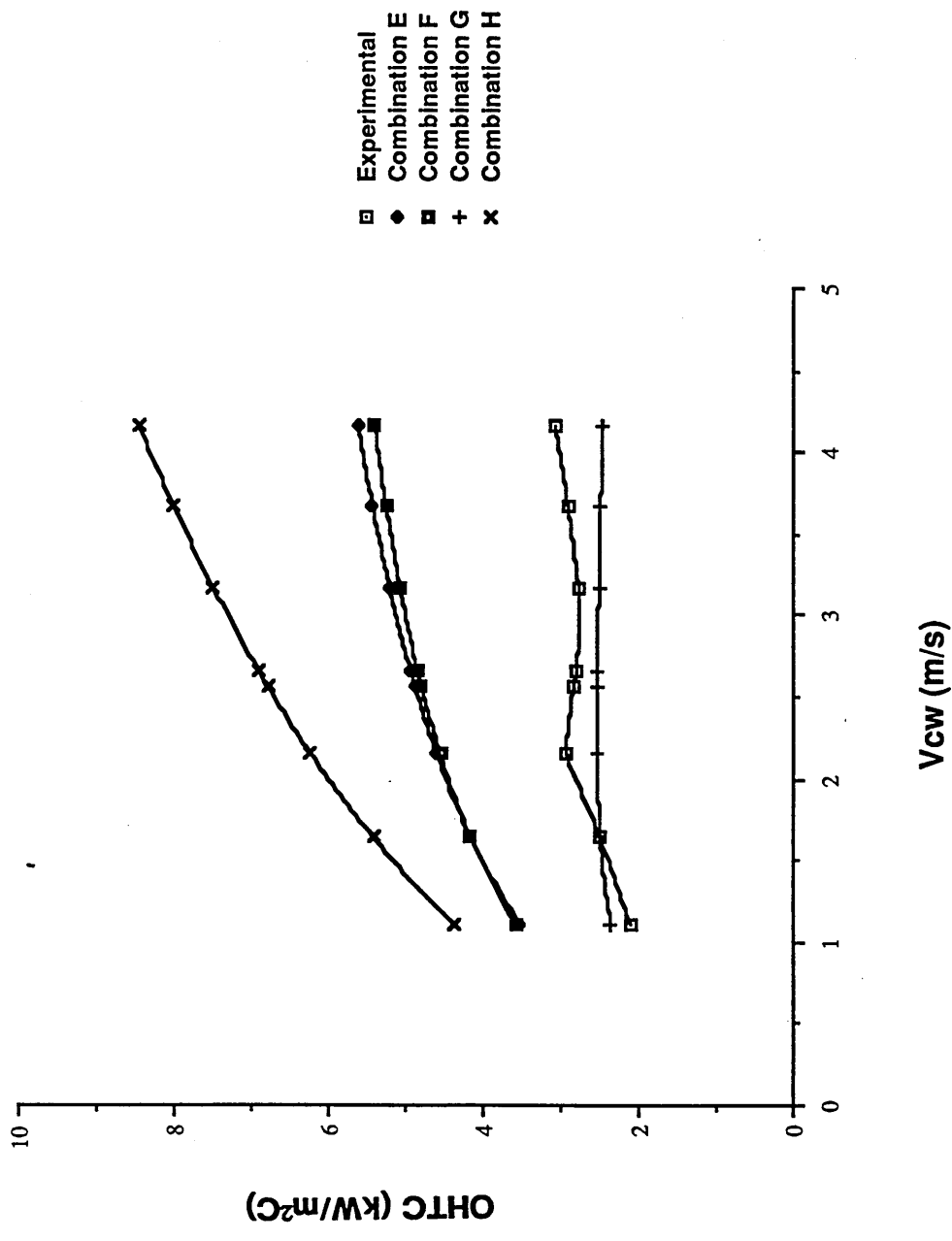


Figure 41: Plain Tube Results Comparison for a Steam Velocity of 0.27 m/s

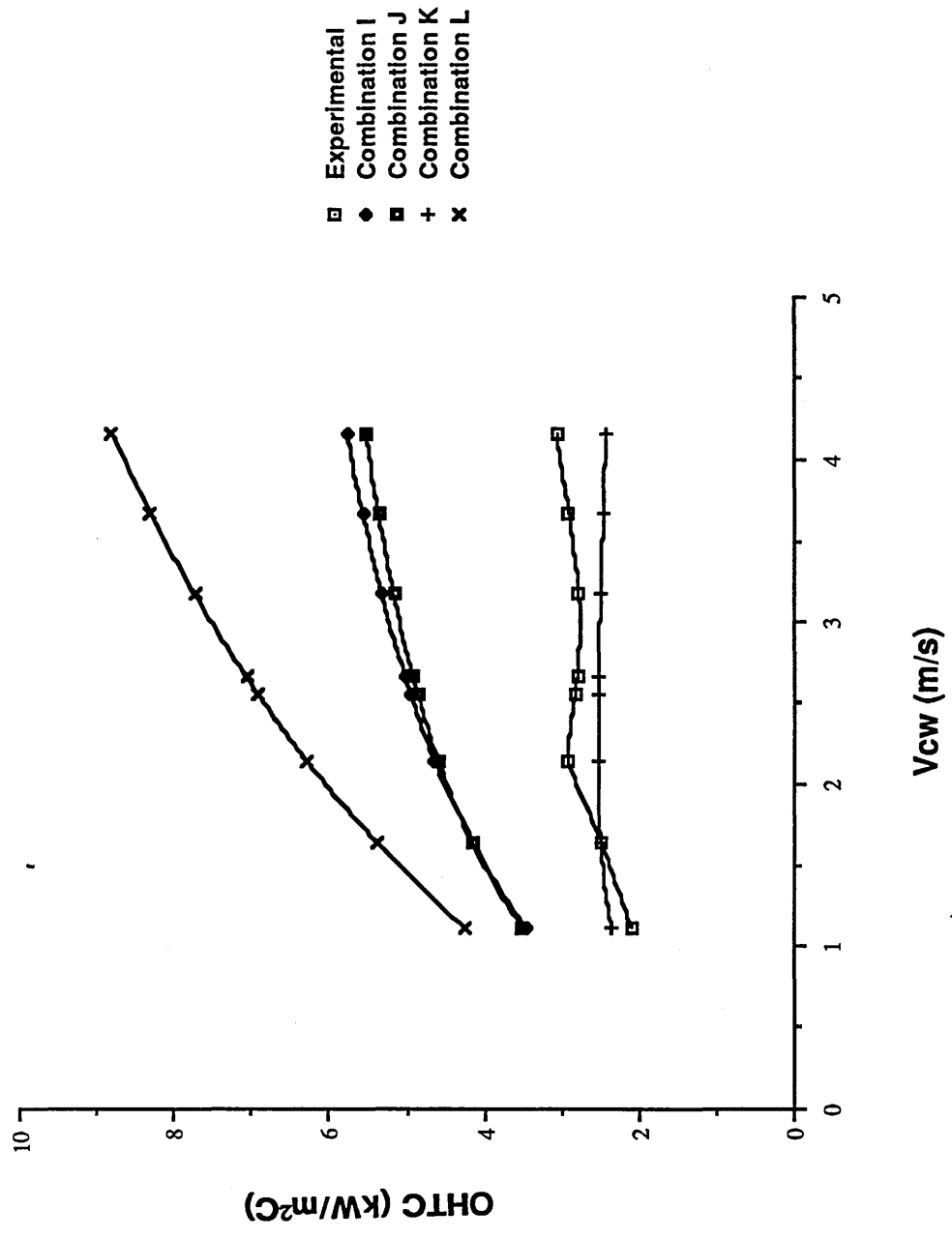


Figure 42: Plain Tube Results Comparison for a Steam Velocity of 0.27 m/s

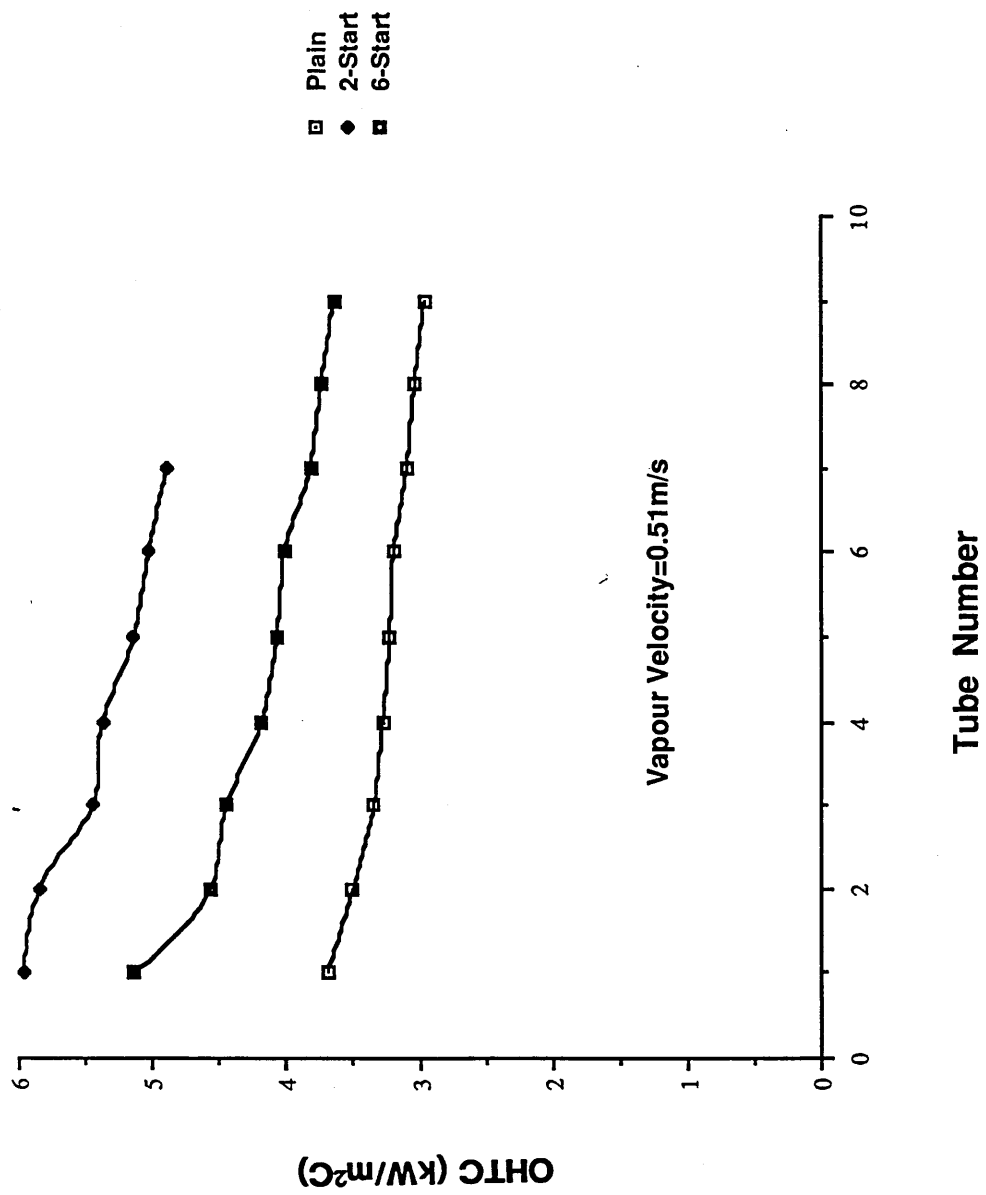


Figure 43: Vapour Shear and Inundation Experimental Results Comparison

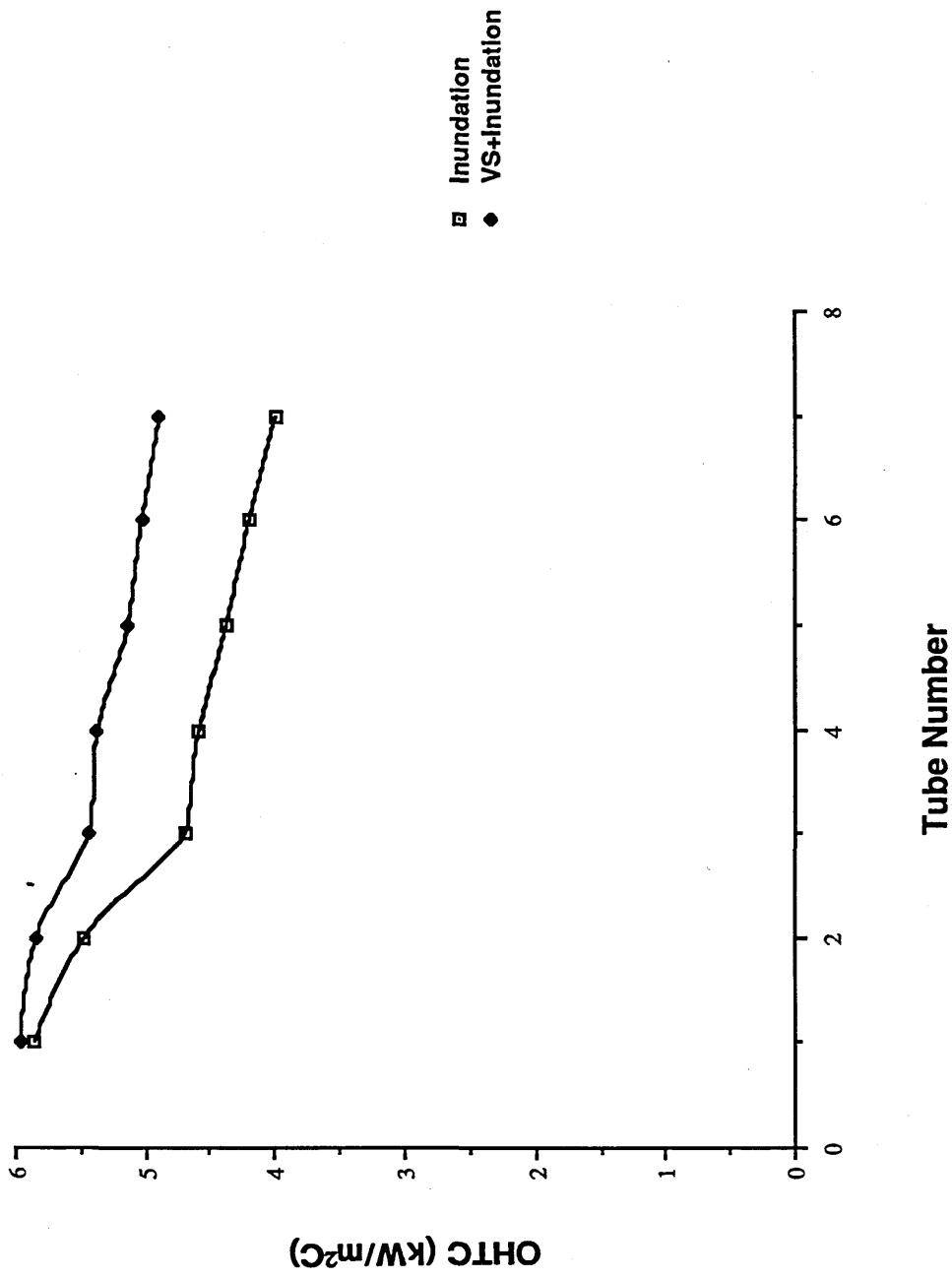


Figure 44: Experimental Results Comparison for 2-Start Roped Tubes

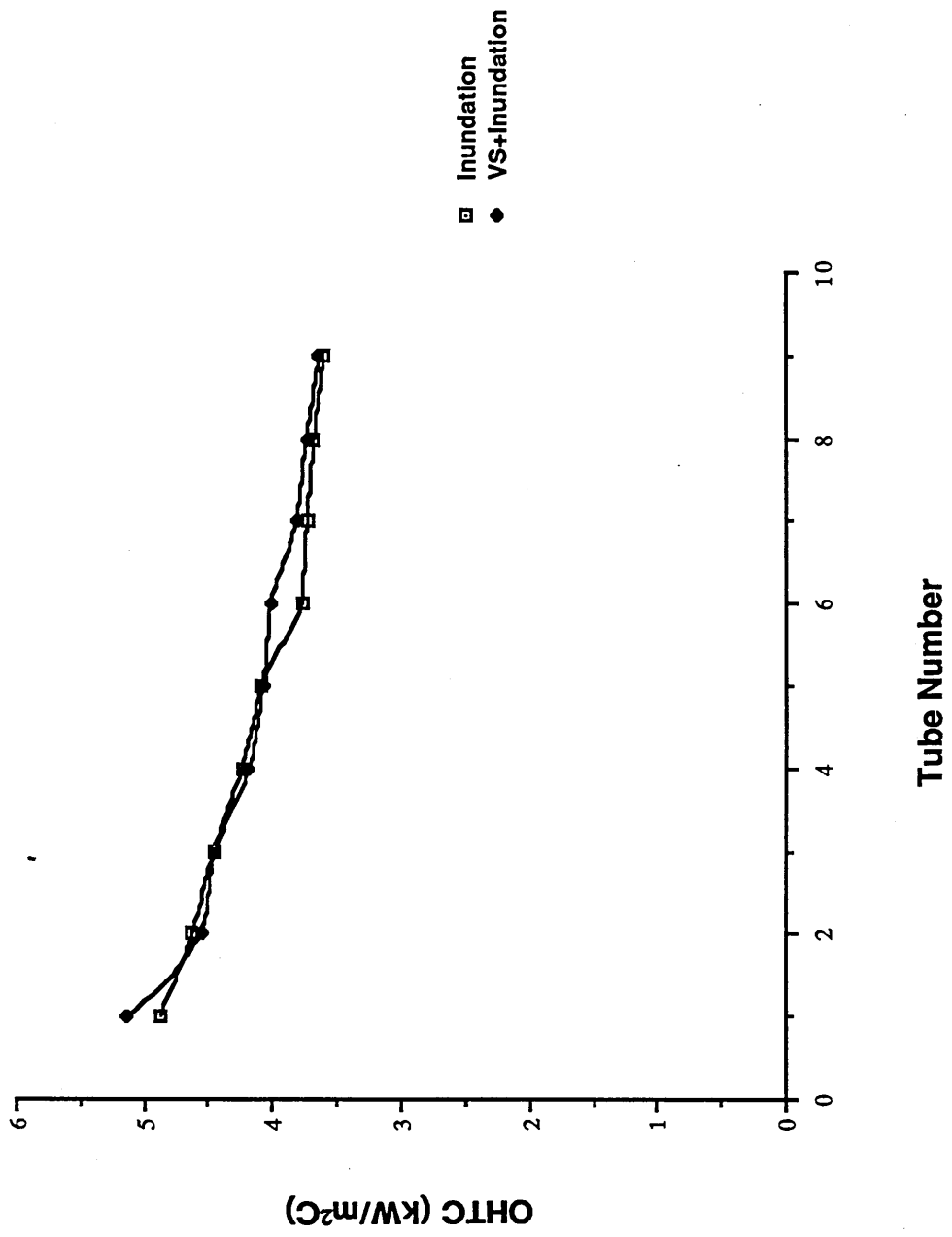


Figure 45: Experimental Results Comparison for 6-Start Roped Tubes

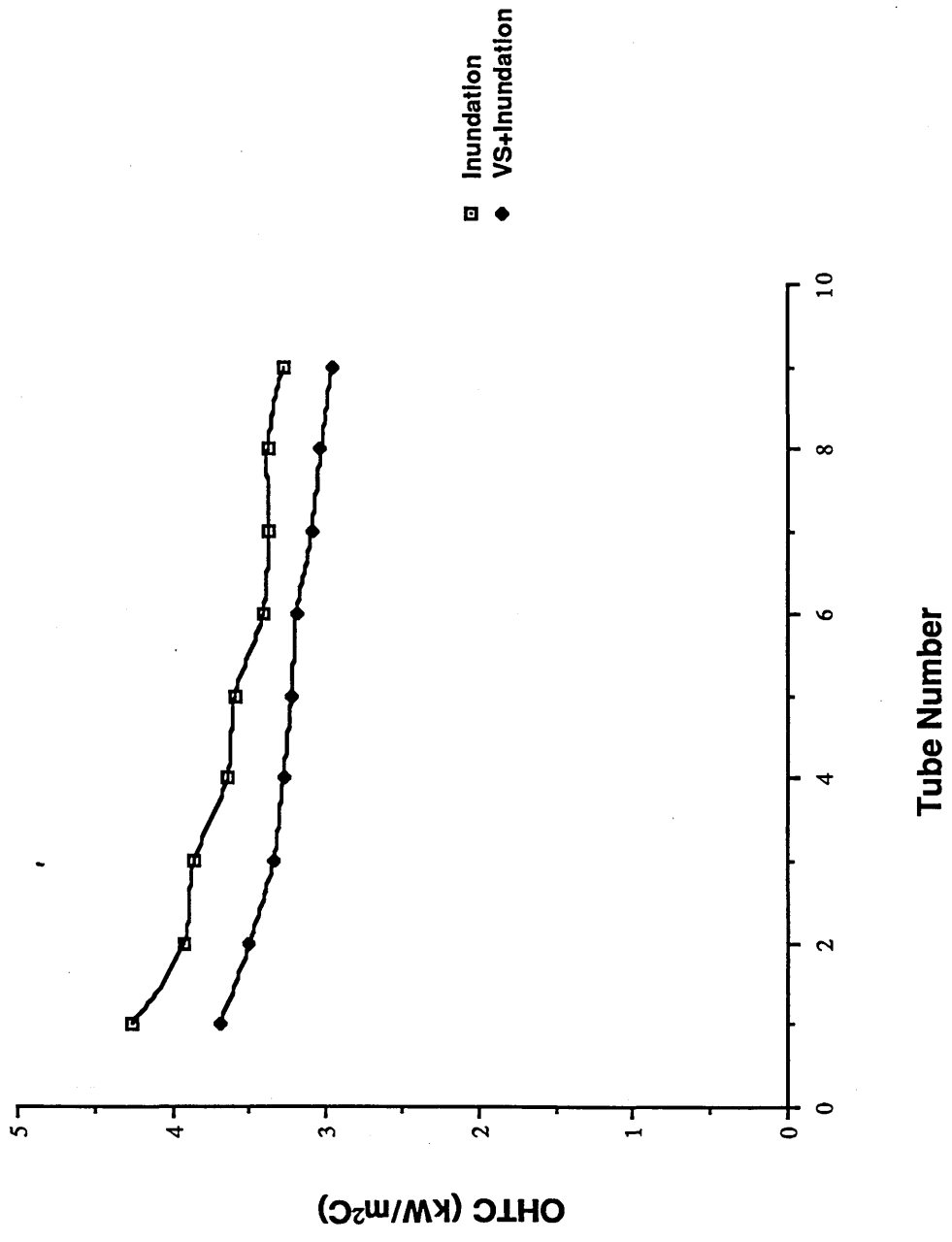


Figure 46: Experimental Results Comparison for Plain Tubes

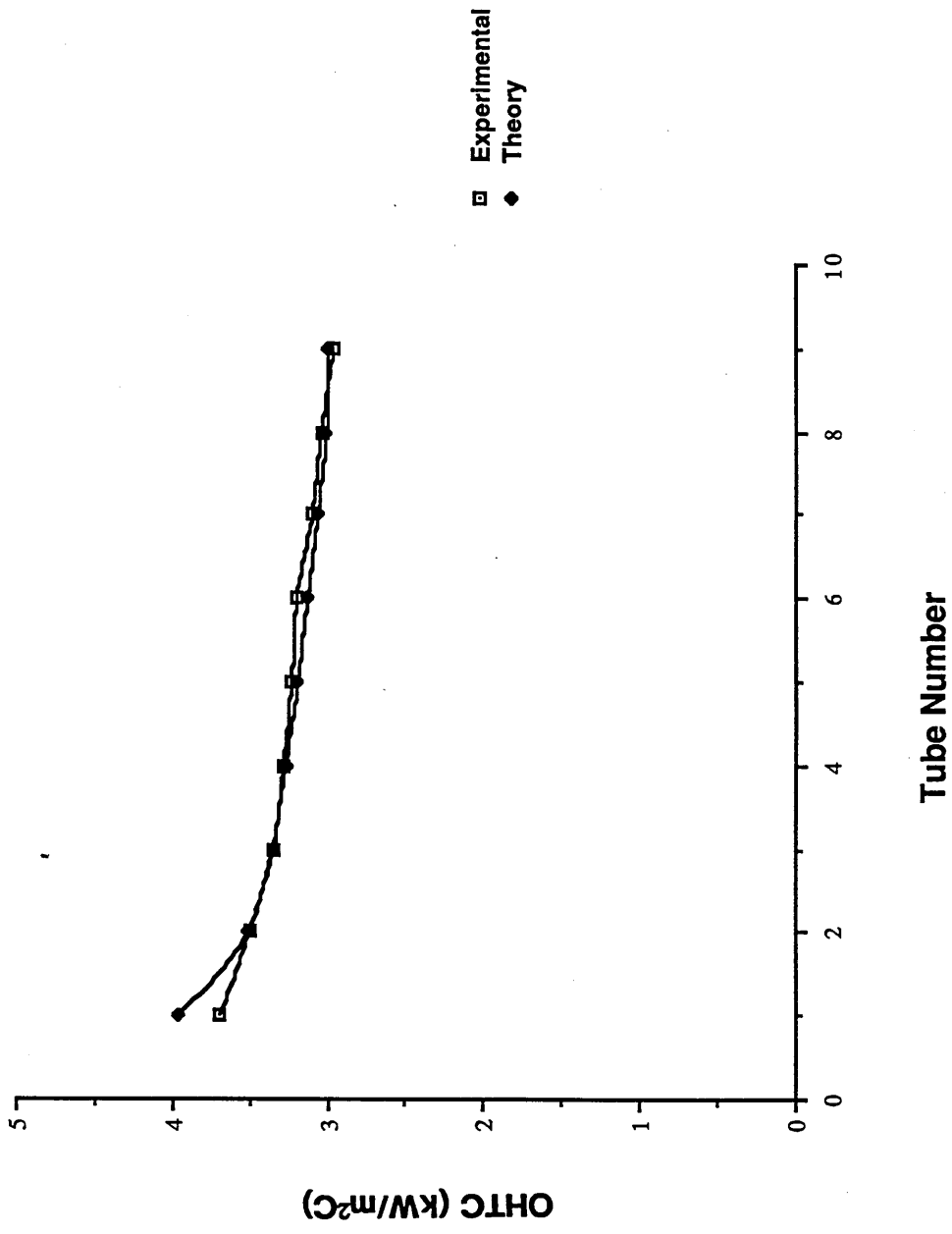


Figure 47: Theoretical and Experimental Results Comparison for Plain Tubes

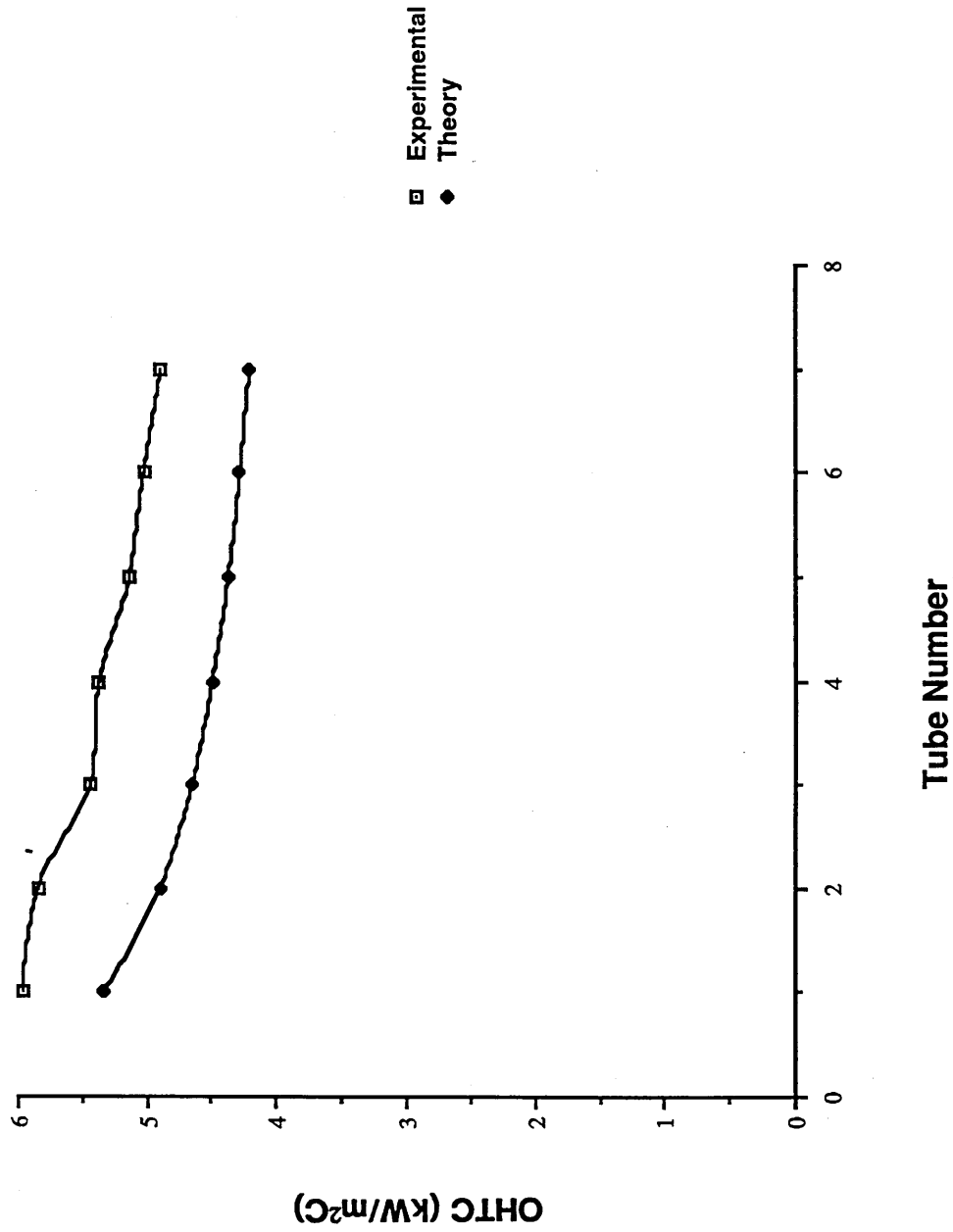


Figure 48: Theoretical and Experimental Results Comparison for 2-Start Roped Tubes

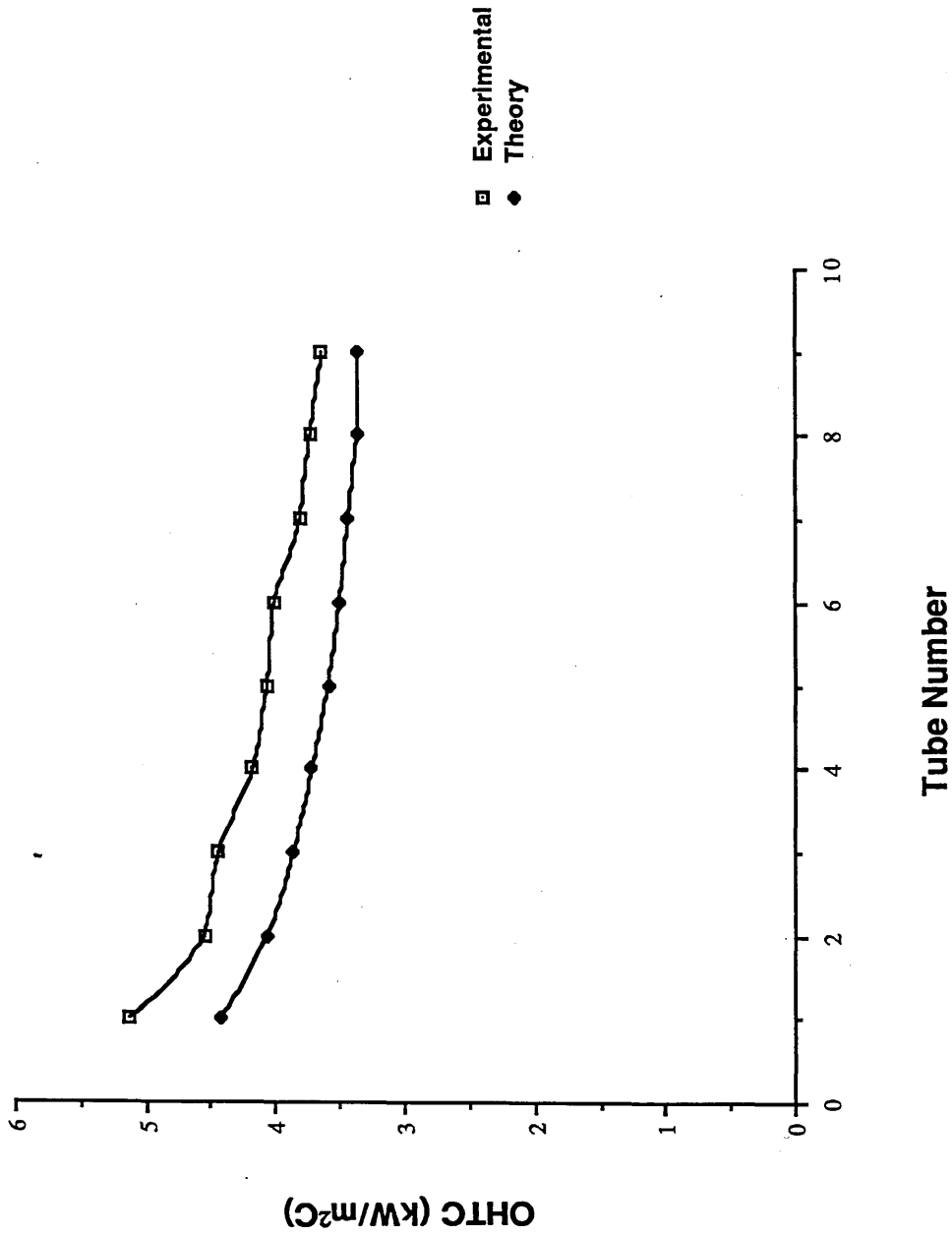


Figure 49: Theoretical and Experimental Results Comparison for 6-Start Tubes